Overexpression and crosslinking of the metallo-chaperone PbrD to calcium alginate nanoparticles as a novel biosorbent for lead ions

by

Vidya Keshav

(0503548y)

Thesis

Submitted in fulfilment of the requirements for the degree

Philosophiae Doctor

in

Molecular and Cell Biology

in the Faculty of Science, University of the Witwatersrand, Johannesburg, South Africa

Supervisor: Dr Kulsum Kondiah

Co-supervisor: Prof. Heinrich Dirr

Co-supervisor: Dr Paul Franklyn

September 2019

Declaration

I, Vidya Keshav (0503548Y), am a student registered for the degree of Doctor of Philosophy (PhD) in the academic year 2019.

I hereby declare the following:

- I am aware that plagiarism (the use of someone else's work without their permission and/or without acknowledging the original source) is wrong.
- I confirm that the work submitted for assessment for the above degree is my own unaided work except where explicitly indicated otherwise and acknowledged.
- I have not submitted this work before for any other degree or examination at this or any other University.
- The information used in the Thesis/Dissertation/Research Report HAS NOT been obtained by me while employed by, or working under the aegis of, any person or organization other than the University.
- I have followed the required conventions in referencing the thoughts and ideas of others.
- I understand that the University of the Witwatersrand may take disciplinary action against me if there is a belief that this is not my own unaided work or that I have failed to acknowledge the source of the ideas or words in my writing.

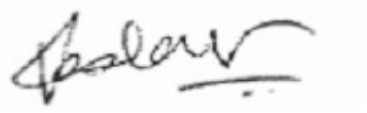

Vidya Keshav

18th day of September 2019 at University of the Witwatersrand

Abstract

Heavy metals are one of the most harmful pollutants found in our fresh water resources; threatening human health, infrastructure and the entire eco-system. Amongst other metals present in water, lead (Pb) has no significance in all forms of life and is toxic even at low concentrations. Despite several reviews on Pb toxicity, the remediation of Pb ions [Pb(II)] from water systems is scarce and understudied. This project aimed to design a novel *in vitro* Pb-nanobiosorbent utilizing a bacterial metallo-chaperone protein PbrD derived from *Cupriavidus metallidurans* CH34. Genetic engineering and molecular techniques were applied to obtain a purified refolded PbrD fusion protein (rPbrD) from *E. coli*; the first for the prokaryotic Pb metallo-chaperone. Western blot and peptide sequencing confirmed the identity of the recombinant rPbrD. Bioinformatics and circular dichroism spectra of rPbrD indicated an arrangement of α-helices, antiparallel β-sheets (Trx-tag), turns and loops which was significantly altered in the presence of Pb(II). Tryptophan fluorescence of rPbrD showed significant fluorophore quenching in the presence of Pb(II) suggesting intermolecular interactions with an appropriately folded rPbrD protein. The refolded fusion protein was cross-linked to calcium alginate nanoparticles (rPbrD-CANPs) for its intended use as a biosorbent. Scanning and transmission electron microscopy (SEM, TEM) coupled with energy dispersive X-ray spectroscopy (EDS), dynamic light scattering (DLS) and zeta potential analysis revealed uniformly synthesized, mono-dispersed nanoparticles displaying a negative surface charge indicative of a stable colloidal system allowing interactions with Pb(II). Binding activity of rPbrD, rPbrD-CANPs and their respective controls were analyzed by quantifying metal uptake using inductively coupled plasma mass spectroscopy (ICP-MS). At the highest concentration of Pb tested (1 mg/L) rPbrD biosorbed 99.7 % at a rate of 64 µg/g. Additionally, surface cross-linked rPbrD-CANPs bisorbed 99.9 % of 100 mg/L Pb(II) at a rate of 8820 µg/g. The Pb binding ability by rPbrD and rPbrD-CANPS was indicative of its maintained functionality even at elevated concentrations of Pb(II). These results suggest that rPbrD-CANPs could be applied in the remediation of Pb-contaminated wastewater. As such, treated wastewater could be recycled for water use in an era where water scarcity is at the forefront of global threats.

Research Outputs

Patent

Kondiah, K., Franklyn, P., and Keshav, V. Process and device for removing lead from a liquid [Nation phase registration (SA, USA, Canada and Australia)] International publication number [WO 2017/051370 A1].

Publications and manuscripts forming part of PhD thesis

1. Keshav, V., and Kondiah, K., 2019. A South African perspective on the bioremediation of heavy metals in water polluted by acid mine drainage. *Mine water and Environment* (under review).
2. Keshav, V., Achilonu, I., Dirr, H.W. and Kondiah, K., 2019. Recombinant expression and purification of a functional bacterial metallo-chaperone PbrD-fusion construct as a potential biosorbent for Pb (II). *Protein Expression and Purification*, *158*, pp. 27–35. DOI: 10.1016/j.pep.2019.02.008
3. Keshav, V., Franklyn, P., and Kondiah, K., 2019 Recombinant fusion protein PbrD cross-linked to calcium alginate nanoparticles for Pb remediation. *American Chemical Society Omega* DOI: 10.1021/acsomega.9b01624

Conferences

1. 4th YWP-ZA Biennial Conference and 1st Africa-wide YWP Conference Pretoria, 16-18th Nov, 2015. *Poster presentation*. To investigate the function of a recombinant metallo-chaperone PbrD to capture soluble lead ions from wastewater. Keshav, V., and Kondiah, K.
2. Molecular Biosciences Research Thrust Postgraduate Research Day, University of the Witwatersrand, Johannesburg, 3rd Dec, 2015. *Oral presentation*. Recombinant synthesis of a bacterial metalloprotein: PbrD to capture soluble lead ions. Keshav, V., Dirr, H.W., Franklyn, P., and Kondiah, K.
3. 19th Biennial Congress - The South African Society for Microbiology Durban, 18-20th Jan, 2016. *Oral presentation*. Developing a bioremediation strategy for lead contaminated water using the metallo- chaperone PbrD. Keshav, V., Dirr, H.W., Franklyn, P., and Kondiah, K.
4. WISA 15-18th May, 2016 Biennial Conference and Exhibition, Durban, 2016. *Oral presentation*. Evaluate the use of a recombinant bacterial metallo-chaperone protein PbrD to capture soluble lead ions from heavy metal contaminated water. Keshav, V., Dirr, H.W., Franklyn, P., and Kondiah, K.

Acknowledgements

॥ अज्ञानतिमिरान्धस्य ज्ञानाञ्जनशालाकया चक्षुरुन्मीलितं येन तस्मै श्रीगुरवे नमः ॥

I would like to offer my sincere gratitude to:

- The Tiso foundation (Archibald Mafeje Scholarship 2015-2017) and National Research Foundation (Innovation Doctoral Scholarship 2016) for their generous financial support.

- Dr Kulsum Kondiah for her continuous support, encouragement, invaluable advice and excellent supervision throughout this project.

- Professor Heinrich Dirr for his co-supervision, valuable critique and recommendations on the biochemistry aspects of this project.

- Dr Paul Franklyn for his co-supervision and guidance on the chemistry aspects of this project.

- Dr Ikechukwu Achilonu for always willing to assist and guide me with his in depth knowledge in biochemistry.

- Dr. Nomvano Keto (Spectra Unit, UJ), Dr. Deran Reddy and Jacques Gerber (MMU, Wits), Dr. Caren Billing (Electrochemistry, Wits) and Professor Lisa Du Toit (Dept. of Pharmacy, Wits) for their effort in training me and granting me permission to use equipment required throughout this project.

- Wits Enterprise for their assistance with the legal and administrative work required in the patent process.

- Family and friends for their immense love and support throughout my academic endeavours.

Contents

List of Figures

List of Tables

List of Abbreviations

α	Alpha
β	Beta
ε	Polanyi potential
θ	Ellipticity
~	Approximately
®	Registered
µg	Microgram(s)
µg/dl	Micrograms per decilitre
µg/g	Microgram(s) per gram
µg/L	Microgram per litre
µg/mL	Microgram per millilitre
µL	Microliter(s)
µm	Micrometre(s)
µM	Micromolar
µmol/g	Micromolar per gram
aa	Amino acid
ACN	Acetonitrile
Al	Aluminium
AMD	Acid mine drainage
Amp	Ampicillin
As	Arsenic
ATP	Adenosine triphosphate
bp	Base pair(s)
C	Carbon
Ca	Calcium
CA	Calcium alginate
$CaCl_2$	Calcium chloride
CANPs	Calcium alginate nanoparticles
Cd	Cadmium
CD	Circular dichroism
cfu/µL	Colony-forming unit per microliter
Cl	Chloride
CMGI-1	Cupriavidus metallidurans genomic island 1
Co	Cobalt
CO_3	Carbonate
Conc	Concentration
COOH	Carboxylic acid
Cr	Chromium
Cu	Copper
CWs	Constructed wetlands
Cys	Cysteine
DLS	Dynamic light scattering
dNTPS	Deoxyribonucleotide triphosphate
D-R	Dubinin–Radushkevich
DTT	Dichlorodiphenyltrichloroethane
DWA	Department of water affairs
DWAF	Department of water affairs and forestry
EDS	Energy-dispersive X-ray spectroscopy
EDTA	Ethylenediaminetetraacetic acid
EPS	Extracellular polymeric substances
Fe	Iron
$Fe(OH)_3$	Ferric hydroxide

FeS_2	Ferrous disulfide (Pyrite)
$FeSO_4$	Ferrous sulfate
FPLC	Fast protein liquid chromatography
FT	Fusion tag
g	Gravity
G	α-L-gluronic acid
GE	Genetic engineering/engineered
h	Hour(s)
H_2SO_4	Sulfuric acid
HCl	Hydrochloric acid
Hg	Mercury
His•Tag®	Histidine tag
HM	Heavy metal(s)
HNO_3	Nitric acid
HPO_4^{2-}	Hydrogen phosphate
IAA	Iodoacetamide
IB	Inclusion body
ICP-MS	Inductively coupled plasma mass spectrometry
IF	Insoluble fraction
IMAC	Immobilize metal affinity chromatography
IPTG	Isopropyl β-D-1-thiogalactopyranoside
kDa	Kilodalton
kV	Kilovoltage
L	Litre
LB	Luria-Bertani
LC-MS/MS	Liquid chromatography mass spectrometry
M	Molar
Mg	Magnesium
mg/g	Milligram(s) per gram
mg/Kg	Milligram(s) per kilo
mg/L	Milligram(s) per litre
mg/mL	Milligram(s) per millilitre
Min	Minute(s)
mL/min	Millilitre(s) per minute
mM	Millimolar
Mn	Manganese
MT	Metallothionein
mV	Millivolts
MWCO	Molecular weight cut off
NaH_2PO_4	Monobasic sodium phosphate
NH_2	Amines
NH_3	Ammonia
NH_4HCO_3	Ammonium bicarbonate
Ni	Nickel
Ni-NTA	Nickel-nitrilotriacetic acid
nm	Nanometre(s)
nm/min	Nanometre(s) per minute
NPs	Nanoparticles
NPs	Nanoparticles
O	Oxygen
^oC	Degree Celsius
OD	Optical density
OH	Hydroxide
Pb	Lead
$Pb(NO_3)_2$	Lead nitrate
PBS	Phosphate buffered saline

PCR	Polymerase chain reaction
PDB	Protein data bank
PDI	Poly dispersity index
ppm	Parts per million
PRBs	Permeable reactive barriers
PVDF	Polyvinylidene difluoride
R^2	Regression line
RL	Separation factor
rPbrD	Refolded PbrD protein fused to an N- terminal Trx•Tag™, His•Tag® and S®Tag™
rpm	Revolutions per minute
s	Second(s)
S	Sulfur
S®Tag™	Peptide derived from pancreatic Ribonuclease A - tag
SA	Sodium alginate
SD	Standard deviation
SDS-PAGE	Sodium dodecyl sulfate polyacrylamide gel Electrophoresis
SEM	Scanning electron microscopy
SF	Soluble fraction
SO_4^{2-}	Sulfate
SRB	Sulfate reducing bacteria
T	Total cell protein
TEM	Transmission electron microscopy
Trp	Tryptophan
Trx	Thioredoxin
Trx•Tag™	Thioredoxin tag
™	Trademark
U	Units
U	Uranium
UniProt	Universal protein resource
Univ	University
UV-Vis	Ultraviolet-visual spectroscopy
v/v	Volume per volume
w/v	Weight per volume
WHO	World health organization
ZAR	South African rand(s)
Zn	Zinc

Chapter 1

Introduction

1.1 Background

The constant release of heavy metals (HMs) into the environment threatens all forms of life (Ayangbenro and Babalola, 2017) and is one of the most common and persistent pollutants found in freshwater systems around the globe (Fernández-Luqueñ *et al.,* 2013). Often, HMs such as arsenic (As), cadmium (Cd), chromium (Cr), cobalt (Co), lead (Pb), mercury (Hg), nickel (Ni), and zinc (Zn) are deposited into the environment through anthropogenic activities (Akpor and Muchie, 2010; Gavrilescu, 2004). Additionally, seepage from acid mine drainage (AMD), mine tailings, rock sediments may also be the contributing factors (Duruibe *et al.,* 2007). Once metals are released into the environment they seep into freshwater resources (rivers, dams, lakes, ponds), soil/plants (fruits and vegetables) and animals (milk, meat) increasing the risk to consumers (Rajaganapathy *et al.,* 2011). Due to the non-biodegradable nature, metals accumulate in living organisms and disrupt vital cellular functions leading to organ failure or even death (Jaishankar *et al.,* 2014; Järup, 2014). Additional problems encountered with the release of HMs are damage to water pipelines, ecological and geotechnical system and urban infrastructure (Report to the Inter- ministerial committee on AMD 2010) which further plummets the country's economy.

In South Africa, HM pollution mainly arises from extensive mining activities which begun over a century ago. Consequently, high concentrations of metals have already seeped into the environment and still continue to accumulate at present (Mhlongo and Amponsah-Dacosta, 2016). Due to the health hazards and financial burden associated with HM pollution, the government enforced strict regulations for mine owners to prevent the release of metals into the environment (Feris and Kotze, 2014). The first governance law in the mining sector was established as early as 1956 (Act 27, 1956) towards the protection of the environment (Wyatt, 2015). Since then considerable precautions have been practiced towards preventing the release of HMs in the environment, however vulnerabilities in the system still remain (Oelofse, 2008). The occurrence of Pb in

levels above the safe limit of 0.01 mg/L within South Africa's freshwater systems (Fatoki *et al.,* 2002; Nyirenda *et al.,* 2013; Olujimi *et al.,* 2015) is of public health concern as the metal has no biological significance and is toxic even in low concentrations (Jaishankar *et al.,* 2014). Considerable numbers of children who were monitored for blood Pb levels in South Africa had levels which exceed (>10 µg/dl) the safe limits described by international guidelines (Mathee *et al.,* 2004). However, children are not the only ones susceptible to Pb toxicity but also healthy individuals who are continuously exposed to the metal. Within the body Pb is distributed to the brain, liver, kidneys, organs, teeth and bones which affect the functioning of cardiovascular, renal, reproductive and central nervous systems (Brochin, 2008; Mason *et al.,* 2014). Therefore it is crucial to find a treatment solution to completely remove or at best reduce toxic metals from polluted water.

To date, both physiochemical (Barakat, 2011; Fu and Wang, 2011; Kurniawan *et al.,* 2006) and bioremediation (Lovely and Coates, 1997; Park *et al.,* 2010; Wu *et al.,* 2012) strategies have been developed and are continuously being improved for the recovery of metals from wastewater. However, bioremediation has been the preferred method as the system offers an eco-friendly, rapid and efficient approach of recovering HMs at a low process cost (Alluri *et al.,* 2007). Biological systems are usually sensitive to harsh environments leading to decreased function and require optimization for efficient remediation. Therefore, there is a continuous effort in exploring new bioremediation material and improving them for industrial application.

This study presents a novel approach to metal bioremediation by using a protein based biosorbent targeted to the uptake of Pb by way of a Pb specific metallo- chaperone. *Cupriavidus metallidurans* CH34 contains several metal resistance genes coded on two megaplasmids and chromosomal genomic islands conferring resistance to at least 20 HMs (Jarosławiecka and Piotrowska-Seget, 2014; Taghavi *et al.,* 1994). The pbr lead resistance operon *pbrUTRABCD* encodes for a number of proteins involved in the uptake, efflux and accumulation of Pb (Borremans *et al.,* 2001). Amongst the proteins that confer Pb resistance, PbrD (241 amino acid) is reported to function as a metallo-chaperone that binds and sequesters Pb(II) via the Cys-7X-Cys-Cys-7X-Cys-7X-His-14DX-Cys metal binding motif (Silver and Phung, 2009). The ability to bind and release Pb(II) was

the basis for selecting the protein as a suitable biosorbent. Additionally, PbrD protein has no homologues (Taghavi *et al.,* 2009) and has not yet been studied *in vitro* further contributing to the novelty of this study.

1.2 Problem Statement

South Africa is a water scarce country. An increase in environmental pollution particularly AMD, population growth and climate change has resulted in a shortage of clean water supply (DWA, 2012). It is estimated that over 70 % of the water used in South Africa comes from freshwater resources (Ochieng *et al.,* 2012) which is polluted with HMs owing largely to AMD. In order to limit the overflow of AMD in freshwater resources openings of abandoned mines are either capped or sealed. Alternatively, AMD water is treated with lime and sulfides followed by an ion-exchange procedure to precipitate metals (Akpor and Muchie, 2010). However, there is a large amount of sludge produced post-treatment which is often dumped into landfills allowing metals to re-enter into the environment via soil. Additionally, ion-exchange is not efficient in removing low concentrations of metals from large volumes of water (Fu and Wang, 2011) and thus traces of soluble metal still remain in the treated water. Other strategies developed in South Africa to treat large volume water are based on either active (physicochemical) or passive (wetlands) treatments (Akcil and Koldas, 2006; Ochieng *et al.,* 2012) which are further discussed in chapter 2. The main problem associated with HM treatment is the variable composition and oxidation form of metals that differ based on their geological locations (Yao *et al.,* 2014). Therefore, a single chemical treatment is not efficient to precipitate all metals present in the effluent. The continuous addition of chemicals in treatment plants has safety concerns, increases the process cost, and produces secondary waste (Fu and Wang, 2011). Although, the utilization of biological material is more plausible than physicochemical treatments some problems encountered with microbial bioremediation include the requirements to maintain physiological parameters during biosorbent growth and the impracticality of applying live or dead microbes in water (Abbas *et al.,* 2014; Akpor and Muchie, 2010). Recently, the use of metallo-proteins engineered onto bacterial strains has been realised as an alternative and efficient treatment to recover toxic metals (Bondarenko *et al.,* 2008; Liu et *al., 2011*; Valls *et al.,* 2000). However, introduction of genetic engineered (GE) bacteria has environmental concerns, particularly the transfer of genetic material to other organisms, and therefore its application is limited.

To overcome some of the disadvantages of using GE bacteria an alternative strategy of utilizing the protein itself as a biosorbent was assessed in this study. Additionally, to address the concerns of the elevated levels of Pb in freshwater systems, a recombinant

Pb specific metallo-chaperone PbrD originating from *Cupriavidus metallidurans* CH34 was chosen as a biosorbent for this study.

1.3 Research Aim and Objectives

1.3.1 Aim

The aim of the study was to overexpress and immobilize a functional PbrD protein for binding of soluble Pb ions under controlled laboratory conditions.

1.3.2 Main Objectives

The purpose of this research was to develop a Pb specific biosorbent that is eco- friendly, sensitive and efficient for recovering both low and high concentrations of Pb(II) from wastewaters. The ability of PbrD metallo-chaperone to bind- accumulate-release the metal ions was exploited as an innovation for Pb bioremediation. For this, the main objectives of the study were:

- To overexpress and purify recombinant PbrD from an *Escherichia coli* expression system (Chapter 3).
- To evaluate the structural and functional characterization of recombinant PbrD protein using circular dichroism and tryptophan fluorescence (Chapter 3).
- To verify the Pb binding function of recombinant PbrD protein using inductively couple plasma mass spectroscopy (Chapter 3).
- To immobilize the recombinant PbrD protein by entrapment in calcium alginate nanoparticles (Chapter 4).
- To evaluate the structural characterization of rPbrD-CANPs nanobiosorbent using scanning and transmission electron microscopy coupled with energy dispersive X-ray spectroscopy, dynamic light scattering and zeta potential (Chapter 4).
- To verify the Pb binding function of the immobilized PbrD protein using inductively couple plasma mass spectroscopy (Chapter 4).

1.4 Chapter Outline

The thesis is structured as follows:

Chapter 1

This chapter provides an overview of the research background and further discusses the problem statement leading to the study aim and the specific objectives.

Chapter 2

This chapter was submitted as a review paper to the Mine water and Environment (2019) and is currently under review. The manuscript entails a comprehensive review of the literature associated with acid mine drainage and heavy metal pollution in South Africa with emphasis on Pb as a pollutant. The manuscript further discusses the drawbacks of current remediation systems in South Africa and paves the way forward by suggesting the synthesis of an environmental friendly, cost-effective immobilized biosorbent that is sustainable and efficient for recovering high concentrations of toxic metal ions from South African wastewater systems.

Chapter 3

This chapter was submitted as a research paper to Protein Expression and Purification and is available online (DOI: 10.1016/j.pep.2019.02.008). The paper presents the recombinant synthesis of PbrD and evaluates the structural and functional characterization of the recombinant metallo-fusion protein through biochemical procedures. Results from the Pb(II) binding ability together with the adsorption isotherm calculations assumes the potential of the biologically functional metallo-fusion protein for future application in the development of a biosorbent for remediation of Pb(II) from wastewater.

Chapter 4

This chapter was submitted as a research paper to ACS Omega (2019) and is available online (DOI: 10.1021/acsomega.9b01624). The paper presents the synthesis, characterization and evaluation of calcium alginate nanoparticles and surface cross-linked rPbrD-CANPs as a potential nanobiosorbent for the remediation of Pb(II). Results from the characterization, Pb(II) binding ability and the adsorption isotherm calculation show the potential for further optimization of the nanobiosorbent for future integration into membrane filters for water treatment within households and their scale-up into existing water treatment plants.

Chapter 5

This chapter draws conclusions to the overall research study and discusses the cost, advantages and drawbacks of the developed nanobiosorbent. Additionally, recommendations for future work entailing cost reduction, method validation and environmental application is also discussed.

1.5 References

1. Abbas, S.H., Ismail, I.M., Mostafa, T.M. and Sulaymon, A.H., 2014. Biosorption of

heavy metals: a review. *Journal of Chemical Science and Technology*, *3*(4), pp.74-102.

2. Akcil, A. and Koldas, S., 2006. Acid mine drainage (AMD): causes, treatment and case studies. *Journal of Cleaner Production*, *14*(12-13), pp.1139-1145. https://doi.org/10.1016/j.jclepro.2004.09.006
3. Akpor, O.B. and Muchie, M., 2010. Remediation of heavy metals in drinking water and wastewater treatment systems: Processes and applications. *International Journal of Physical Sciences*, *5*(12), pp.1807- 1817.
4. Alluri, H.K., Ronda, S.R., Settalluri, V.S., Bondili, J.S., Suryanarayana, V. and Venkateshwar, P., 2007. Biosorption: An eco-friendly alternative for heavy metal removal. *African Journal of Biotechnology*, *6*(25).
5. Ayangbenro, A. and Babalola, O., 2017. A new strategy for heavy metal polluted environments: a review of microbial biosorbents. *International Journal of Environmental Research and Public Health*, *14*(1), p.94. https://doi.org/10.3390/ijerph14010094
6. Barakat, M.A., 2011. New trends in removing heavy metals from industrial wastewater. *Arabian Journal of Chemistry*, *4*(4), pp.361-377. https://doi.org/10.1016/j.arabjc.2010.07.019
7. Bondarenko, O., Rõlova, T., Kahru, A. and Ivask, A., 2008. Bioavailability of Cd, Zn and Hg in soil to nine recombinant luminescent metal sensor bacteria. *Sensors*, *8*(11), pp.6899-6923. https://doi.org/10.3390/s8116899
8. Borremans, B., Hobman, J.L., Provoost, A., Brown, N.L. and van Der Lelie, D., 2001. Cloning and functional analysis of the pbr lead resistance determinant of *Ralstonia metallidurans* CH34. *Journal of Bacteriology*, *183*(19), pp.5651-5658. https://doi.org/10.1128/JB.183.19.5651-5658.2001
9. Brochin, R., Leone, S., Phillips, D., Shepard, N., Zisa, D. and Angerio, A., 2008. The cellular effect of lead poisoning and its clinical picture. *Issues*, *5*(2).
10. Duruibe, J.O., Ogwuegbu, M.O.C. and Egwurugwu, J.N., 2007. Heavy metal pollution and human biotoxic effects. *International Journal of physical sciences*, *2*(5), pp.112-118.
11. DWA, Department of Water Affairs., 2012. The annual national state of water resource report October 2011 to September 2012. Accessed online from http://www.dwa.gov.za/groundwater/documents/2011-12%20Annual%20National%20State%20of%20Water%20Resources%20report.pdf
12. Fatoki, O.S., Lujiza, N. and Ogunfowokan, A.O., 2002. Trace metal pollution in Umtata River. *Water SA*, *28*(2), pp.183-190.

https://doi.org/10.4314/wsa.v28i2.5160

13. Feris, L. and Kotze, L.J., 2014. The regulation of acid mine drainage in South Africa: law and governance perspectives. *Potchefstroom Electronic Law Journal*, *17*(5), pp.2104-2163.
14. Fernández-Luqueñ, F., López-Valdez, F., Gamero-Melo, P., Luna-Suárez, S., Aguilera-González, E.N., Martínez, A.I., García-Guillermo, M.D.S., Hernández-Martínez, G., Herrera-Mendoza, R., Álvarez-Garza, M.A. and Pérez-Velázquez, I.R., 2013. Heavy metal pollution in drinking water-a global risk for human health: A review. *African Journal of Environmental Science and Technology*, *7*(7), pp.567-584.
15. Fu, F. and Wang, Q., 2011. Removal of heavy metal ions from wastewaters: a review. *Journal of Environmental Management*, *92*(3), pp.407-418.

    https://doi.org/10.1016/j.jenvman.2010.11.011
16. Gavrilescu, M., 2004. Removal of heavy metals from the environment by biosorption. *Engineering in Life Sciences*, *4*(3), pp.219-232.

    https://doi.org/10.1002/elsc.200420026
17. Jaishankar, M., Tseten, T., Anbalagan, N., Mathew, B.B. and Beeregowda, K.N., 2014. Toxicity, mechanism and health effects of some heavy metals. *Interdisciplinary Toxicology*, *7*(2), pp.60-72.
    https://doi.org/10.2478/intox-2014-0009
18. Jarosławiecka, A. and Piotrowska-Seget, Z., 2014. Lead resistance in micro-organisms. *Microbiology*, *160*(1), pp.12-25.
    https://doi.org/10.1099/mic.0.070284-0
19. Järup, L., 2003. Hazards of heavy metal contamination. *British Medical Bulletin*, *68*(1), pp.167-182.
    https://doi.org/10.1093/bmb/ldg032
20. Kurniawan, T.A., Chan, G.Y., Lo, W.H. and Babel, S., 2006. Physico– chemical treatment techniques for wastewater laden with heavy metals. *Chemical Engineering Journal*, *118*(1-2), pp.83-98.

    https://doi.org/10.1016/j.cej.2006.01.015
21. Liu, S., Zhang, F., Chen, J. and Sun, G.X., 2011. Arsenic removal from contaminated soil via biovolatilization by genetically engineered bacteria under laboratory conditions. *Journal of Environmental Sciences* (China). *23*, pp. 1544-50.
22. Lovley, D.R. and Coates, J.D., 1997. Bioremediation of metal contamination. *Current Opinion in Biotechnology*, *8*(3), pp.285-289.
    https://doi.org/10.1016/S0958-1669(97)80005-5

23. Mason, L.H., Harp, J.P. and Han, D.Y., 2014. Pb neurotoxicity: neuropsychological effects of lead toxicity. *Biomed Research International*, *2014*, pp.1-8. https://doi.org/10.1155/2014/840547
24. Mathee, A., von Schirnding, Y., Montgomery, M. and Röllin, H., 2004. Lead poisoning in South African children: the hazard is at home. *Reviews on Environmental Health*, *19*(3-4), pp.347-361.
25. Mhlongo, S.E. and Amponsah-Dacosta, F., 2016. A review of problems and solutions of abandoned mines in South Africa. *International Journal of Mining, Reclamation and Environment*, *30*(4), pp.279-294. https://doi.org/10.1080/17480930.2015.1044046
26. Nyirenda, M., Ramoabi, T.E., Dzoma, B.M. and Motsei, L.E., 2013. A comparative study of the levels of heavy metals in dam water, borehole water and cattle serum around the Modimola dam of the Mafikeng, North West province, South Africa. *Life*, *10*(1), pp.3096-3100.
27. Ochieng, G.M., Seanego, E.S. and Nkwonta, O.I., 2010. Impacts of mining on water resources in South Africa: A review. *Scientific Research and Essays*, *5*(22), pp.3351-3357.
28. Oelofse, S.H., 2009. Mine water pollution-acid mine decant, effluent and treatment: a consideration of key emerging issues that may impact the state of the environment. The Icfai University Press.
29. Olujimi, O.O., Fatoki, O.S., Odendaal, J.P. and Oputu, O.U., 2015. Variability in heavy metal levels in river water receiving effluents in Cape Town, South Africa. *In Research and Practices in Water Quality*. InTech, pp.193-211. https://doi.org/10.5772/59077
30. Park, D., Yun, Y.S. and Park, J.M., 2010. The past, present, and future trends of biosorption. *Biotechnology and Bioprocess Engineering*, *15*(1), pp.86-102. https://doi.org/10.1007/s12257-009-0199-4
31. Rajaganapathy, V., Xavier, F., Sreekumar, D. and Mandal, P.K., 2011. Heavy metal contamination in soil, water and fodder and their presence in livestock and products: a review. *Journal of Environmental Science and Technology*, *4*(3), pp.234-249. https://doi.org/10.3923/jest.2011.234.249
32. Report to the Inter-Ministerial committee on acid mine drainage (2010) Mine water management in the Witwatersrand Gold Fields with special emphasis on acid mine drainage. Pretoria: Department of Water Affairs. Accessed online

from http://www.dmr.gov.za/Portals/0/Resource%20Center/Reports%20and%20Other%20Documents/2010_Report_Interministerial%20Committee_Acid%20Mine%20Drainage.pdf?ver=2018-03-13-020432-273 [Accessed 18 June 2018]

33. Silver, S. and Phung, L.T., 2009. Heavy metals, bacterial resistance. *Environmental Microbiology and Ecology*, pp. 220-227. https://doi.org/10.1016/B978-012373944-5.00267-4

34. Taghavi, S., Lesaulnier, C., Monchy, S., Wattiez, R., Mergeay, M. and van der Lelie, D., 2009. Lead (II) resistance in *Cupriavidus metallidurans* CH34: interplay between plasmid and chromosomally-located functions. *Antonie Van Leeuwenhoek*, 96(2), p.171. https://doi.org/10.1007/s10482-008-9289-0

35. Taghavi, S., Van der Lelie, D. and Mergeay, M., 1994. Electroporation of *Alcaligenes eutrophus* with (mega) plasmids and genomic DNA fragments. *Applied and Environmental Microbiology*, *60*(10), pp.3585- 3591.

36. Valls, M., Atrian, S., de Lorenzo, V. and Fernández, L.A., 2000. Engineering a mouse metallothionein on the cell surface of *Ralstonia eutropha* CH34 for immobilization of heavy metals in soil. *Nature Biotechnology*, *18*(6), p.661. https://doi.org/10.1038/76516

37. Wu, Y., Li, T. and Yang, L., 2012. Mechanisms of removing pollutants from aqueous solutions by microorganisms and their aggregates: a review. *Bioresource Technology*, *107*, pp.10-18. https://doi.org/10.1016/j.biortech.2011.12.088

38. Wyatt, A., 2015. Report on the implementation evaluation of the effectiveness of environmental governance in the mining sector. Accessed online from https://www.environment.gov.za/sites/default/files/reports/report_environmentalgovernance_miningsector.pdf [Accessed 16 March 2018].

39. Yao, H., Qian, X., Gao, H., Wang, Y. and Xia, B., 2014. Seasonal and spatial variations of heavy metals in two typical Chinese rivers: concentrations, environmental risks, and possible sources. *International Journal of Environmental Research and Public Health*, *11*(11), pp.11860- 11878. https://doi.org/10.3390/ijerph111111860

Chapter 2

A South African perspective on the bioremediation of heavy metals in water polluted by acid mine drainage

Keshav, V and Kondiah, K.

Revised manuscript submitted (2019) to *Mine, Water and Environment* (under review).

This review presents an overview on the (1) source, formation and composition of acid mine drainage and heavy metal pollution in South Africa, and further provide details on (2) the current physiochemical and biological treatments, with their advantages and drawbacks. Thereafter there is a core focus on the (3) occurrence of lead (Pb) ions, its toxic effects on human health and introduce a novel concept of proposal for recovering Pb ions using metal resistance proteins.

Author contributions: Vidya Keshav and Dr Kulsum Kondiah contributed towards the conceptualization of this manuscript. Vidya Keshav further contributed towards data curation, writing of initial drafts and revisions of manuscript. Dr Kulsum Kondiah contributed towards student supervision, editing and proof reading of the manuscript.

A South African Perspective on the Bioremediation of Heavy Metals in Water Polluted by Acid Mine Drainage

Keshav, V[1] and Kondiah, K[2*]

[1]School of Molecular and Cell Biology, University of Witwatersrand, Private bag 3, Wits 2050, Johannesburg, South Africa
[2*]Department of Biotechnology and Food Technology, University of Johannesburg, P.O. Box 17011, Doornfontein 2028, Johannesburg, South Africa, Tel:+27 11 5596102, kulsumk@uj.ac.za

Abstract

Metal pollution in the environment and the exploration for plausible treatment solutions is at the forefront of environmental studies mainly due to the toxicity arising from the ingestion of metals and the financial burden to treat freshwater resources. In South Africa, mining activities not only largely contribute to the country's economy but also constitute one of the primary sources for heavy metal (HM) pollution of the environment. In order to maintain a steady growth in mining activities as well as sustain drinking water quality there is an increasing demand to develop an efficient and eco-friendly remediation strategy for removal of toxic metals from water. The purpose of this review is to provide an overview on acid mine drainage (AMD) as a source of HM pollution of water in South Africa, and discuss promising bioremediation strategies thereof with a focus on bacterial based biosorbents. This review further describes a novel bioremediation strategy, using lead (Pb) as an example, for the removal of metals from water using a genetically engineered protein based biosorbent which can be immobilized onto biodegradable calcium alginate nanoparticles for environmental applications.

Key words: Acid mine drainage, bioremediation, heavy metals, lead (Pb), nanoparticles, protein-based biosorbents

Introduction

South Africa's rich legacy of mineral resources has and continues to extensively contribute to the country's economy. However, excessive mining operations, negligence and mismanagement by mine owners, improper discharge of mine tailings into landfills and the termination of underground mine water extraction from abandoned mines has resulted in the production of acid mine drainage (AMD) (Mhlongo and Amponsah-Dacosta 2016). AMD is formed by the oxidation of mineral pyrite (FeS_2) (McCarthy 2011) whereby the release of H^+ is responsible for the acidic conditions characteristic of AMD and subsequent solubilization of heavy metals (HMs) present in the AMD.

The types of mineral ores commonly found in South African mines vary according to their geographical distribution. Subsequently the overall quality of AMD and its impact on the environment is dependent on

the climate and degree of distribution. For example, the Witwatersrand basin contains large amounts of gold and coal tailings which are deposited mainly around the Vaal and Olifant river catchment. These regions are reported to receive high levels of rainfall which oxidizes the exposed pyrite subsequently contaminating the Vaal and Olifant rivers with AMD (McCarthy 2011) containing elevated concentrations of lead (Pb), copper (Cu), nickel (Ni), cobalt (Co), zinc (Zn) and uranium (U), amongst others (Durand 2012; Humphries et al. 2017). The Vaal River System meets the water resource needs of 60% of the national economy and serves approximately 45% of South Africa's population (Van Wyk et al. 2010). It supplies water to Eskom's power stations for electricity production, Sasol petro-chemical plants in Free State, North-west, Mpumalanga Highveld and Kimberly for petrol, Sappi for paper production and Iscor near Vanderbijlpark for iron and steel products (Van Wyk et al. 2010). It is also a raw water source for several informal settlements alongside the river bank**.** The persistent pollution of such river systems with AMD is therefore of major concern to both urban (industries) and rural (public health) regions.

In South Africa, the communities that reside in informal settlements around acid mine polluted water sources use untreated water for domestic and subsistence/homestead farming while their domestic animals consume the untreated water and graze on contaminated plants. Thus HMs enter the food chain either directly or indirectly via the consumption of contaminated water, plants, meat or animal by-products (Ali et al. 2019; Nyirenda et al. 2013; Rajaganapathy et al. 2011). Metal exposure is not only limited to these communities but may also affect the urban population when they consume contaminated home-grown fruits and vegetables irrigated with such water and sold as a source of income by local traders (Bvenura and Afolayan 2012). While certain HMs are required at low concentrations for normal metabolic activities, at elevated levels they disrupt vital cellular mechanisms leading to organ failure, or carcinogenesis in humans (Ali et al. 2019; Järup 2014; Tchounwou et al. 2014). Several case studies in South Africa have documented the impact of such exposure to HMs (Ali 2010; Bvenura and Afolayan 2012, Masika and Mafu 2004; Olujimi et al. 2015).

The impact of AMD in South Africa has been reviewed extensively (McCarthy, 2011; Mhlongo and Amponsah-Dacosta 2016; Naidoo, 2017; Ochieng et al. 2010). However, the treatment of AMD and HM pollution are often reported separately (Feng, 2000; Masindi et al. 2018) with a core focus on physicochemical and wetland strategies. The purpose of this review is to provide a summary of the current strategies for the removal of HMs from AMD with a specific focus on biological treatment. Thus far, biological based biosorbents (discussed below) offer an ecofriendly alternative to chemical treatments. However, these technologies rarely get commercialized due to variations in remediation efficiencies when applied under harsh environmental conditions and an increase in treatment cost due to the requirement for immobilization (Fosso-Kankeu and Mulaba-Bafubiandi 2014). Hence, the search for an "ideal" biosorbent

product is still a continuing process around the globe with very few commercialized to date. In this review, we further describe the concept of developing protein based targeted biosorbents for potential use in wastewater treatment using Pb as a specific example. Lead is the most important toxic element in the environment (Ali et al. 2019; Wani et al. 2015). While it may not be the most dominant metal found in AMD in South Africa, it is frequently reported in freshwater systems (Jooste et al. 2015; Malan et al. 2015; Nyirenda et al. 2013); one of the sources of its exposure in majority of the African countries being mining activities (WHO 2014). Moreover, China has listed Pb as one of the four highest priority metal pollutants in its five year plan for comprehensive prevention and control of HM pollution (Fu et al. 2017) further confirming its significance as a hazardous pollutant. Despite several papers that discuss the health hazards of Pb exposure (Hess et al. 2013; Mathee et al. 2017; Röllin et al. 2017) the remediation of Pb ions from water systems in developing countries like South Africa is understudied.

Remediation of HMs in AMD

A number of anthropogenic activities shown in Fig. 1 are known to add to the metal load in the environment resulting in metal pollution. In South Africa, mining activities form a key contributor to such HM pollution due to limited efficiency in their removal from large volumes of AMD using current physicochemical treatment strategies. Trace concentrations of HMs do not present a visible change in colour or distinctive smell thereby resulting in their unknown consumption either directly or indirectly with detrimental health impacts. It is therefore imperative to completely remove or substantially reduce the concentration of HMs in wastewaters like AMD prior to their discharge into the environment.

Short-term management of AMD in South Africa involves first capping or sealing openings in abandoned mines to prevent the overflow of toxic water. In the event of AMD overflow, the acidic pH of the contaminated water is neutralized with either limestone, sulfides, soda ash or CO_2 bubbling to neutralize the acidic pH and precipitate HMs (Masindi et al. 2017, 2018) followed by ion-exchange for HM removal. In the case of alkaline mine drainage found in some coal mines, neutralization is not required and metals (predominantly iron (Fe)) are precipitated by chemical oxidation or as sulfides. In addition to these solutions, long term goals to prevent, treat and/or limit decant of AMD water and subsequent HM pollution in South Africa were proposed in an Inter-ministerial committee (IMC) report (2010) and are briefly summarized in Table 1. An overview of the strengths and weaknesses of remediation strategies currently developed and/or implemented to treat AMD is provided hereafter with a distinct focus on the removal of HMs.

Current Physicochemical Strategies for AMD Remediation

The varying composition of AMD makes it almost impossible to utilize a single technique for its treatment.

The quality of discharged effluent can range from acidic to neutral pH which may contain high or low concentrations of sulfate and variable forms of HMs (McCarthy 2011). Hence, treatment of AMD focuses on neutralizing the acidic pH and precipitating the metals. Table 2 lists the different active and passive technologies developed over time in South Africa used in the treatment of AMD. These technologies are inherently based on the three most common physicochemical processes used to remediate metals from water in general: chemical precipitation, reverse osmosis and ion exchange. Other neutralization agents such as magnesite and bentonite clay are currently under investigation for their application in AMD pretreatment. However, existing neutralization agents such as lime and caustic soda perform better (Masindi et al. 2017)

Chemical precipitation is versatile and can be used to treat large volumes of water (Masindi et al. 2017), but there are several limitations that should be considered during AMD treatment. These include the need for further coagulation/flocculation of tiny metal flocs, the generation of large volumes of toxic sludge that require disposal and the dissolution of one metal when adjusting the pH to precipitate another. Ion exchange and reverse osmosis are also limited due to selective removal of pollutants, poor performance when large volumes are treated and energy requirements (Masindi et al. 2017). Overall, active treatment is not sensitive or efficient enough to remediate minute concentrations of metals from large volumes of water (Fu and Wang 2011). The continuous addition of chemicals in treatment plants significantly adds to the cost and safety concerns. The large quantities of toxic sludge or waste produced post treatment is often dumped into open pits or landfills, thereby re-contaminating the environment (Fu and Wang 2011). Additionally, these methods require employing skilled personnel to design and operate the plant. Thus owing to high operational cost and the final quality of treated water which still contains sulfates and metals, the active treatment process is considered unsuitable for treating large volumes of AMD water.

Conversely, passive treatment based on the construction of wetlands (CWs), or open pits/ landfills, diversion of wells or filtering the discharged effluent through permeable reactive barriers (PRBs) (Ochieng et al. 2010; Shabalala 2013; Sheridan et al. 2013) requires low maintenance and has a low operational cost. Since the passive system relies on the natural process of using plants and bacteria to take up metals, it is not always efficient to remediate high concentrations of sulfates and metals as environmental conditions are not controlled. This is different to the use of biosorbents (discussed further) where the optimal conditions for maximal uptake of metals are provided externally in a controlled manner. Other limitations of passive systems include: the availability of land to construct the wetlands, the accumulation of solid residue within the CW plants, seasonal variations may affect the functionality of the plants and therefore the remediation performance cannot be predicted.

The limitations experienced with physicochemical treatment of AMD drives the search for new/innovative

strategies that can either supplement existing treatments or be applied as an alternative treatment to remediate HMs from such wastewater. The treatment strategy should preferably have a low operational cost, high efficiency and specificity to remediate high and low concentrations of HMs, allow the regeneration of the sorbent and be able to recover metal ions post sorption to minimize secondary pollution.

Bioremediation of AMD by Bacteria

Bioremediation utilizes microorganisms that can bind, accumulate and/or detoxify metal ions into a less toxic form (Gadd and Griffiths 1978). It is regarded as an attractive alternative to physicochemical processes for AMD treatment due to its innovative, cost effective and environmentally friendly characteristics (Singh et al. 2011; Vieira and Volesky 2000). Contrary to the toxic effects of AMD contaminated water or soil on most living organisms, a unique world of microbial life consisting of algae, bacteria, fungi and yeast was discovered to thrive in these extreme conditions (Panda et al. 2016). This intrigued many scientists to investigate the ability of such microorganisms to survive and therefore remediate toxic metal ions in a reproducible manner. The use of bacteria over other microorganisms is preferable due to their ubiquity, increased metal adsorbent capacities, resistant to various environmental conditions, their high surface-to-volume ratios (size) and a high content of chemisorption sites in their cell walls (Fosso-Kankeu and Mulaba-Bafubiandi 2014). For the purpose of this review, a core focus on bacterial based biosorbents is specified for the remediation of HMs from AMD.

The application of sulfate-reducing bacteria (SRB) has been suggested as an alternative treatment for AMD (Ayangbenro et al. 2018; Panda et al. 2016). In the presence of organic compounds (as a carbon source) and anaerobic conditions, SRBs convert sulfates into hydrogen sulfide which reacts with dissolved divalent metal ions to form insoluble sulfides. The organic compounds are converted to carbonate thereby increasing the alkalinity of treated effluent (Fu and Wang 2011). Using SRB in sulfidogenic bioreactors to treat AMD offers several advantages over passive systems with regard to more predictable performance and control, selectivity of heavy metals and lowered sulfate concentrations in processed water (Panda et al. 2016). However, their application in metal remediation is limited due (1) to the unpredictable function of SRBs under low pH and high metal concentrations, (2) requires continuous supply of biomass, and (3) the requirement for alkaline material and organic substrate increase the process cost (Ayangbenro et al. 2018; Panda et al. 2016).

Other bacterial strains capable of metal biosorption are considered for bioremediation of HMs in AMD. Table 3 lists some bacterial species that have been recommended for bioremediation of common toxic metals but is in no way exhaustive.

Bacteria interact with metals in the environment by a number of mechanisms; some of which can be

exploited for bioremediation of toxic metal ions as seen in Fig. 2. Different bacteria require a different range of optimum parameters such as pH, temperature, nutritional content etc. in which to function efficiently. Nonetheless once the optimum conditions are achieved, they make attractive sorbents for bioremediation of metal ions.

Natural bacterial biosorbents

The biological uptake of metal ions by bacteria can occur via a passive mechanism known as biosorption which can further be enhanced actively through bioaccumulation. Biosorption is metabolically independent as it involves the physicochemical interaction between the metal ions and functional groups on the surface of the bacterial cell (Perpetuo et al. 2011) without the need for cellular energy. Functional groups involved in the biosorption process include carbonyl, carboxyl, hydroxyl, phosphoric, phenolic, sulfhydryl and sulfonate, which are present in bacterial cell walls and extracellular polymeric substances (EPS) (Vieira and Volesky 2000). The interaction of the metal ions with these groups results in their physical adsorption, ion-exchange, complexation, coordination, electrostatic interaction, chelation and/or precipitation (Atkinson et al. 1998; Fu and Wang 2011). Additional interactions with cell wall components such as peptidoglycan layer, teichoic and/or teichuronic acids (Gram positive bacteria) and phospholipids and lipopolysaccharides (Gram negative bacteria) also play a role in biosorption capacity (Fosso-Kankeu and Mulaba-Bafubiandi 2014).

Further uptake of metal ions can occur in living cells through bioaccumulation enabling remediation of higher concentrations of metals as they use both extra and intracellular mechanisms to bind metal ions (Gadd and Griffiths 1978). Bioaccumulation occurs through one of two mechanisms. A chemiosmotic gradient facilitates the rapid and non-specific transportation of extracellular metal inside the cell without the need for energy (ATP). However, since there is no control/limit of the type and concentration of the metals that can move across the cell wall, intracellular accumulation of these metals often leads to cell death (Spain 2003). On the other hand, energy driven efflux pumps enable the slower intracellular accumulation of metal ions circumventing metal toxicity due to accumulation. Intracellular metal ions can further be remediated by enzymatic detoxification, intracellular sequestration and/or enhanced siderophores production (Naik and Dubey 2013).

The choice of biosorbent plays a vital role in biosorption capacity owing to factors such as the number of binding sites in the biosorbent, the accessibility and availability of these sites, the chemical configuration of the site and affinity and binding strength between metal ion and site (Vieira and Volesky 2000; Wu et al. 2012). The rate of metal uptake is also dependent on the structural difference and oxidation potential of each metal ion that interacts with the biosorbent together with external factors such as pH, temperature,

biomass concentration and the presence of other metal ions (Abbas et al. 2014). A detailed summary on the biosorption of different HMs and their rates of uptake by various bacterial species can be found in Kanamarlapudi et al. (2018) and Shamim (2018).

The advantages and disadvantages of metal bioremediation over physicochemical treatment are summarized as follows (Akpor and Muchie 2010; Wu et al. 2012):

Advantages of bioremediation:

1. Moderate capital investment compared to physicochemical treatment.
2. Highly specific to different metal ions allowing targeted treatment of AMD depending on its composition.
3. Environmentally friendly as it does not produce toxic sludge waste post treatment.
4. Faster and higher concentration of metal ions are remediated compared to physicochemical process.
5. Can be applied *ex situ* or *in situ*.
6. Some bacteria can detoxify metals making them biologically unavailable thus limiting contamination to other living organisms.

Disadvantages of bioremediation:

1. Bioremediation capacity is dependent on the availability of suitable growth conditions i.e. the process requires the continuous monitoring of pH, temperature, nutritional and dissolved oxygen levels.
2. If bioremediation is to be performed on site, recovery of dead cells will increase the process time whereas use of live cells may negatively increase the pollution in water bodies.
3. Even though a number of studies have shown impressive bioremediation capacities at bench-scale, commercialization of this system is hindered due to lack of reproducibility in remediation efficiency (quantity) due to complex mixtures present in the environment such as organic and inorganic chemicals, radionuclides and other HMs present in the environment.
4. Seasonal variations may affect the bioremediation capacity when used *in situ*.
5. Although development of the bioremediation process is simple, industrial implementation of this strategy requires skilled personnel to design a feasible system that can efficiently treat contaminated water on a large scale per day (megalitres).

These limitations can be circumvented to some extent with the immobilization of the biosorbent onto a

solid biopolymeric or polymeric matrix. By immobilizing the biosorbent, its performance is improved due to increased capacity, improved mechanical strength and resistance to chemicals (Kanamarlapudi et al. 2018). Additionally, the biomass with bound metal ions can be easily separated from the AMD thereby enabling non-destructive recovery and eradicating any safety concerns. The immobilization material itself may also enhance the metal binding capacity (Atkinson et al. 1998). When natural polymers such as alginate, cellulose, chitosan etc. are used as the immobilization support, the system is entirely biodegradable preventing secondary pollution. These benefits improve the overall efficiency of bioremediation of HMs and increase the sustainability of the system as the biosorbent is recovered for reuse and the metal ions can be recycled back to industry.

The biosorption process can further be improvised by genetic engineering of the bacterial strains to enhance the metal remediation specificity and capacity and to increase their resistance to ambient conditions (Vijayaraghavan and Yun 2008) especially given the harsh conditions characteristic of AMD. Recent advances in the field of molecular biology have enabled the understanding of the interaction between metal ions and bacteria and the genetic mechanisms involved in metal resistance. Currently, several kinds of cysteine-rich peptides and proteins such as metallothioneins (MTs) (Bae et al. 2001; Pazirandeh et al. 1998; Perpetuo et al. 2011; Valls et al. 2000) have been synthesized to bind and sequester metal ions to biologically inactive forms. The use of genetically engineered (GE) MTs in bioremediation has resulted in an increase in specificity, affinity and biosorptive capacities, making this a promising technology for the development of bacterium-based biosorbents (Pazirandeh et al. 1998) that could be used in the treatment of AMD.

GE bacterial biosorbents

De novo design of incorporating metal resistance genes in bacterial cells to introduce/enhance the remediation capacity and specificity of bacterial based biosorbents has recently been studied. Thus far a number of bacterial strains have been genetically engineered with (1) metal uptake regulator genes to enhance the bioaccumulative properties, (2) metal chelators and (3) metal transporter genes to confer the cell with detoxification and efflux mechanism, (4) metallo-chaperone genes involved in maintaining cell homeostasis as well as with (5) genes that enhances the survival of the bacterial strain in biotic or abiotic stressed conditions (Singh et al. 2011). A few examples of GE bacterial strains that were transformed with genes involved in metal resistance for Cd, Hg, Ni, Cr, and Zn and As are described in Table 4.

Although construction of GE bacterial biosorbents is at the forefront of innovation in the field of bioremediation, several concerns with regard to their environmental application have been raised. Herewith is a summary of the advantages and disadvantages of GE bacterial biosorbents (Perpetuo et al. 2011; Singh et al. 2011).

Advantages of GE bacterial biosorbents:

1. Molecular biology tools enable the chemical synthesis of specific metal resistance genes and allows for sequence adaptation of genes and/or metabolic pathways to enhance the biosorbent properties.
2. Capable of reducing the bioavailability of pollutants by altering its chemical form/oxidation state.
3. Enhancement of the monitoring, yield control and efficiency of process.
4. Allows specific metal remediation from a consortium of metals and complex compounds.
5. The technique offers low operational cost and high efficiency.
6. Provided the GE biosorbent is immobilized onto a solid matrix for recovery post treatment, the technique is eco-friendly in nature.

Disadvantages of GE bacterial biosorbents:

1. The unpredictability of GE bacteria to retain the inserted genetic material (recombinant vector, anchored genes, etc.) in a stable manner raises environmental concerns.
2. Transfer of genetic material to indigenous organisms when applied to treat metal pollution in the environment.
3. Competition of GE bacteria with natural microorganisms for nutrients and other resources within the environment.

In practice, the following may affect the large scale production of GE biosorbent: Poor growth of the host, inclusion body (IB) formation, protein inactivity, and even not obtaining any protein at all.

The Occurrence of Pb in South African Water Systems

Access to clean drinking water is essential to all living organisms however, in South Africa two-thirds of the population depends entirely upon groundwater (which is frequently reported to be contaminated by AMD and other industrial effluent) for drinking (Edokpayi et al. 2018). High concentrations of Pb have been detected in South Africa's river systems (discussed below) and thus people who consume/utilize the untreated water are at risk of Pb poisoning (and other HMs). In order to improve the access of rural communities to safe drinking water, a cost effective and practical remediation process needs to be implemented in order to treat wastewater effluent prior to its release into the environment. Alternatively, a treatment strategy at the point of use may also be of value to communities who reside in informal settlements in close proximity to freshwater sources.

Lead (Pb) Pollution, Toxicity and Remediation

Pb is a mutagenic and teratogenic element that naturally persists in the environment and bioaccumulates in all living entities (Naik and Dubey 2013). Upon exposure, Pb intoxication affects several vital functions in the human body with the most severe effect on the central nervous system (CNS), liver, kidneys, circulatory, reproductive and cardiovascular system, which may lead to coma and death (Järup 2014; Mathee et al. 2017). Pb enters into the blood-brain barrier and blocks the N-methyl-D-aspartate receptor which causes permanent brain damage (Järup 2014). Additionally, it also affects the cellular and genetic material by replacing Ca(II) which is the most abundant and vital metal required for cell regulation. Intracellularly, Pb binds to calmodulin which alters the protein conformational structure, resulting in either activation or inactivation of other vital proteins required for cellular processes such as further activating enzymes, altering membrane permeability, promoting synthesis of certain proteins, stimulating or inhibiting metabolic pathways, and initiating secretion of hormones and other substances (Brochin et al. 2008).

Pb may also enter soil and water via industrial waste produced from the manufacturing of batteries, paint, cosmetics, automobile products etc. or alternatively through AMD (Abbas et al. 2014, WHO 2014). A case study reported by Naicker et al. (2013) showed elevated concentrations of Pb ions (average of four seasonal variations) in ground (0.484 ppm), surface (0.573 ppm) and seepage (1.170 ppm) water located within the Witwatersrand region (mining district) in Johannesburg, South Africa. Similarly, Humphries et al. (2017) reported 60 ppm of Pb in a wetland that receives water from mining, industrial or sewage effluent and 311 mg/kg Pb was found in soil samples polluted with mine tailings in South Africa (Titshall et al. 2013). High concentrations of HMs are often diluted downstream when discharged into streams, lakes and dams within the area. However, in South Africa, certain studies have reported Pb concentrations exceeding the safe limit of 0.01 mg/L Pb as stipulated by the Department of Water Affairs and Forestry (DWAF 1996) in freshwater resources. These range from 0.004-0.087 mg/L in Western Cape (Olujimi et al. 2015), 0.24-1.11 mg/L in the Eastern Cape (Fatoki et al. 2002) and 0.02-0.03 mg/L in Limpopo (Edokpayi et al. 2018). Thus, exposure to Pb continues to be a major public health problem and its removal from wastewaters is of utmost importance. Pb-containing wastewater is commonly treated by physicochemical means before release into the environment. However, too often treatment is ineffective resulting in higher than acceptable concentrations being discharged into soil and water.

Despite the concerns of Pb in drinking water only few GE bacteria have been developed to specifically remediate Pb ions from wastewater. A Pb binding peptide ThrAsnThrLeuSerAsnAsn was anchored onto the surface of *E. coli* Top 10 cells and was reported to biosorb 240 µmol/g cell of Pb(II) in solution (Nguyen et al. 2013). In a separate study by Maruthamuthu et al. (2015) an ompC-lead binding peptide was expressed on the cell surface of the same bacterial strain which was then reported to biosorb 427

µmol/g cell of Pb(II) present in wastewater. However, as previously discussed there are several concerns around the use of GE based biosorbents. To address some of these concerns, it may be worthwhile pursuing an alternative strategy to develop GE protein based biosorbents.

Using a GE protein based biosorbent may circumvent the use of live bacterial cells which have the ability to transfer genetic material to other native microorganisms present in the environment to be treated. Furthermore, the proteins incorporated into the biosorbent can be selected to target specific metal ions based on their binding preferences. While there are several bacterial proteins such as smtA and zraP that are able to bind Pb, they prefer to bind Zn^{2+} because their main function is to transport essential metals such as Zn^{2+} to maintain cell homeostasis. Therefore, targeted removal of Pb would require the development of a biosorbent with a protein that exhibits high specificity for the metal. Such proteins have been found in the bacterium *Cupriavidus metallidurans* CH34 which serves as a model organism to understand the genetic pathways underlying Pb resistance in bacteria.

Pb Resistance in *C. metallidurans* CH34

C. metallidurans CH34 (formerly *Ralstonia metallidurans* and *Alcaligenes eutrophus*) is resistant to 20 HMs (Taghavi et al. 1994), but is the only bacterial species reported to date to have a dedicated operon to Pb resistance. Serving as a model organism, it was discovered that full resistance to Pb ions is due to the combined function of several genes located on both plasmid and chromosomal DNA (Taghavi et al. 1994). The first defense mechanism to Pb ions is through the transcription of *pbrUTRABCD* operon located on the pMOL30 plasmid (Jarosławiecka and Piotrowska-Seget, 2014). In the event of the cell undergoing a mutation in the plasmid resistance genes or if the cell loses the entire plasmid due to environmental stressed conditions, the second line defense mechanism transcribes resistance genes encoded on *pbrR2 cadA pbrC2* operon located on CMG-1 (genomic island) on chromosome 1 (Taghavi et al. 2009) .

When Pb ions are present in the surrounding environment, they may be transported across the cell membrane into the cytoplasm by PbrT (a protein that consists of a cytochrome domain and transmembrane metal transport domain) (Borremans et al. 2001). The Pb ions then signal the regulator protein PbrR to bind to the promoter/operator (P/O) region to initiate transcription of the Pb dependent *pbrUTRABCD* operon (shown in Fig. 3). Upon intracellular accumulation of Pb ions they either bind directly to an integral membrane protein PbrB or to the cysteine rich metallo-chaperone protein PbrD. PbrB coordinates with the prolipoprotein signal peptidase PbrC to detoxify the Pb ions into an insoluble form, thus preventing their re-entry into the cell (Taghavi et al. 2009). Additionally, Pb ions bound to PbrD are shuttled to PbrA (a P_{IB}-type ATPase transporter protein) and eventually transported into the

periplasm for detoxification by PbrB/C (Borremans et al. 2001).

In the event of a mutation occurring in the PbrT protein, PbrA may function in both influx (uptake) and efflux (discharge) of Pb ions. However, if a mutation in PbrA occurs, the cell relies on CadA and ZntA proteins for efflux of Pb ions (Jarosławiecka and Piotrowska-Seget 2014). Should the *pbrUTRABCD* operon become inactivated, the chromosomal encoded *pbrR2 cadA pbrC2* operon synergistically transcribes proteins to maintain the reduced concentrations of Pb ions within the cell (Taghavi et al. 2009). The $PbrC_2$ protein is known to compensate for deletions in the *pbrA* and *pbrD* genes (Taghavi et al. 2009).

PbrD as a protein based biosorbent

Inactivation of the *pbrD* gene has been associated with a decrease in the cytoplasmic accumulation of Pb ions (Taghavi et al. 2009). Since PbrD is a metallo-chaperone, it functions as a "temporary intracellular metal storage" that can bind-accumulate-release Pb but is not vital for conferring Pb resistance. However, it does protect the cell against an ineffectual cycle of Pb import and export (energy efficient). There are no homologs of PbrD (Taghavi et al. 2009) and thus far no other Pb-specific metallo-chaperone has been reported.

Due to its specificity for Pb and the ability to bind and release the metal ions, PbrD (or other metal specific metallo-chaperones) could be used in the development of protein biosorbents for the metal concerned. However, owing to the delicate nature of proteins, an immobilization support would be required to preserve its structure and functionality in any application, especially within the harsh conditions characteristic of AMD. The enhanced binding of metal ions usually offered by the support itself could also be of added benefit.

An example of such a support matrix is calcium alginate (CA) particles which are formed in a three dimensional network by binding divalent calcium ions to the α-L-guluronic acid (G) polymer of sodium alginate (SA), forming a cross linked gel. A high content of G polymers may form a stronger, firmer and more porous gel, making it ideal for the immobilization of DNA and proteins (Paques et al. 2014). Since SA is a natural polysaccharide derived from brown algae and bacteria, CA particles are biocompatible, biodegradable, low in cost and nontoxic to living organisms (Paques et al. 2014). Consequently they are sought after for environmental applications that could especially impact indirectly on human health. Subhashini et al. (2013) showed that SA beads were able to remediate 62.5 mg/g Pb ions at pH 7 and 35 ^{o}C reaching an equilibrium state within 16 hours. These findings support their use as a Pb biosorbent and the potential to treat and prevent heavy metal intoxications, further emphasizing their biocompatibility.

There are few studies documenting the stability of peptides (Xing et al. 2003) and proteins (Nesamony et

al. 2012; Wells and Sheardown 2007) immobilized in/on CA particles. This evidence and the ability of CA to adsorb Pb ions make it a favorable support matrix for PbrD. The development of an immobilized protein biosorbent using PbrD and CA particles further allows the recovery of the metal while enabling the regeneration of the system for reuse. Such a protein based biosorbent could be implemented in the targeted bioremediation of Pb from AMD and other industrial wastewaters with the added advantage of being able to recycle the metal back to industry.

Concluding Remarks

Decanting of AMD from abandoned mines began in South Africa as early as 2001 and still continues to overflow into natural water sources. Despite the recent changes made in the legislations, regulations and attitude towards the management of AMD, the ceaseless accumulation and circulation of metals of AMD origin in the environment will have a long-lasting impact on South Africa's freshwater systems. Although several improvements in treatment methods have been developed, the variation in AMD composition from different geographical locations poses a challenge to find a single, effective, all-in-one treatment strategy. In this regard, researchers have shifted focus to the development of hybrid treatment systems which combine physicochemical and biological processes to remove or reduce metal ion concentrations in water to within recommended safe limits. Natural bacterial biosorbents can be integrated into existing AMD treatment strategies where they not only increase the remediation efficiency of metals but also reduce the operational cost. Alternatively, bacterial whole cell or protein based biosorbents can be genetically engineered with the capability to target specific metal contaminants which may be used in synergy to treat AMD of varying composition without compromising the efficiency of metal uptake. For example, a biosorbent comprising a genetically engineered PbrD protein immobilized onto CA nanoparticles can be used in conjunction with sulfate reducing bacteria to remediate both Pb and sulfates, respectively, from AMD. While the increase in population, industrialization, climate change and the exploitation of water use have significantly exhausted the natural water resources, the irresponsible discharge of mine water contributes greatly to the pollution of the remaining freshwater available for use. Though the prevention of AMD formation at the source is more desirable in the protection of the environment and especially scarce freshwater resources, this is not possible. The continuous development of innovative technologies for the treatment and possible recycling of AMD contaminated water therefore offers a short-term solution to a worldwide problem. It is envisioned that with more stringent practices during and post mining operations, metal pollution of AMD origin will eventually decline in freshwater systems.

References

Abbas SH, Ismail IM, Mostafa TM, Sulaymon AH (2014) Biosorption of heavy metals: a review. J Chem Sci Technol 3:74-102

Akcil A, Koldas S (2006) Acid mine drainage (AMD): causes, treatment and case studies. J Clean Prod 14:1139-1145

Akpor OB, Muchie M (2010) Remediation of heavy metals in drinking water and wastewater treatment systems: Processes and applications. Int J Phys Sci 5:1807-1817

Ali YD (2010) Toxic elements in food chain: exposure pathways to infants in selected areas of Limpopo Province. PhD Diss, Univ of South Africa

Ali H, Khan E, Ilahi I (2019) Environmental chemistry and ecotoxicology of hazardous heavy metals: Environmental persistence, toxicity, and bioaccumulation. J Chem 2019: https://doi.org/10.1155/2019/6730305

Atkinson BW, Bux F, Kasan HC (1998) Considerations for application of biosorption technology to remediate metal-contaminated industrial effluents. Water SA 24:129-135

Ayangbenro AS, Olanrewaju OS, Babalola OO (2018) Sulfate-reducing bacteria as an effective tool for sustainable acid mine bioremediation. Front Microbiol 9:1986

Bae W, Mehra RK, Mulchandani A, Chen W (2001) Genetic engineering of *Escherichia coli* for enhanced uptake and bioaccumulation of mercury. Appl Environ Microbiol 67:5335-5338

Baldiris R, Acosta-Tapia N, Montes A, Hernández J, Vivas-Reyes R (2018) Reduction of hexavalent chromium and detection of chromate reductase (ChrR) in *Stenotrophomonas maltophilia*. Molecules 23:406

Bologo V, Maree JP, Carlsson F (2012) Application of magnesium hydroxide and barium hydroxide for the removal of metals and sulphate from mine water. Water SA 38:23-28

Bondarenko O, Rõlova T, Kahru A, Ivask A (2008) Bioavailability of Cd, Zn and Hg in soil to nine recombinant luminescent metal sensor bacteria. Sensors 8:6899-6923

Borremans B, Hobman JL, Provoost A, Brown NL, van Der Lelie D (2001) Cloning and functional analysis of the pbr lead resistance determinant of *Ralstonia metallidurans* CH34. J Bacteriol 183:5651-5658

Brochin R, Leone S, Phillips D, Shepard N, Zisa D, Angerio A (2008) The cellular effect of lead poisoning and its clinical picture. Issues 5:2

Bvenura C, Afolayan AJ (2012) Heavy metal contamination of vegetables cultivated in home gardens in the Eastern Cape. S Afr J Sci 108:1-6

Chellaiah ER (2018) Cadmium (heavy metals) bioremediation by *Pseudomonas aeruginosa*: a minireview. Appl Water Sci 8:154

Choi SB, Yun YS (2004) Lead biosorption by waste biomass of *Corynebacterium glutamicum* generated from lysine fermentation process. Biotechnol Lett 26:331-336

De Beer M, Maree JP, Wilsenach J, Motaung S, Bologo L, Radebe V (2010) Acid mine water reclamation using the ABC process. International Mine Water Association Symposium. Cape Brenton Univ, Sydney, Nova Scotia, Canada

Deng X, Li QB, Lu YH, He N, Jiang J (2005) Genetic engineering of *E. coli* SE5000 and its potential for Ni^{2+} bioremediation. Process Biochem 40:425-430

Dey U, Chatterjee S, Mondal NK (2016) Isolation and characterization of arsenic-resistant bacteria and possible application in bioremediation. Biotechnol Rep 10:1-7

Durand JF (2012) The impact of gold mining on the Witwatersrand on the rivers and karst system of Gauteng and North West Province, South Africa. J Afr Earth Sci 68:24-43

DWAF (1996). South African water quality guidelines. Department of Water Affairs and Forestry, Pretoria. http://www.dwa.gov.za/Groundwater/documents/Pol_saWQguideFRESHDomesticusevol1.pdf Accessed 2019-04-16

Edokpayi JN, Enitan AM, Mutileni N, Odiyo JO (2018) Evaluation of water quality and human risk assessment due to heavy metals in groundwater around Muledane area of Vhembe District, Limpopo Province, South Africa. Chem Cent J 12:2

Fatoki OS, Lujiza N, Ogunfowokan AO (2002) Trace metal pollution in Umtata River. Water SA 28:183-190

Feng D, Aldrich C, Tan H (2000) Treatment of acid mine water by use of heavy metal precipitation and ion exchange. Miner Eng 13:623-642

Fosso-Kankeu E, Mulaba-Bafubiandi AF (2014) Review of challenges in the escalation of metal-biosorbing processes for wastewater treatment: applied and commercialized technologies. Afr J Biotechnol 13:17

Fu F, Wang Q (2011) Removal of heavy metal ions from wastewaters: a review. J Environ Manage 92:407-418

Fu Z, Guo W, Dang Z, Hu Q, Wu F, Feng C, Zhao X, Meng W, Xing B, Giesy JP (2017) Refocusing on nonpriority toxic metals in the aquatic environment in China. Environ Sci Technol 51:3117-3118

Gadd GM, Griffiths AJ (1978) Microorganisms and heavy metal toxicity. Microb Ecol 4:303-317

Ginisty P, Besnainou B, Sahut C, Guezennec J (1998) Biosorption of cobalt by *Pseudomonas halodentrificans*: influence of cell wall treatment by alkali and alkaline-earth metals and ion-exchange mechanisms. Biotechnol Lett 20:1035-1039

Giri AK, Patel RK, Mishra PC (2012) Biosorption of As (V) from aqueous solutions by living cells of *Bacillus cereus.* Water Sci Technol 66:1699-1707

Hess CA, Cooper MJ, Smith MJ, Trueman CN, Schutkowski H (2013) Lead exposure in adult males in urban Transvaal Province, South Africa during the apartheid era. PloS One 8:e58146

Howard D, Grobler C, Robinson REG, Cole PM (2009) Sustainable purification of mine water using ion exchange technology. In International Mine Water Conference pp. 447-453

Humphries MS, McCarthy TS, Pillay L (2017) Attenuation of pollution arising from acid mine drainage by a natural wetland on the Witwatersrand. S Afr J Sci 113:1-9

Jarosławiecka A, Piotrowska-Seget Z (2014) Lead resistance in micro-organisms. Microbiology 160:12-25

Järup L (2003) Hazards of heavy metal contamination. Brit Med Bull 68:167-182

Jooste A, Marra SM, Addo-Bediakoa A, Luus-Powella WJ (2015) Metal bioaccumulation in the fish of the Olifants River, Limpopo province, South Africa, and the associated human health risk: a case study of rednose labeo *Labeo rosae* from two impoundments. Afr J Aquat Sci 39:271-277

Kalita D, Joshi SR (2017) Study on bioremediation of lead by exopolysaccharide producing metallophilic bacterium isolated from extreme habitat. Biotechnol Rep 16:48-57

Kanamarlapudi SLRK, Chintalpudi VK, Muddada S (2018) Application of biosorption for removal of heavy metals from wastewater. In: Biosorption, IntechOpen http://dx.doi.org/10.5772/intechopen.77315

Kotwal DR, Shewale NB, Tambat US, Thakare MJ, Bholay AD (2018) Bioremediation of mercury using mercury resistant bacteria. Res J Life Sci, Bioinformat, Pharm and Chem Sci 4:145

Kumar M, Kumar V, Varma A, Prasad R, Sharma AK, Pal A, Arshi A, Singh J (2016) An efficient approach towards the bioremediation of copper, cobalt and nickel contaminated field samples. J Soil Sediment 16:2118-2127

Loukidou MX, Karapantsios TD, Zouboulis AI, Matis KA (2005) Cadmium (II) Biosorption by *Aeromonas caviae*: kinetic modeling. Sep Sci Technol 40:1293-1311

Malan M, Müller F, Cyster L, Raitt L, Aalbers J (2015) Heavy metals in the irrigation water, soils and vegetables in the Philippi horticultural area in the Western Cape Province of South Africa. Environ Monit Assess 187:4085

Maruthamuthu KM, Ganesh I, Ravikumar S, Hong SH (2015) Evaluation of *zraP* gene expression characteristics and construction of a lead (Pb) sensing and removal system in a recombinant *Escherichia coli*. Biotechnol Lett 37:659-664

Masika PJ, Mafu JV (2004) Aspects of goat farming in the communal farming systems of the central Eastern Cape, South Africa. Small Ruminant Res 52:161-164

Masindi V, Akinwekomi V, Maree JP, Muedi KL (2017) Comparison of mine water neutralisation efficiencies of different alkaline generating agents. J Environ Chem Eng 5:3903-3913

Masindi V, Chatzisymeon E, Kortidis I, Foteinis S (2018) Assessing the sustainability of acid mine drainage (AMD) treatment in South Africa. Sci Total Environ 635:793-802

Mathee A, De Jager P, Naidoo S, Naicker N (2017) Lead poisoning in shooting-range workers in Gauteng Province, South Africa: Two case studies. SAMJ: S Afr Med J 107:302-303

McCarthy TS (2011) The impact of acid mine drainage in South Africa. S Afr J Sci 107:01-07

Mhlongo SE, Amponsah-Dacosta F (2016) A review of problems and solutions of abandoned mines in South Africa. Int J Min, Reclam Env 30:279-294

Mutiat F-BY, Gbolahan B, Olu O (2018) A comparative study of the wild and mutated heavy metal resistant *Klebsiella variicola* generated for cadmium bioremediation. Bioremediat J 22:28-42

Naicker K., Cukrowska E, McCarthy TS (2003) Acid mine drainage arising from gold mining activity in Johannesburg, South Africa and environs. Environ Pollut 122:29-4

Naidoo S (2017) Acid mine drainage in South Africa. SpringerBriefs in Environmental Science. Springer, Cham. DOI https://doi.org/10.1007/978-3-319-44435-2_1.

Naik MM, Dubey SK (2013) Lead resistant bacteria: lead resistance mechanisms, their applications in lead bioremediation and biomonitoring. Ecotox Environ Safe 98:1-7

Nesamony J, Singh PR, Nada SE, Shah ZA, Kolling WM (2012) Calcium alginate nanoparticles synthesized through a novel interfacial cross-linking method as a potential protein drug delivery system. J Pharm Sci 101:2177-2184

Nguyen TT, Lee HR, Hong SH, Jang JR, Choe WS, Yoo IK (2013) Selective lead adsorption by recombinant *Escherichia coli* displaying a lead-binding peptide. Appl Biochem Biotechnol 169:1188-1196

Nyirenda M, Ramoabi TE, Dzoma BM, Motsei LE (2013) A comparative study of the levels of heavy metals in dam water, borehole water and cattle serum around the Modimola dam of the Mafikeng, North West province, South Africa. Life 10:1

Ochieng GM, Seanego ES, Nkwonta OI (2010) Impacts of mining on water resources in South Africa: a review. Sci Res Essays 5:3351-3357

Olujimi OO, Fatoki OS, Odendaal JP, Oputu OU (2015) Variability in heavy metal levels in river water receiving effluents in Cape Town, South Africa. In Research and Practices in Water Quality. InTech

Panda S, Mishra S, Akcil A (2016) Bioremediation of acidic mine effluents and the role of sulfidogenic biosystems: a mini-review. Euro-Mediterr J Environ Integr 1:8

Paques JP, Van der Linden E, Van Rijn CJ, Sagis LM (2014) Preparation methods of alginate nanoparticles. Adv Colloid Interfac 209:163-171

Pazirandeh M, Wells BM, Ryan RL (1998) Development of bacterium-based heavy metal biosorbents: enhanced uptake of cadmium and mercury by *Escherichia coli* expressing a metal binding motif. Appl Environ Microb 64:4068-4072

Peña-Montenegro TD, Lozano L, Dussán J (2015) Genome sequence and description of the mosquitocidal and heavy metal tolerant strain *Lysinibacillus sphaericus* CBAM5. Stand Genomic Sci 10:2

Perpetuo EA, Souza CB, Nascimento CAO (2011) Engineering bacteria for bioremediation. In: Progress in Molecular and Environmental Bioengineering-From Analysis and Modeling to Technology Applications. Intech Open Access Publisher, Rijeka, Croatia, pp 605–632

Prasad KS, Ramanathan AL, Paul J, Subramanian V, Prasad R (2013) Biosorption of arsenite (As^{+3}) and arsenate (As^{+5}) from aqueous solution by *Arthrobacter sp*. biomass. Environ Technol 34:2701-2708

Pulles W, Juby GJG, Busby RW (1992) Development of the slurry precipitation and recycle reverse osmosis (SPARRO) technology for desalinating scaling mine waters. Water Sci Technol 25:177-192

Rajaganapathy V, Xavier F, Sreekumar D, Mandal PK (2011) Heavy metal contamination in soil, water and fodder and their presence in livestock and products: a review. J Environ Sci Technol 4:234-249

Ray L, Paul S, Bera D, Chattopadhyay P (2006) Bioaccumulation of Pb (II) from aqueous solutions by *Bacillus cereus* M1 16. J Hazard Subst Res 5:1

Rehman A, Ali A, Muneer B, Shakoori AR (2007) Resistance and biosorption of mercury by bacteria isolated from industrial effluents. Pak J Zool 39:137

Report to the Inter-Ministerial committee on acid mine drainage (2010) Mine water management in the Witwatersrand Gold Fields with special emphasis on acid mine drainage. Pretoria: Department of Water Affairs. http://www.dmr.gov.za/Portals/0/Resource%20Center/Reports%20and%20Other%20Documents/2010_Report_Interministerial%20Committee_Acid%20Mine%20Drainage.pdf?ver=2018-03-13-020432-273

Röllin HB, Olutola B, Channa K, Odland JØ (2017) Reduction of in utero lead exposures in South African populations: Positive impact of unleaded petrol. PloS One 12:e0186445

Rose P (2013) Long-term sustainability in the management of acid mine drainage wastewaters–development of the Rhodes biosure process. Water SA 39:582-592

Şahin Y, Öztürk A (2005) Biosorption of chromium (VI) ions from aqueous solution by the bacterium *Bacillus thuringiensis*. Process Biochem 40:1895-1901

Seadira, TWP (2014) Treatment of acid mine drainage using constructed wetland and UV/TiO_2 photocatalysis. PhD Diss, Vaal Univ of Technology

Shabalala AN (2013) Assessment of locally available reactive materials for use in permeable reactive barriers (PRBs) in remediating acid mine drainage. Water SA 39:251-256

Shamim S (2018) Biosorption of heavy metals. In: Biosorption, IntechOpen, http://dx.doi.org/10.5772/intechopen.72099

Sheridan G, Harding K, Koller E, De Pretto A (2013) A comparison of charcoal-and slag-based constructed wetlands for acid mine drainage remediation. Water SA 39:369-374

Singh JS, Abhilash PC, Singh HB, Singh RP, Singh DP (2011) Genetically engineered bacteria: an emerging tool for environmental remediation and future research perspectives. Gene 480:1-9

Smit JP (1999) The purification of polluted mine water. Proceedings of the International Symposium on Mine Water & Environment for the 21st Century, Seville, Spain

Spain A (2003) Implications of microbial heavy metal tolerance in the environment. Rev Undergrad Res 2:1-6

Srivastava N, Jha M, Mall I, Singh D (2010) Application of genetic engineering for chromium removal from industrial wastewater. Int J Chem Biol Eng 4:633-638

Subhashini SS, Velan M, Kaliappan S (2013) Biosorption of lead by *Kluyveromyces marxianus* immobilized in alginate beads. J Environ Biol 34:831

Taghavi S, Van der Lelie D, Mergeay M (1994) Electroporation of *Alcaligenes eutrophus* with (mega) plasmids and genomic DNA fragments. Appl Environ Microbiol 60:3585-3591

Taghavi S, Lesaulnier C, Monchy S, Wattiez R, Mergeay M, Van der Lelie D (2009) Lead (II) resistance in *Cupriavidus metallidurans* CH34: interplay between plasmid and chromosomally-located functions. Anton Leeu 96:171

Tchounwou PB, Yedjou CG, Patlolla AK, Sutton DJ (2012) Heavy metal toxicity and the environment. In Molecular, Clinical and Environmental Toxicology, Springer, Basel, pp 133-164

Titshall LW, Hughes JC, Bester HC (2013). Characterisation of alkaline tailings from a lead/zinc mine in South Africa and evaluation of their revegetation potential using five indigenous grass species. S Afr J Plant Soil 30:97-105

Valls M, Atrian S, de Lorenzo V, Fernández LA (2000) Engineering a mouse metallothionein on the cell surface of *Ralstonia eutropha* CH34 for immobilization of heavy metals in soil. Nat Biotechnol 18:661

Van Wyk JJ, Rademeyer JI, Van Rooyen JA (2010) Position statement on the Vaal River system and acid mine drainage. Department of Water Affairs, Pretoria. http://www6.dwa.gov.za/AMDFSLTS/Documents/Vaal%20River%20System%20&%20AMD%20Version%203.pdf

Vieira RH, Volesky B (2000) Biosorption: a solution to pollution?. Int Microbiol 3:17-24

Vijayaraghavan K, Yun YS (2008) Bacterial biosorbents and biosorption. Biotechnol Adv 26:266-291

Villadangos AF1, Ordóñez E, Pedre B, Messens J, Gil JA, Mateos LM (2014) Engineered coryneform bacteria as a bio-tool for arsenic remediation. Appl Microbiol Biotechnol 98, 10143–10152

Wani AL, Ara A, Usmani JA (2015) Lead toxicity: a review. Interdiscip Toxicol 8:55–64

Wells LA, Sheardown H (2007) Extended release of high Pi proteins from alginate microspheres via a novel encapsulation technique. Eur J Pharm Biopharm 65:329-335

WHO (2014) Chemicals of public health concern in the African Region and their management - Regional Assessment Report, Republic of Congo. https://www.afro.who.int/sites/default/files/2017-06/9789290232810.pdf Accessed 2019-05-30

Wu Y, Li T, Yang L (2012) Mechanisms of removing pollutants from aqueous solutions by microorganisms and their aggregates: A Review. Bioresource Technol 107:10-18

Xing L, Dawei C, Liping X, Rongqing Z (2003) Oral colon-specific drug delivery for bee venom peptide: development of a coated calcium alginate gel beads-entrapped liposome. J Control Release 93:293-300

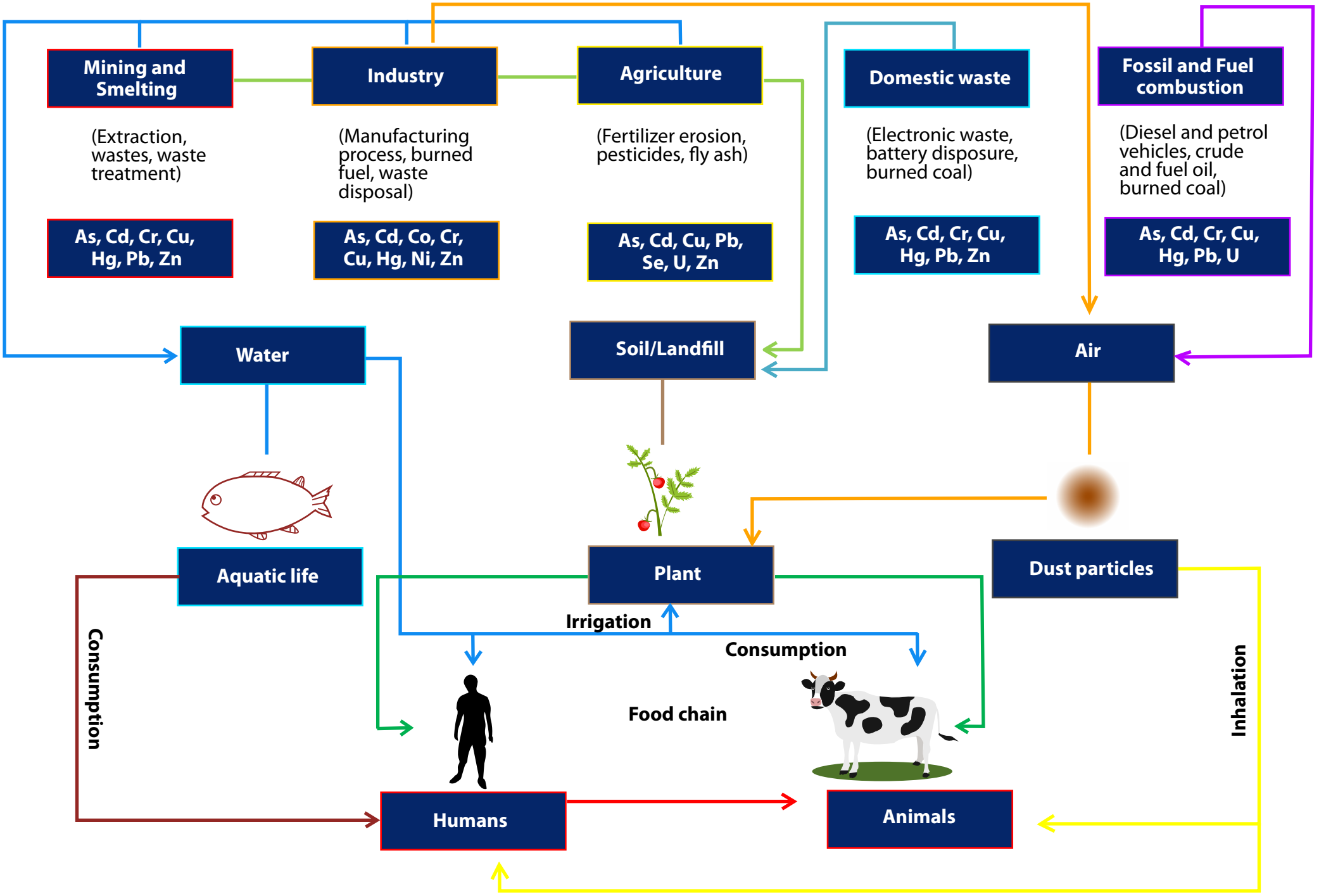
Mining and Smelting
Industry
Agriculture
Domestic waste
Fossil and Fuel combustion
(Extraction, wastes, waste treatment)
(Manufacturing process, burned fuel, waste disposal)
(Fertilizer erosion, pesticides, fly ash)
(Electronic waste, battery disposure, burned coal)
(Diesel and petrol vehicles, crude and fuel oil, burned coal)
As, Cd, Cr, Cu, Hg, Pb, Zn
As, Cd, Co, Cr, Cu, Hg, Ni, Zn
As, Cd, Cu, Pb, Se, U, Zn
As, Cd, Cr, Cu, Hg, Pb, Zn
As, Cd, Cr, Cu, Hg, Pb, U
Water
Soil/Landfill
Air
Aquatic life
Plant
Dust particles
Irrigation
Consumption
Consumption
Food chain
Inhalation
Humans
Animals

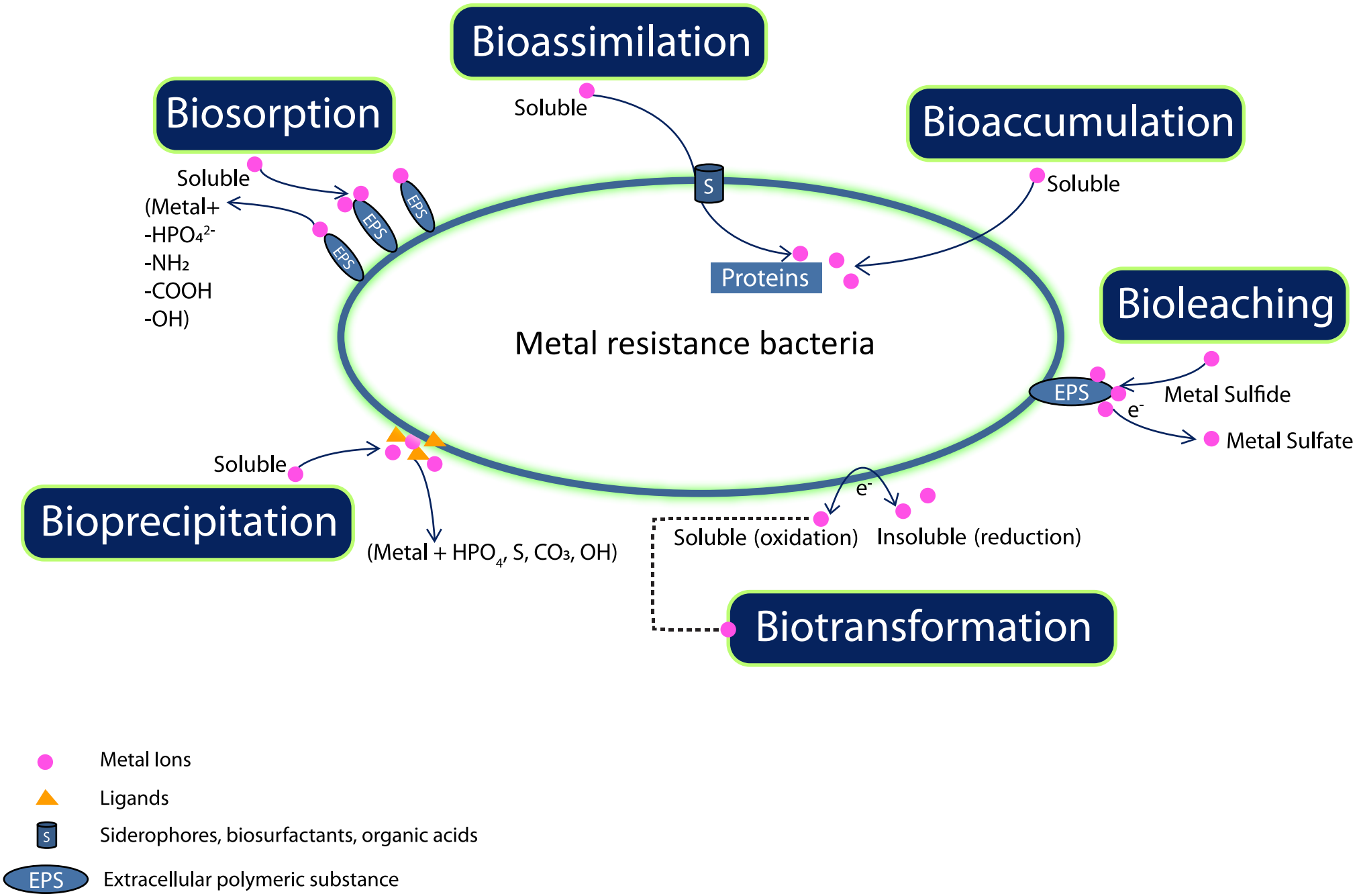
Bioassimilation
Soluble
S
Proteins
Biosorption
Soluble
(Metal+
-HPO4 2-
-NH2
-COOH
-OH)
EPS
EPS
EPS
Bioaccumulation
Soluble
Metal resistance bacteria
Bioleaching
EPS
Metal Sulfide
e-
Metal Sulfate
Soluble
Bioprecipitation
(Metal + HPO4, S, CO3, OH)
e-
Soluble (oxidation)
Insoluble (reduction)
Biotransformation
Metal Ions
Ligands
S
Siderophores, biosurfactants, organic acids
EPS
Extracellular polymeric substance

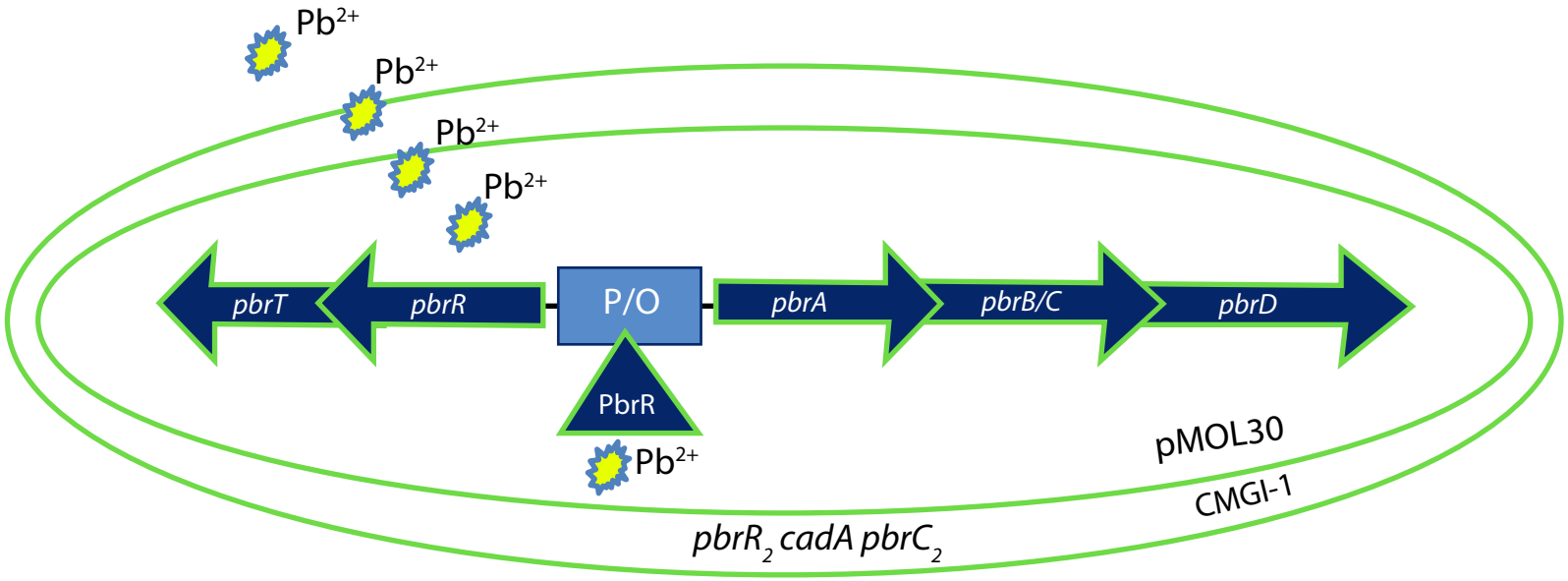
Pb2+
Pb2+
Pb2+
Pb2+
pbrT
pbrR
P/O
pbrA
pbrB/C
pbrD
PbrR
Pb2+
pMOL30
CMGI-1
pbrR2 cadA pbrC2

Table 1 Immediate and intermediate-long term goals formulated to prevent, treat and monitor AMD water in South Africa (IMC 2010)

	Proposed	Advantage	Disadvantage
Short term goals	Water must be pumped from Western, Central and Eastern basins below environmental critical levels	Prevent discharge of AMD into the environment	Pumping is costly
	Reduce the ingress of water in underground workings	Reduce the amount of AMD water to be pumped and treated, thereby reducing the cost in the long term	Could have high capital costs
	Treatment of pumped water to a suitable quality prior to its discharge into river systems	Neutralizing the pumped water will increase the pH, thereby reduce the iron and metal content	High salinity and facilities for sludge disposal required
Long term goals	Establish a multi-institutional monitoring committee Monitor mine, ground and surface waters, seismic activity, geotechnical impacts and mine residues	Monitoring AMD will highlight changes in the quality of water that may impact on future management strategies	The current monitoring systems are inadequate to assess the extent and degree of problems
	Investigating the implementation of an environmental levy by operating mines	Prevent AMD negligence by mine owners and recover cost of past mining activities	Higher levies could lead to increased unemployment of mine workers

Table 2 Summary of active and passive treatment processes developed to treat AMD water in South Africa

	Technique	Principle	Reference
Active Treatment	Slurry Precipitation and Recycle Reverse Osmosis (SPARRO)	Tubular reverse osmosis to desalinate $CaSO_4$ scaling	Pulles et al. 1992
	SAVMIN	Lime, H_2SO_4 and CO_2 precipitate SO_4^{2-}	Smit 1999
	Gypsum cation exchange (GYP-CIX) Process	Resin regenerated with H_2SO_4 and lime slurry binds Ca and SO_4^{2-}. The $CaSO_4$ is used as fertilizer	Akcil and Koldas 2006
	Ion exchange	Cation (HNO_3) and anion exchange (NH_3) bind U and SO_4^{2-}. The eluant is used as fertilizer	Howard et al. 2009
	Alkaline-Barium-Calcium (ABC)	ABC neutralizes pH, reduces SO_4^{2-} and metal load	de Beer et al. 2010
	Magnesium-Barium-Alkali (MBA)	MBA neutralizes pH, precipitates SO_4^{2-} and Mg	Bologo et al. 2012
	BioSURE Process	Sewage sludge binds acidic SO_4^{2-}	Rose 2013
Passive Treatment	Construction of Wetlands (CWs)	In house CWs amended with charcoal and basic oxygen furnace remove Fe, SO_4^{2-} from stimulated AMD water	Sheridan et al. 2013
	Permeable Reactive Barriers (PRBs)	Fly ash adsorbs or precipitates Fe, Mn, Mg and SO_4^{2-}	Shabalala 2013
	Construction of Wetlands (CWs)	Sand and clinoptilolite adsorb Fe, Cr, Mg, Ca, Be, Zn, Co, Ni, Mn and SO_4^{2-}	Seadira et al. 2014

Table 3 Examples of bacteria studied for bioremediation of HMs

Heavy metal/metalloid	Bacterial based biosorbents
Arsenic (As)	*Aneurinibacillus aneurinilyticus* (Dey et al. 2016), *Arthrobacter sp.* (Prasad et al. 2013), *Bacillus cereus* (Giri et al. 2012)
Cadmium (Cd)	*Aeromonas cavia* (Loukidou et al. 2004), *Pseudomonas aeruginosa* (Chellaiah, 2018), *Klebsiella variicola* (Mutiat et al. 2018)
Chromium (Cr)	*Bacillus thuringiensis* (Şahin and Öztürk 2005), *Stenotrophomonas maltophilia* (Baldiris et al. 2018)
Cobalt (Co)	*Lysinibacillus sphaericus* (Peña-Montenegro et al. 2015), *Proteus vulgaris* (Kumar et al. 2016), *Pseudomonas halodenitrificans* (Ginisty et al. 1998)
Lead (Pb)	*Bacillus cereus* (Ray et al. 2006), *Corynebacterium glutamicum* (Choi and Yun 2004), *Pseudomonas aeruginosa and Pseudomonas alcaligenes* (Kalita and Joshi 2017)
Mercury (Hg)	*Bacillus licheniformis* and *Pseudomonas aeruginosa* (Kotwal et al. 2018), *Brevibacterium casei* (Rehman et al. 2007)

Table 4 GE bacterial strains involved in metal remediation

Recombinant strain(s)	Gene (Protein)	Function	Reference
Pseudomonas fluorescens OS8, *Bacillus subtilis* BR151, *Staphylococcus aureus* RN4220	*cadR/cadA* (CadR-regulatory protein/CadA-transporting ATPase)	Transport of Cd, Pb, Hg and Zn	
Escherichia coli MC1061	*zntR/zntA* (ZntR-zinc regulatory protein/ZntA-translocating P-type ATPase)	Transport of Zn, Cd and Pb	Bondarenko et al. 2008
	merR/merB (MerR-regulatory protein/MerB-alkyl mercury lyase)	Detoxification of Hg by cleavage of the carbon-mercury bond	
Escherichia coli	*Mtb* (Mtb-mouse metallothionein)	Engineered onto the cell surface of *Ralstonia eutropha* CH34 for Cd resistance	Valls et al. 2000
Escherichia coli	*arsD* (ArsD)	Accumulation of inorganic As as As(V) or As(III)	Villadangos et al. 2014
Alcaligenes eutrophus	*chrBA* (Cr-regulator and transporter)	Reduction of Cr^{6+} to Cr^{3+}	Srivastava et al. 2010
Escherichia coli SE5000	*nixA* /MT (NixA-transporting protein/ Metallothionein)	Specific uptake and accumulation of Ni^{2+}	Deng et al. 2005

Chapter 3

Recombinant expression and purification of a functional bacterial metallo-chaperone PbrD-fusion construct as a potential biosorbent for Pb(II)

Keshav, V., Achilonu, I., Dirr, H.W and Kondiah, K.

Protein Expression and Purification, 2019 **DOI:** 10.1016/j.pep.2019.02.008

This paper describes the synthesis of recombinant rPbrD protein fused to an N-terminal the N-terminal Trx•Tag™, His•Tag® and S®Tag™ for biosorption of Pb(II) in solution. This is the first report displaying the *in vitro* synthesis of a Pb metallo-chaperone in *E. coli*. Functional assessment of rPbrD-fusion protein showed potential for the development of a biosorbent for remediation of Pb(II) from wastewater.

Author contributions: Vidya Keshav contributed towards all the experimental work, data analysis, data curation, writing of initial drafts and revisions of manuscript. Professor Heinrich Dirr contributed towards co-supervision and proof reading of manuscript. Dr Ikechukwu Achilonu contributed towards data interpretation. Dr Kulsum Kondiah contributed towards student supervision, data analysis, data editing and proof reading of the manuscript.

Protein Expression and Purification 158 (2019) 27–35

Contents lists available at ScienceDirect

Protein Expression and Purification

journal homepage: www.elsevier.com/locate/yprep

Recombinant expression and purification of a functional bacterial metallo-chaperone PbrD-fusion construct as a potential biosorbent for Pb(II)

Keshav V[a,*], Achilonu I[a], Dirr HW[a], Kondiah K[a,b]

[a] School of Molecular and Cell Biology, University of Witwatersrand, Private Bag 3, Wits, 2050, Johannesburg, South Africa
[b] Department of Biotechnology and Food Technology, University of Johannesburg, P.O. Box 17011, Doornfontein, 2028, Johannesburg, South Africa

ARTICLE INFO

Keywords:
Biosorption
Metallo-chaperone
Pb(II)
PbrD protein

ABSTRACT

PbrD is a lead (II) binding protein encoded by the *pbr* lead resistance operon found exclusively in *Cupriavidus metallidurans* CH34. Its ability to sequester Pb(II) shows potential for it to be developed as a biosorbent for Pb in the bioremediation of contaminated wastewaters. In this study the *pbrD* gene from *C. metallidurans* CH34 was transformed and overexpressed in *Escherichia coli* BL21 (DE3) using the pET32 Xa/Lic vector. Optimal expression of recombinant (r)PbrD (~50 kDa) was achieved post-induction with IPTG within inclusion bodies (IBs). Inclusion bodies were solubilised by denaturation and purified by Ni-NTA affinity chromatography. The purified denatured protein containing the N-terminal Trx•Tag™, His•Tag® and S®Tag™ was refolded *in vitro* via dialysis to a biologically functional form. Circular dichroism spectra of refolded rPbrD-fusion protein indicated a high degree of turns, β-sheets and 3_{10} helices content and tryptophan fluorescence showed a structural conformational change in the presence of Pb(II). Refolded rPbrD-fusion protein bound 99.7% of Pb(II) when mixed with lead nitrate in ten-fold increasing concentrations. Adsorption isotherms including Langmuir, Freundlich, Temkin and Dubinin-Radushkevich models were applied to determine the biosorption mechanism. A biologically functional rPbrD-fusion protein has potential application in the development of a biosorbent for remediation of Pb(II) from wastewater.

1. Introduction

Lead (Pb) exposure is responsible for 494 550 deaths annually in developing countries [1]. Environmental contamination by Pb waste particularly in low-income countries like South-East Asia and sub Saharan-Africa occurs due to mismanagement of mining and industrial effluent and the disposal of non-biodegradable electronic waste (McCarthy, 2011; [2,3]. A number of studies report that the levels of Pb (II) in surface and ground water of several areas in South Africa for example exceed the acceptable safe limit of < 0.01 mg/L in drinking water [4–9]. Although the concentration of Pb(II) is usually low in surface waters, over time they accumulate in the environment and pose various health risks to the communities who utilize the water without further purification [4]; Järup, 2014). The current chemical strategies applied to treat wastewaters are inefficient at removing minute concentrations of Pb(II). In addition the large-scale waste that is produced post chemical treatment is often dumped into landfills which re-contaminate the environment through soil pollution [10]. Bioremediation of heavy metals like Pb from contaminated water using predominantly bacterial biosorbents presents an attractive alternative to current chemical processes.

Moreover, the use of bacteria genetically engineered (GE) with metallothionein (MTs) or metallo-chaperones have been studied for the remediation of specific metal ions. Several studies describing the use of GE biosorbents for cadmium (Cd) [11–14], mercury (Hg) [13,15,16], arsenic (As) [17] and Nickel (Ni) [18] have been reported. Despite the concerns of Pb in drinking water the synthesis of GE bacteria for the remediation of Pb(II) is scarce. Nguyen and co-workers [19] synthesised a highly specific Pb binding peptide ThrAsnThrLeuSerAsnAsn anchored onto the surface of *Escherichia coli* Top 10 cells via the outer membrane protein C (OmpC) for the remediation of Pb(II). Their results showed a rapid biosorption (30 min) of > 80% (240 μmol/g cell) Pb(II) in solution. A dual functional *E. coli* strain which acts as a biosensor and biosorbent for Pb(II) was developed by Maruthamuthu and co-workers (2015). In the presence of environmental Pb(II) the GE strain emits fluorescence due to the expression of green fluorescent protein (GFP) under the control of the *zraP* promoter. Additionally, an ompC-lead binding peptide (that was cloned downstream of *gfp*) is expressed on the cell surface functioning as a metal binding motif for biosorption of Pb (II). Their results showed that the GE strain biosorbed 85.3%

* Corresponding author.
E-mail address: kulsumk@uj.ac.za (K. V).

https://doi.org/10.1016/j.pep.2019.02.008
Received 16 November 2018; Received in revised form 25 January 2019; Accepted 11 February 2019
Available online 15 February 2019

(427 μmol/g cell) of Pb(II) present in wastewater.

Using GE improved bacterial strains for the biosorption of Pb results in high yield recovery of metal ions at a low cost. However, their implementation is currently hindered due to the risk associated with the addition of live/dead transgenic bacterial cells into the environment. A plausible way to circumvent such implications is to use the metal binding protein itself as a biosorbent when immobilized on a suitable platform such as biodegradable matrices. Such an approach may further improve the remediation capacity, sensitivity, affinity, and specificity of the biosorbent. Here we report the overexpression and purification of an N-terminal fusion rPbrD, a metallo-chaperone for Pb found exclusively in *Cupriavidus metallidurans* CH34 [20] and its Pb binding capacity for future application as a protein based biosorbent.

2. Materials and methods

2.1. Strains, vectors, reagents and media

The pET32Xa/LIC cloning kit containing the expression vector pET32Xa/LIC and *E. coli* strain BL21 (DE3), pET32a vector and BugBuster™ Protein Extraction Reagent were purchased from Novagen (Madison, USA). The *pbrD* gene (GenBank accession number CP000354.2) from *C. metallidurans* CH34 was synthesised by Genscript (USA). High-fidelity DNA polymerase ExTaKaRa was purchased from Takara (Otsu, Japan). Wizard® SV Gel and PCR cleanup system and PureYield™ Plasmid Miniprep System were purchased from Promega (Madison, USA). Primer synthesis and DNA sequencing were performed by Inqaba Biotech (Pty) Ltd (Pretoria, South Africa). His-probe (H-3) monoclonal antibody was purchased from Santa Cruz Biotechnology (Dallas, USA). Goat anti-Mouse HRP antibody and Clarity™ ECL western blotting substrate were purchased from Bio-Rad (California, USA). Unless stated otherwise, all other chemicals and media were of analytical grade and purchased from Sigma-Aldrich (Missouri, USA).

2.2. Gene amplification and construction of the expression plasmid

The synthesised *pbrD* gene supplied in the vector pUC57 was used as a template (1 μg/mL) for PCR amplification. A 50 μL reaction mixture [1.25 U TaKaRa Ex Taq, 10X Ex Taq Buffer (5 μL), 0.2 mM of each dNTP, and 1 μM of each forward and reverse primer] was prepared according to the manufacturer's instructions. The forward primer PbrDpET32Xa/LICF1 5′- GGTATTGAGGGTCGCTTGGCAATTGAG-3′ and reverse primer PbrDpET32Xa/LICR1 5′-GGTATTGAGGGTCGCTTG GCAATTGAG-3′ were designed using PrimerQuest software (Integrated DNA Technologies Inc., USA) to enable ligation of the full length gene into pET32 Xa/LIC vector. PCR amplifications were performed in a Bio-Rad Mycycler™ (Bio-Rad) under the following conditions: 95 °C for 2 min (x1 cycle), 95 °C for 30 s, 62 °C for 30 s and 72 °C for 45 s (x35 cycles) and 72 °C for 7 min (x1 cycle). The amplified products were electrophoresed on a 1.5% (w/v) agarose gel pre-stained with GelRed™ solution (Biotium, USA) and visualised under the ChemiDoc™ MP imaging system (Bio-Rad) (Fig. S1). The amplified product was gel purified using the Wizard® SV Gel and PCR cleanup system according to the manufacturer's instructions without modification. The purity of the extracted product was assessed on a 1.5% agarose gel and quantified using the dsDNA broad range assay kit with the Qubit® 2.0 Fluorometer (Thermo-Fisher Scientific). The purified *pbrD* gene was ligated into the pET32 Xa/LIC expression vector following the manufacturer's instructions to create the recombinant plasmid pET32Xa/LIC-*pbrD* which contains a N-terminal Trx•Tag™, His•Tag® and S®Tag™.

2.3. Transformation of E. coli BL21 (DE3)

The recombinant plasmid pET32Xa/LIC-*pbrD* was used to transform chemically competent *E. coli* BL21 (DE3) by heat shock.

Transformants were primarily selected on Luria–Bertani (LB) agar plates supplemented with 50 μg/mL ampicillin and further screened for the *pbrD* insert by colony PCR. Positive transformants were subsequently processed for small scale plasmid isolations using the PureYield™ Plasmid Miniprep System according to the manufacturer's instructions. Purified plasmids were sent to Inqaba Biotech (Pty) Ltd (Pretoria, South Africa) for sequencing with the universal T7 promoter and terminator primers in order to confirm the orientation and full length gene sequence of *pbrD* inserts. The data was analysed in CLC main workbench 8; sequences were aligned using ClustalOmega (https://www.ebi.ac.uk/Tools/msa/clustalo/) and compared to existing *pbrD* sequences available in the Genbank Database (http://www.ncbi.nlm.nih.gov/). Transformants identified to contain full length *pbrD* were selected for downstream application and maintained in glycerol stocks.

In addition, self-ligated “empty” pET32a plasmid that carries the same N-terminal Trx•Tag™, His•Tag® and S®Tag™ was transformed into *E. coli* BL21 (DE3) cells in a similar manner to serve as a Pb binding control.

2.4. Overexpression of rPbrD

A recombinant *E. coli* strain containing the target gene or the control pET32a vector was grown overnight in LB media supplemented with 50 μg/mL ampicillin (LB/Amp) at 37 °C in an orbital shaker at 250 rpm. A fresh inoculum was prepared by diluting 3 mL of overnight culture into 100 mL of LB/Amp media and grown to an optical density (OD_{600}) of ~0.5. A fraction of the cells were collected hourly and processed as “uninduced” cells depicting the control. The remaining cells were induced with a final concentration of 1 mM isopropyl β-D-1-thiogalactopyranoside (IPTG). Both induced and control samples were collected hourly for the first 5 h and after 24 h to determine the optimal time for expression of recombinant PbrD fused to an N-terminal Trx•Tag™, His•Tag® and S®Tag™ and herewith referred to as rPbrD. Collected samples were re-suspended in 5 mL 1x BugBuster™ buffer per gram of wet cell pellet weight. The cell suspension was incubated at room temperature with gentle agitation (150 rpm) for 20 min to complete cell lysis. The soluble (SF) and insoluble fractions (IF) were separated by centrifugation at 16 000 *g* for 20 min at 4 °C (Heraeus™ Multifuge™ X1R Centrifuge, Thermo-Fisher scientific). Each fraction was separated and assessed on a normalised mini protean SDS-PAGE gel prepared with 10% TGX Stain-Free™ FastCast™ Acrylamide Kit (Bio-Rad) and visualised under the ChemiDoc™ MP imaging system. The identity of the recombinant protein was further confirmed by Western blot using the His-probe (H-3) monoclonal antibody (1:5000) directed against the N-terminal 6x-histidine fusion tag and secondary goat anti-Mouse HRP antibody (1:15000). The antibody bound PVDF membrane was treated with Clarity™ ECL western blotting substrate and the fluorescence detected under the ChemiDoc™ MP imaging system. To obtain sufficient protein for purification, expression was scaled up to 1 L under the optimal conditions selected from the pilot study following the protocol described. Cells were pelleted by centrifugation at 16 000 *g* for 10 min at 4 °C and the resulting pellet was stored at −20 °C until purification.

2.5. Purification of rPbrD by Ni-NTA affinity chromatography

The cell pellet was lysed in 1x BugBuster™ buffer as described above and the insoluble fraction containing protein inclusion bodies (IBs) was collected for purification. The IBs were washed twice by re-suspending the pellet in 10 fold diluted 1x Bugbuster buffer and once with buffer B (100 mM sodium phosphate, 10 mM Tris-HCl, pH 8). The re-suspended fractions were centrifuged at 16000 *g* for 15 min at 4 °C between each wash and the supernatant was discarded. The washed IBs were solubilised in buffer B containing 8 M urea by centrifugation at 16 000 *g* for 20 min at 4 °C. The supernatant containing the solubilised protein fraction was passed through a 0.45 μm syringe filter prior to IMAC purification. Purification was performed using the Äkta FPLC (Fast

performance liquid chromatography) prime plus protein purification system (GE Healthcare Life Sciences, USA). Clarified supernatant was loaded onto a HisTrap HP column charged with Ni^{2+} (GE Healthcare Life Sciences, USA) previously equilibrated with binding buffer [50 mM sodium phosphate, 300 mM NaCl, 8 M urea, 5 mM imidazole, pH 8]. After loading, the column was washed with 10 column-volumes of wash buffer [50 mM sodium phosphate, 300 mM NaCl, 8 M urea, 10 mM imidazole, pH 8], then eluted with elution buffer [50 mM sodium phosphate, 300 mM NaCl, 8 M urea, 400 mM imidazole, pH 8] at a flow rate of 4 mL/min. All eluted fractions were collected and analysed by SDS-PAGE as described previously. All protein quantification was done using the Qubit® Protein assay kit with the Qubit® 2.0 Fluorometer (Thermo-Fisher Scientific).

The fractions containing rPbrD were pooled and refolded by dialysis in a 3 mL, 10K MWCO Slide-A-Lyzer™ Dialysis Cassette (Thermo-Fisher Scientific, USA). Briefly the dialysis cassette was hydrated in dialysis buffer (50 mM Tris, 0.5 M L-arginine, 6 M urea, 10% (v/v) glycerol, 5 mM DTT, pH 8) for ~2 min. The eluted fraction (3 mL) was inserted into the dialysis cassette and the cassette submerged in 3 L dialysis buffer for 4 h at room temperature with gentle agitation. The original buffer was sequentially replaced with 3 L dialysis buffer containing reduced concentrations of urea (4 M and 2 M) and DTT (3 mM and 1 mM) under the same conditions. A final buffer (3 L) containing 1 M urea and 1 mM DTT was used for an overnight dialysis at 4 °C. The refolded protein was harvested, assessed on a normalised 10% (w/v) SDS-PAGE gel with densitometric analysis and further confirmed by Western blot as described above. Additionally, purified refolded protein was quantified using the Qubit® Protein assay kit with the Qubit® 2.0 Fluorometer (Thermo-Fisher Scientific) and assayed for the presence of soluble aggregates by absorbance spectroscopy (240–340 nm) and size exclusion chromatography on HiLoadTM 16/60 SuperdexTM grade column (GE healthcare). rPbrD was maintained as the fusion protein for all subsequent experimental work since it was intended for use as a biosorbent thereby stabilizing the protein itself whilst eliminating additional purification steps and cost.

The fusion tag (N-terminal Trx•Tag™, His•Tag® and S®Tag™) was overexpressed in *E. coli* as a soluble protein and purified under native conditions using Ni-NTA affinity chromatography (Fig. S2).

2.6. Peptide sequencing by mass spectroscopy

SDS-PAGE analysis of the purified denatured recombinant protein revealed the presence of the expected ~50 kDa PbrD-fusion protein together with an additional protein of ~32 kDa in size. The amino acid sequences of both proteins were determined by LC-MS/MS (Liquid chromatography-mass spectroscopy) at the CSIR (Council for Scientific and Industrial Research, Pretoria, South Africa). For in-gel digestions, the two protein bands were individually excised from a Coomassie-stained SDS-PAGE and destained using 50% methanol/50 mM ammonium bicarbonate (NH_4HCO_3). Following dehydration in 75% acetonitrile (ACN) solution, 10 mM DTT and 55 mM iodoacetamide (IAA) in 25 mM NH_4HCO_3 were added. Cleavage of proteins into peptides was achieved overnight at 37 °C with 0.1 μg/μL tryspin. The peptides were eluted in a sterile Protein Lo-Bind tube using 50% ACN and 5% formic acid.

The extracted peptides were ionised by an electrospray ionisation and the mass of the ions were measured by the ScieX TripleTOF 6600 (SCIEX) coupled to a Dionex Ultimate 3000 UHPLC system (Thermo Scientific). Data obtained from the LC-MS/MS spectra were analysed with the Paragon database search algorithm using the ProteinPilot™ Software (SCIEX) [21]. Identification of protein/peptides sequences was obtained with the protein blast search using the NCBI database (http://www.ncbi.nlm.nih.gov/). Furthermore, the peptide sequence of the fusion PbrD protein was used to construct a hypothetical structure using Phyre2 [22] and PyMol [version 1.7.4, Schrodinger] [23].

2.7. Circular dichroism (CD)

The secondary structure of rPbrD was evaluated using far-UV circular dichroism. Spectral measurements of 5 μM rPbrD (50 mM Tris-HCl, 1 mM DTT, pH 8) were obtained using a J-1500 Circular Dichroism Spectrometer (Jasco Analytical Instruments, Japan) from 200 to 250 nm. Measurements were recorded at 100 nm/min scan speed, 5 accumulations and 1 nm bandwidth. Data obtained from CD measurements (θ) were initially corrected for interference from buffer solution, and thereafter was converted to molar residue ellipticity (θ_{MRE}) using equation (1) [24].

$$\theta_{MRE} = \frac{\theta(100)}{(l)(c)(n)} \quad (1)$$

where: θ = ellipticity (m.deg), ^{l} = path length (cm), c = protein concentration (μM), and n = number of amino acid residues.

The CD spectrum data was analysed using BeStSel software available at http://bestsel.elte.hu/to predict the proportion of secondary structures in the rPbrD-fusion protein [25,26].

2.8. Tryptophan fluorescence

Tryptophan fluorescence of denatured rPbrD and refolded rPbrD was used to determine if there are any tertiary structural changes in the presence of 5 μM and 500 μM Pb(II). Fluorescence spectra of 5 μM denatured (50 mM Tris, 0.5 M L-arginine, 8 M urea, 1 mM DTT, pH 8) and 5 μM refolded rPbrD (50 mM Tris, 0.5 M L-arginine, 1 mM DTT, pH 8) was recorded using a JASCO FP-6300 spectrofluorometer (Jasco Analytical Instruments, Japan). The emission spectra were recorded under the following parameters; excitation at 295 nm and emission from 280 to 450 nm, 500 nm/min scan speed, 3 accumulations and 2.5 nm emission bandwidth.

2.9. Pb binding assay (Batch adsorption study)

To determine whether the refolded PbrD-fusion protein was biologically functional *in vitro*, 5 μM of protein was incubated with 10-fold dilutions of $Pb(NO_3)_2$ between 0.005 and 5 μM for 30 min at room temperature under constant agitation (150 rpm). Thereafter the solution was filtered through a 10K MWCO Amicon® Ultra-15 spin centrifugal filter (Merck, SA) by centrifugation at 5000*g* for 30 min at 4 °C. The filtrate was acidified with 1% (v/v) nitric acid and analysed using the NexION® 300 Induction Coupled Plasma Mass Spectrometer (ICP-MS) (Perkin Elmer, USA) to measure the concentration of residual unbound ^{208}Pb. Controls consisting of $Pb(NO_3)_2$ without the protein and with the fusion tag were prepared and treated under the same conditions for each concentration tested. The experimental data reported is based on three replicates. The biosorption capacity which is the amount of sorbed metal (Pb ions) per gram of sorbent (rPbrD) was determined using equation (2) and the biosorption efficiency (%) was calculated using equation (3) [27].

$$Q_e = \frac{(C_i - C_e)V}{w} \quad (2)$$

$$Q\% = \left(\frac{C_i - C_e}{C_i}\right) \times 100 \quad (3)$$

where: Q_e = the amount of metal adsorbed from solution by the biosorbent (μg/g), C_i = initial metal concentration (μg/L), C_e = residual metal concentration (μg/L), V = solution volume (L), w = amount of adsorbent in solution (g).

2.10. Adsorption isotherm models

Since, PbrD has not been studied for its metal-binding characteristics *in vitro*; no theoretical data is currently available to support the

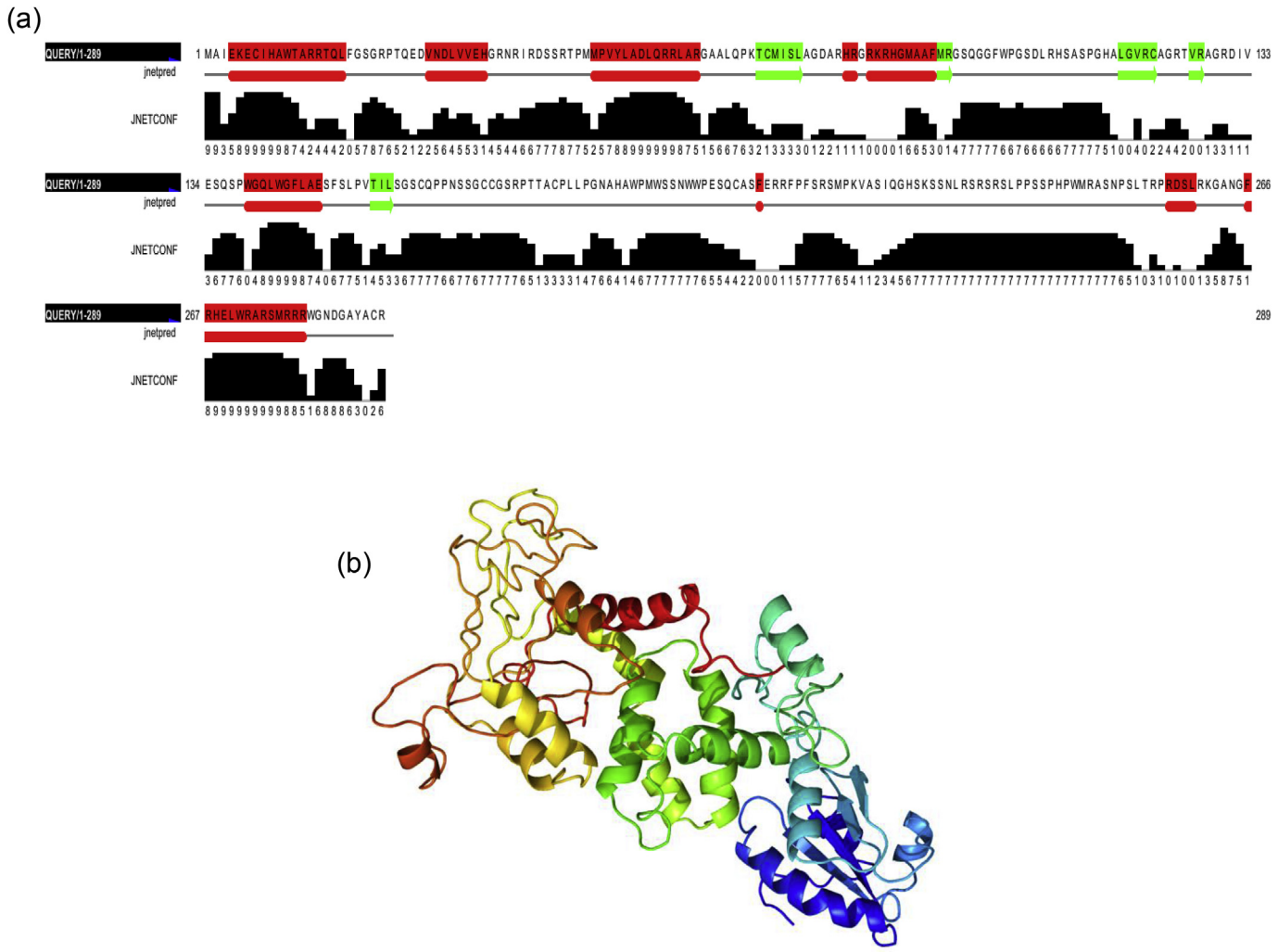

Fig. 1. Secondary structure and 3-dimensional model of rPbrD. Secondary structure of rPbrD (UniProt accession: Q1LAL8) protein as predicted by Jpred 4 server [35] and associated confidence "JNETCONF" (a). Red bars, green arrows, and grey lines represent α-helices, β-sheets and coils, respectively. Secondary 3-dimensional structure of rPbrD (b) as predicted by Phyre2 software [22] and PyMol [version 1.7.4, Schrodinger] [23] covering 144 residues modelled at > 90% accuracy.

mechanisms of the proposed sorbent. To further understand the adsorption mechanism; four isotherm models were used to obtain theoretical data on the thermodynamics of the biosorption process.

3. Langmuir adsorption isotherm

The Langmuir model is indicative of a complete monolayer formation of Pb(II) on the surface of the rPbrD protein provided that the protein contains a finite number of identical sites containing a homogenous surface [28]. The linearised equation (4) [29] were used to calculate the isotherm constants from the plot of 1/Ce vs. 1/Qe.

$$\frac{1}{Q_e} = \frac{1}{Q_m} + \frac{1}{Q_m K_L C_e} \tag{4}$$

where: Q_m = maximum adsorption capacity (μg/g) and K_L = Langmuir equilibrium constant (μg/L).

4. Freundlich adsorption isotherm

The Freundlich model is indicative of an exponential distribution of active sites of rPbrD protein and its affinity towards Pb(II). This isotherm is suitable for a heterogeneous surface [28]. The empirical linearised equation (5) [30] was used to calculate the isotherm constants from the plot of log Qe vs. log Ce.

$$\log Q_e = logK_f + \frac{1}{n} logC_e \tag{5}$$

where: K_f = Freundlich adsorption constant (μg/g) and n = adsorption intensity. The 1/n value is indicative of the adsorption intensity between rPbrD and Pb(II). If 1/n < 1 then the adsorption is favourable, if 1/n > 1 then it is a cooperative adsorption, and if 1/n = 0 then it indicates a more heterogeneous surface.

5. The Temkin adsorption isotherm

The Temkin model gives a more clear indication on the interactions between rPbrD protein and Pb(II) provided that the very low and high Pb(II) concentrations are ignored. As Pb(II) bind and cover the surface of the protein; the heat generated from the molecules would decline linearly instead of logarithmically [31]. The linearised equation (6) [32] was used to calculate the thermodynamic parameters from the plot of Qe vs. *ln* Ce.

$$Q_e = \frac{RT}{B_t} ln(A_t) + \frac{RT}{B_t} ln(C_e) \tag{6}$$

where: R = Universal gas constant (8.314 J/mol/k), T = absolute temperature in kelvin (298 K) A_t = equilibrium binding constant, and B_t = Temkin isotherm constant.

6. Dubinin–Radushkevich (D-R) isotherm model

The D-R model is used to determine the sorption free energy and to identify whether the bonding of Pb(II) to rPbrD protein is a physisorption or chemisorption mechanism [33]. The linearised equations (7)–(9) [34] were used to calculate the thermodynamic parameters by plotting ln Qe vs ε^2.

$$\varepsilon = RT\ ln\left(1 + \frac{1}{C_e}\right) \tag{7}$$

$$ln(Q_e) = ln(Q_s) - K_{ad}\varepsilon^2 \tag{8}$$

$$E = \frac{1}{\sqrt{2B_{DR}}} \tag{9}$$

where: ε = Polanyi potential, Q_s = theoretical saturation capacity (μg/g), K_{ad} = D-R adsorption energy constant (mol^2/kJ^2), B_{DR} = isotherm constant, related to the mean free energy of adsorption.

7. Results and discussion

7.1. Amplification and cloning of the pbrD gene

PCR amplification of the synthesised *pbrD* gene yielded a single product of expected size (~870 bp) (Fig. S1). The purified PCR product was treated with T4 DNA polymerase and successfully ligated into the pET32Xa/LIC vector to construct the recombinant expression vector pET32 Xa/LIC-*pbrD*. The expression vector was transformed into *E. coli* BL21 (DE3) cells at a transformation efficiency of ~1×10^7 cfu/μL. A positive transformant carrying recombinant plasmid DNA confirmed to contain the full length gene sequence of *pbrD* with no mutational errors was selected and subsequently used for expression.

The protein sequence of PbrD from *C. metallidurans* CH34 (290 amino acids) referenced during this study was used to predict its secondary structure with Jpred 4 server [35] and a 3-dimensional model of rPbrD (PbrD with N-terminal fusion tag) was constructed with Phyre2 and PyMol [version 1.7.4, Schrodinger] [23] as represented in Fig. 1. This is the first hypothetical model reported for an N-terminal tagged PbrD protein in the absence of a known structure for the native protein.

7.2. Expression of PbrD protein

Recombinant PbrD was expressed as a ~50 kDa fusion protein comprising of 32 kDa native protein fused to a 17.8 kDa N-terminal Trx•Tag™, His•Tag® and S®Tag™. Optimal expression was achieved 5 h post induction with a final concentration of 1 mM IPTG (Fig. 2a). Cells cultured in the absence of IPTG did not show any detectable over-expressed protein. Various attempts to obtain PbrD in the soluble fraction including induction at lower temperatures (25 °C, 30 °C), using different growth medium (Enpresso® B, BioSilta) and solubilisation with 5% sodium lauroyl sarcosinate were unsuccessful. The highest expression of PbrD-fusion protein was consistently found in the insoluble fraction within IBs (Fig. 2a). The expression of rPbrD protein was further confirmed by Western blot using antibodies directed against the N-terminal His tag. Protein was again only detected in the insoluble fraction (Fig. 2b).

7.3. Purification of rPbrD under denaturing conditions

PbrD was purified from washed IBs under denaturing conditions. Recombinant protein was completely solubilised in buffer B containing 8 M urea and loaded onto a Ni affinity column (Fig. 3a). Eluates were normalised and analysed by SDS-PAGE (Fig. 3b) and the densitometry analysis showed the fraction to contain < 7% aggregates (most likely, consisting of protein dimers ~94 kDa and trimers ~141 kDa due to the cysteine rich regions), > 85% full length rPbrD (N-tagged PbrD) and < 6% of a ~32 kDa protein which consistently co-eluted with rPbrD under several buffer conditions. Both the full length rPbrD and ~32 kDa protein were sequenced using mass spectroscopy. The peptide sequence of the full length rPbrD was confirmed while the sequence of the ~32 kDa protein revealed a truncated form of rPbrD protein with 30% coverage from the N-terminus. The C-terminus of rPbrD contains the cysteine-rich hypothetical metal binding site which was lacking in the truncated form and while Pb(II) may also coordinate to nitrogen donors on the histidine tag, their coordination bond is weak [36]. Eluted protein was refolded by dialysis in buffer containing reduced concentrations of urea and DTT in the presence of 0.5 M L-arginine. The presence of arginine in the refolding buffer reduces protein aggregation, prevents the misfolding of proteins and increases protein recovery. Since rPbrD is a metallo-chaperone that contains a high proportion of cysteine residues, DTT was added to prevent disulfide bonds formation thereby maintaining the cysteine residues in their reduced state during refolding. Fig. 3b shows rPbrD to be the major constituent of the total protein in the denatured, purified and refolded fraction; the presence of soluble aggregates in the refolded protein fraction was eliminated (Figs. S3 and S4). The refolded fusion protein was subsequently characterized by CD and tryptophan fluorescence and evaluated for its functionality using a Pb binding assay.

7.4. Circular dichroism (CD)

Circular dichroism is the absorption of left-handed and right-handed circularly polarized light used to study the secondary structure of a protein [24]. The CD spectrum derived using BeStSel for denatured and refolded rPbrD and refolded rPbrD in the presence of Pb(II) is shown in Table 1. Regular helices account for 9.6% of the refolded structure while the β-sheet structure of the Trx protein originating from the fusion tag is also accounted for. Irregular structures, loops and turns appear to constitute majority of the protein structure. The hypothetical structure of rPbrD constructed using Phyre2 and PyMol [version 1.7.4, Schrodinger] and Jpred 4 (Fig. 1a and b) further correlated to the composition of secondary structure obtained by CD in this study with some contribution from the N-terminal Trx•Tag™, His•Tag® and S®Tag™ (Fig. S3).

In the presence of 5 μM $Pb(NO_3)_2$ Pb(II), the refolded protein undergoes a major change in the structural conformation by further adopting left and right twisted antiparallel β-sheets (Table 1). It is

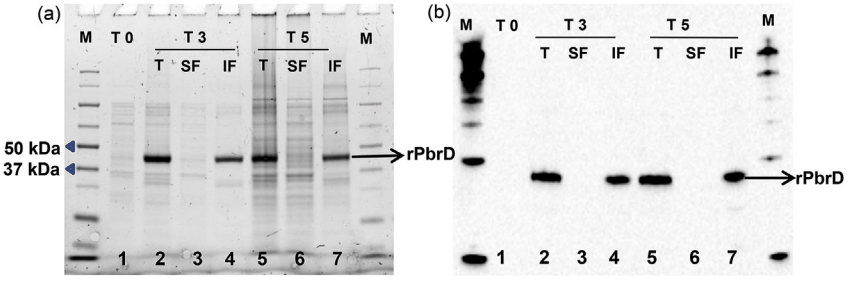

Fig. 2. 10% normalised SDS-PAGE gel (a) and western blot analysis (b) of small-scale expression of rPbrD. Lane M, Precision Plus Protein™ Unstained Standards (Bio-Rad). (a): lanes 1, 2 and 5, total cell fraction (T) of *E. coli* BL21 (DE3) cell lysate at time 0, 3 and 5 h, respectively post-induction; lanes 3 and 6, soluble fractions (SF) of *E. coli* BL21 (DE3) cell lysate at time 3 and 5 h post-induction with no evidence of PbrD expression; lanes 4 and 7, insoluble fractions (IF) of *E. coli* BL21 (DE3) cell lysate at time 3 and 5 h post-induction showing overexpression of PbrD. (b): corresponding western blot showing bands correlating to the rPbrD protein on the SDS-PAGE gel.

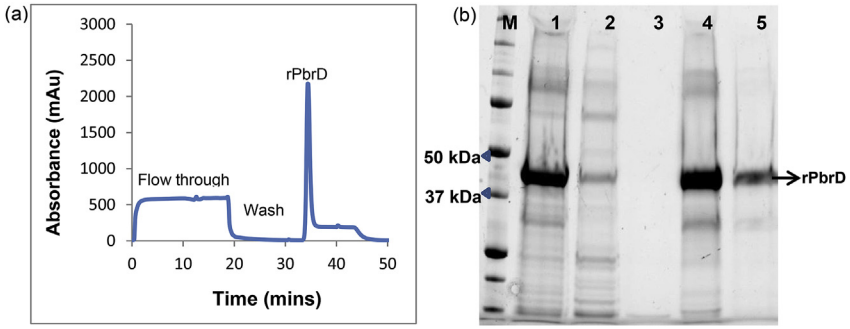

Fig. 3. Elution profile of rPbrD through Ni-NTA IMAC chromatography. (a) Chromatogram showing elution of rPbrD (3) from a 5 mL HisTrap HP column in binding buffer (50 mM sodium phosphate, 300 mM NaCl, 8 M urea, 5 mM imidazole, pH 8) and eluted with 350 mM imidazole. (b) Corresponding 10% SDS-PAGE analysis of normalised fractions collected from the IMAC purification of rPbrD. Lane M indicates Precision Plus Protein™ Unstained standards (Bio-Rad). Lane 1 represents the solubilised IBs; Lanes 2, 3 and 4 represents the flow through, wash and elution fractions respectively; Lane 5 represents refolded rPbrD fraction.

Table 1
Secondary structure composition of rPbrD-fusion protein determined from single-spectrum CD analysis in BeStSel [25,26].

Secondary structure	Denatured PbrD Content (%)	Refolded PbrD Content (%)	Refolded PbrD with Pb Content (%)
Helix (regular)	0	9.6	3.1
β-sheet (parallel)	0	0	0
β-sheet (antiparallel)[a]	0	25	67.5
Turn	30.2	28.4	29.4
Other[b]	69.8	37	0

[a] Right-handed twisted, left handed twisted and relaxed antiparallel β-sheet structure.
[b] Composed of 3_{10} helices, bends, π-helices, β-bridges, irregular structures and loops.

reported that twisted antiparallel β-sheets increase the stability of a protein [37]. Since Pb is toxic to cellular organisms, it is probable that within the native organism PbrD undergoes a structural conformation upon binding Pb(II) in order to maintain cell homeostasis. The change in the conformational structure of rPbrD also indirectly confirmed the ability of the refolded protein to bind Pb(II). Conversely, CD analysis of denatured rPbrD showed a complete loss of α and β structures with majority of the protein found as distorted helices, turns, irregular and random coil structures.

7.5. Tryptophan fluorescence

Tryptophan (Trp) residues in proteins are largely responsible for the intrinsic fluorescence of proteins at an emission wavelength of ~350 nm [38]. Upon denaturation or involvement in ligand binding, the change in the solvent environment surrounding the Trp residues may lead to Trp fluorescence quenching which has been used widely to provide information on the macromolecular structure of proteins. Within the primary sequence of rPbrD, ten Trp residues are contributed by the native protein and two from the fusion tag. Based on the hypothetical structure of rPbrD, Trp 32 (from the fusion tag), Trp 264, Trp 353, Trp 357 and Trp 406 are exposed and may be involved in Pb(II) binding that would result in Trp fluorescence quenching. Therefore, tryptophan fluorescence was performed on denatured and refolded rPbrD protein in the presence of 5 μM Pb(II) and 500 μM Pb(II).

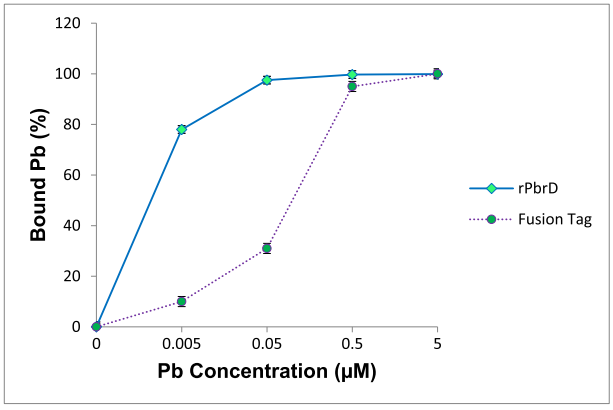

Fig. 5. Pb binding analysis of rPbrD. In the presence of Pb(II), rPbrD (5 μM) increasingly binds the metal ion until reaching 99% biosorption efficiency at concentrations higher than 0.5 μM. The fusion tag protein contributed 10–30% of Pb(II) binding until saturation was achieved at 0.5 μM. Error bars represent the standard deviation from triplicate treatments.

Table 2
Adsorption isotherm constants for biosorption of Pb(II) with rPbrD.

Langmuir			Freundlich			
R^2	q_{max}	kL	R^2	1/n	n	K_f
0.3475	0.36	1.12	0.7733	5.58	0.18	1096.5
Temkin			**Dubinin-Radushkevich**			
R^2	**At**	**Bt**	**R^2**	**Qs**	**Kad**	**E**
0.9783	4.15	39.31	0.8382	1628.15	$5x10^{-7}$	1000

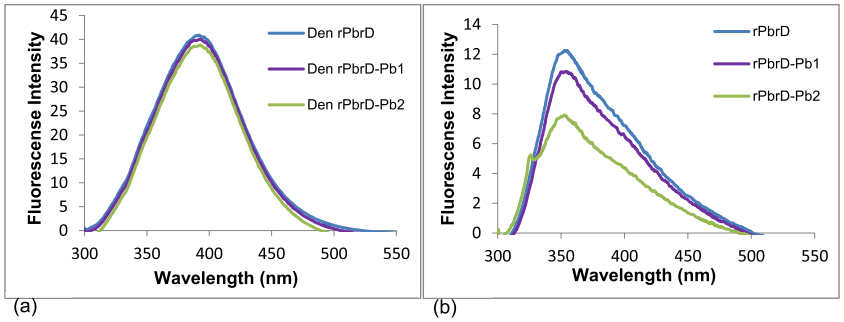

Fig. 4. Tryptophan fluorescence of denatured and refolded rPbrD. Fluorescence emission spectra of 5 μM denatured rPbrD (a) and 5 μM refolded rPbrD (b) in the presence of 5 and 500 μM Pb(II) as Pb1 and Pb2, respectively. Spectra were measured from 280 to 450 nm using an excitation wavelength of 295 nm.

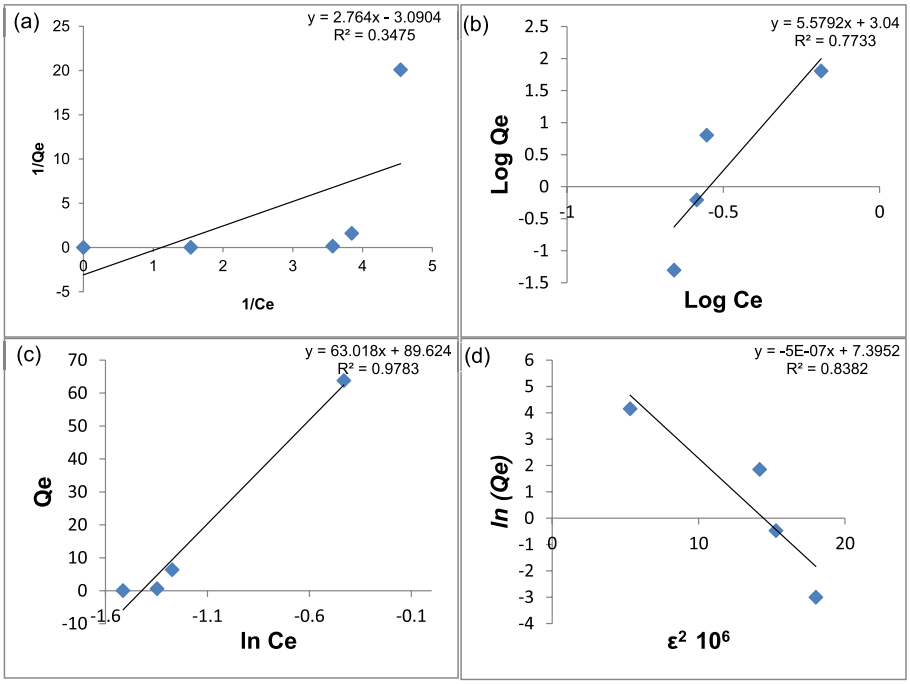

Fig. 6. Plots of the Langmuir (a), Freundlich (b), Temkin (c), and Dubinin–Radushkevich (d) isotherms, respectively. The graphs represent the adsorption capacity (Qe) of rPbrD versus residual concentrations of Pb(II) in solution.

The maximum fluorescence intensity of refolded rPbrD occurred at 347 nm, whereas the maximum fluorescence intensity of denatured protein occurred at 385 nm (Fig. 4). The red shift in the emission wavelength maxima of the denatured protein suggests the exposure of Trp residues located within the protein hydrophobic interior to an aqueous environment. Trp fluorescence was quenched more in the refolded PbrD-fusion protein than the denatured protein suggesting that Trp residues on rPbrD protein were within close proximity to polar residues. The refolded rPbrD protein was further quenched in the presence of 5 and 500 µM Pb(II) as compared to the denatured state where the lower fluorescence emission was within error and is negligible (Fig. 4a and b). There were no wavelength shifts in the spectra of the denatured protein however a slight blue shift was observed in the refolded rPbrD-Pb1 and rPbrD-Pb2; indicating a decrease in the polarity due to the quenching of the fluorophore within the protein. These findings suggest that the fusion protein (rPbrD) expressed in this study was able to bind Pb(II) as Trp fluorescence is known to be quenched upon metal ion binding [39,40]. These findings further suggest that for Pb-binding to occur, PbrD-fusion protein must be folded into its native state. This correlates to the native function of PbrD as a Pb-binding protein.

7.6. Pb binding assay

PbrD is a metallo-chaperone that contains a cysteine rich metal binding motif along with large numbers of proline and serine residues which facilitates sequestration of Pb(II) within the cytoplasm of the bacterial cell [41]. To further confirm that the refolded protein which included an N-terminal fusion tag would function similarly to native PbrD, a Pb binding analysis was performed. Histidine is not involved in Pb(II) binding [42] while the influence of the S-tag or Trx-tag on Pb(II) binding has not been reported. However, thioredoxin (Trx) protein is known to bind to other divalent metal ions such as nickel [Ni(II)] [43], cadmium [Cd(II)] [44], copper [Cu(II)] and mercury [Hg(II)] [45]. For this reason, the fusion tag (N-terminal Trx•Tag™, His•Tag® and S®Tag™) was overexpressed, purified and its contribution to Pb binding was evaluated. A standard concentration of 5 µM of rPbrD protein or fusion tag protein was incubated separately in the presence of varying concentrations of Pb that ranged between 0.005 and 5 µM. Fig. 5 shows that the fusion tag on its own contributed between 10 and 30% binding in the presence of 0.005–0.05 µM Pb. This is likely due to the Cys-X-X-Cys metal-binding motif present at the N-terminal of Trx protein. At similar concentrations, rPbrD was able to bind more Pb(II) in the range of 78–97%. Both rPbrD and the fusion tag were saturated at 0.5 µM (99% binding) where a further increase in metal concentration did not lead to increased binding. Although the fusion tag contributes some metal binding, it is a relatively small protein (~18 kDa) which is usually unstable for application as a biosorbent. Furthermore, the non-specificity of the fusion tag for divalent cations would compromise its activity in natural water systems where a complex mix of metals is present. The findings indicate that under the conditions used in the present study rPbrD was able to function and biosorb (99%) Pb(II) at concentrations reported to be present in natural water systems commonly contaminated with Pb. The specificity and preferential order of binding metal ions in complex metal systems still needs to be elucidated for rPbrD. However, PbrD has only been reported to sequester Pb(II) within *C. metallidurans* CH34 indicating that rPbrD could be used a Pb-specific biosorbent.

7.7. Adsorption isotherms

Adsorption isotherms are essential for studying the thermodynamic properties between the proposed sorbent (rPbrD) and metal ion [Pb(II)] at equilibrium for downstream optimisation of the adsorption system. Herewith, we present the Langmuir, Freundlich, Temkin and Dubinin-Radushkevich adsorption isotherms. The modeling analyses were based on mathematical calculations (Table 2) by plotting graphs between the solid-phase (Qe) and its residual concentration (Ce) derived from their respective equations.

Based on the linear isotherm plots (Fig. 6) the experimental data exhibited high correlation coefficient values (r^2 - Table 2) with the Temkin isotherm exhibiting the highest r^2 of 0.98. Thereafter, the correlation coefficient was closest to the D-R isotherm and Freundlich isotherm which best describes the heterogeneous coverage (unrestricted multilayer formation) of Pb(II) on the surface of rPbrD protein. The maximum adsorption capacity obtained from Langmuir (q_{max}), Freundlich (K_f) and D-R (Q_s) isotherms were 0.35, 1096.5, and

1628 μg/g respectively. A high adsorption value is indicative of a high binding capacity [28]. Based on the adsorption values from Freundlich and D-R isotherm, rPbrD showed a high binding capacity to Pb(II). However, a very low binding capacity was observed from the Langmuir isotherm. With regards to the Freundlich isotherm, the adsorption intensity (1/n) is an indication of the binding strength between rPbrD and Pb(II). The exponent, $1/n > 1$ was indicative of a cooperative adsorption [46] which is favoured by the multi-layer behavior of adsorption observed in this study. The Temkin isotherm constants (B_t) and equilibrium binding constant (A_t) showed low heat of adsorption (4.15 and 39.31 J/mol) which is indicative of a physisorption process [47]. Additionally, the calculated value of E (1 kJ/mol) obtained from the D-R isotherm is also indicative of a physisorption process [48].

The physisorption process depicts the following conditions of binding between rPbrD and Pb(II): it does not require activation energy, it occurs at low temperatures, the attraction between Pb(II) and rPbrD are based on Van der Waal's forces and hence the binding is reversible and it forms multi-layer adsorption.

8. Conclusions

Our findings show that PbrD is expressed within inclusion bodies from *E. coli* BL21 (DE3) transformed using the constructed plasmid pET32Xa/LIC-*pbrD*. Furthermore, purification and refolding of rPbrD resulted in a fusion protein capable of binding Pb (II) in high concentrations. From this study, binding of Pb(II) to rPbrD *in vitro* most likely occurred by physisorption and likely follows the D-R isotherm. To the best of our knowledge, this is the first report on the expression and purification of a functional fusion PbrD protein using an *E. coli* expression system. The ability of the expressed protein to bind Pb(II) in the presence of concentrations higher than those reported in ground/surface water in South Africa suggest its potential to be developed into a biosorbent for the treatment of Pb contaminated water. Future work would include developing a suitable immobilization strategy to maintain the activity of the protein under varying environmental conditions such as pH and temperature.

Acknowledgments

This work is based on the research supported in part by the National Research Foundation of South Africa for the Thuthuka grant (Grant No. TTK13062820091 to K.K). Any opinion, finding and conclusion or recommendation expressed in this material is that of the author(s) and the NRF does not accept any liability in this regard.

Appendix A. Supplementary data

Supplementary data to this article can be found online at https://doi.org/10.1016/j.pep.2019.02.008.

References

[1] World Health Organisation, Lead poisoning and health (Internet communication of 2018 at web site,, 2018. www.who.int/en/news-room/fact-sheets/detail/lead-poisoning-and-health.
[2] N.R. Nengovhela, M. De Beer, H.A. Greben, J.P. Maree, C.A. Strydom, May. Iron (II) oxidation to support limestone neutralization in acid mine water, Proceedings of Wisa 2002 Conference, 2002.
[3] L. Zheng, K. Wu, Y. Li, Z. Qi, D. Han, B. Zhang, C. Gu, G. Chen, J. Liu, S. Chen, X. Xu, X. Huo, Blood lead and cadmium levels and relevant factors among children from an e-waste recycling town in China, Environ. Res. 108 (2008) 15–20.
[4] G. Darko, S. Chigome, S. Lillywhite, Z. Tshentu, J. Darkwa, N. Torto, Sorption of toxic metal ions in aqueous environment using electrospun polystyrene fibres incorporating diazole ligands, WaterSA 39 (2013) 39–46.
[5] M. Dikole, Seasonal Analysis of Water and Sediment along the Umgeni River, South Africa (Doctoral Dissertation), (2016).
[6] J.N. Edokpayi, A.M. Enitan, N. Mutileni, J.O. Odiyo, Evaluation of water quality and human risk assessment due to heavy metals in groundwater around Muledane area of Vhembe District, Limpopo Province, South Africa, Chem. Cent. J. 12 (2018) 2.
[7] O.S. Fatoki, N. Lujiza, A.O. Ogunfowokan, Trace metal pollution in umtata river, WaterSA 28 (2002) 183–190.
[8] O.O. Olujimi, O.S. Fatoki, J.P. Odendaal, O.U. Oputu, Variability in heavy metal levels in river water receiving effluents in Cape Town, South Africa, Research And Practices In Water Quality, 2015, pp. 194–211.
[9] A.J. Reinecke, R.G. Snyman, J.A.J. Nel, Uptake and distribution of lead (Pb) and cadmium (Cd) in the freshwater crab, Potamonautes perlatus (Crustacea) in the eerste river, South Africa, Water Air Soil Pollut. 145 (2003) 395–408.
[10] M.K. Maruthamuthu, I. Ganesh, S. Ravikumar, S.H. Hong, Evaluation of zraP gene expression characteristics and construction of a lead (Pb) sensing and removal system in a recombinant *Escherichia coli*, Biotechnol. Lett. 37 (2015) 659–664.
[11] X. Deng, X.E. Yi, G. Liu, Cadmium removal from aqueous solution by gene-modified *Escherichia coli* JM109, J. Hazard Mater. B139 (2007) 340–344.
[12] M. Pazirandeh, Development of a metallothionein based heavy metal biosorbent, Biochem. Mol. Biol. Int. 39 (1996) 789–795.
[13] M. Pazirandeh, B.M. Wells, R.L. Ryan, Development of bacterium-based heavy metal biosorbents: enhanced uptake of cadmium and mercury by *Escherichia coli* expressing a metal binding motif, Appl. Environ. Microbiol. 64 (1998) 4068–4072.
[14] M. Valls, S. Atrian, V. de Lorenzo, L.A. Fernández, Engineering a mouse metallothionein on the cell surface of *Ralstonia eutropha* CH34 for immobilization of heavy metals in soil, Nat. Biotechnol. 18 (2000) 661–665.
[15] W. Bae, R.K. Mehra, A. Mulchandani, W. Chen, Genetic engineering of *Escherichia coli* for enhanced uptake and bioaccumulation of mercury, Appl. Environ. Microbiol. 67 (2001) 5335–5338.
[16] X.W. Zhao, M.H. Zhou, Q.B. Li, Y.H. Lu, N. He, D.H. Sun, X. Deng, Simultaneous mercury bioaccumulation and cell propagation by genetically engineered *Escherichia coli*, Process Biochem. 40 (2005) 1611–1616.
[17] S. Singh, A. Mulchandani, W. Chen, Highly selective and rapid arsenic removal by metabolically engineered *Escherichia coli* cells expressing *Fucus Vesiculosus* metallothionein, Appl. Environ. Microbiol. 74 (2008) 2924–2927.
[18] X. Deng, Q.B. Li, Y.H. Lu, N. He, J. Jiang, Genetic engineering of *E. coli* SE5000 and its potential for Ni^{2+} bioremediation, Process Biochem. 40 (2005) 425–430.
[19] T.T.L. Nguyen, H.R. Lee, S.H. Hong, J.-R. Jang, W.-S. Choe, I.-K. Yoo, Selective lead adsorption by recombinant *Escherichia coli* displaying a lead-binding peptide, Appl. Biochem. Biotechnol. 169 (2013) 1188–1196.
[20] S. Taghavi, C. Lesaulnier, S. Monchy, R. Wattiez, M. Mergeay, D. van der Lelie, Lead (II) resistance in *Cupriavidus metallidurans* CH34: interplay between plasmid and chromosomally-located functions, Antonie Leeuwenhoek 96 (2009) 171–182.
[21] I.V. Shilov, S.L. Seymourt, A.A. Patel, A. Loboda, W.H. Tang, S.P. Keating, C.L. Hunter, L.M. Nuwaysir, D.A. Schaeffer, The paragon algorithm, a next generation search engine that uses sequence temperature values and feature probabilities to identify peptides from tandem mass spectra, Mol. Cell. Proteomics 6 (2007) 1638–1655.
[22] L.A. Kelley, M.J. Sternberg, Protein structure prediction on the Web: a case study using the Phyre server, Nat. Protoc. 4 (2009) 363–371.
[23] W.L. DeLano, The PyMOL Molecular Graphics System, Delano Scientific, San Carlos, 2002.
[24] N.J. Greenfield, Using circular dichroism spectra to estimate protein secondary structure, Nat. Protoc. 1 (2006) 2876–2890.
[25] A. Micsonai, F. Wien, L. Kernya, Y.H. Lee, Y. Goto, M. Réfrégiers, J. Kardos, Accurate secondary structure prediction and fold recognition for circular dichroism spectroscopy, Proc. Natl. Acad. Sci. Unit. States Am. 112 (24) (2015) E3095–E3103 201500851.
[26] A. Micsonai, F. Wien, É. Bulyáki, J. Kun, É. Moussong, Y.-H. Lee, Y. Goto, M. Réfrégiers, J. Kardos, BeStSel: a web server for accurate protein secondary structure prediction and fold recognition from the circular dichroism spectra, Nucleic Acids Res. 46 (W1) (2018) W315–W322.
[27] B. Volesky, Biosorption and me, Water Res. 41 (2007) 4017–4029.
[28] S. Ayoob, A.K. Gupta, Insights into isotherm making in the sorptive removal of fluoride from drinking water, J. Hazard Mater. 152 (2008) 976–985.
[29] I. Langmuir, The constitution and fundamental properties of solids and liquids, J. Am. Chem. Soc. 38 (1916) 2221–2295.
[30] H.M. Freundlich, Over the adsorption in solution, J. Phys. Chem. 57 (1906) 385–470.
[31] K.Y. Foo, B.H. Hameed, Insights into the modeling of adsorption isotherm systems, Chem. Eng. J. 156 (2010) 2–10.
[32] M.I. Temkin, V. Pyzhev, Kinetic of ammonia synthesis on promoted iron catalyst, Acta physiochimi. URSS 12 (1940) 327–356.
[33] A.O. Dada, A.P. Olalekan, A.M. Olatunya, O. Dada, Langmuir, Freundlich, Temkin and Dubinin–Radushkevich Isotherms studies of equilibrium sorption of Zn^{2+} unto phosphoric acid modified rice husk, J. Appl. Chem. 3 (2012) 38–45.
[34] M.M. Dubinin, L.V. Radushkevich, Equation of the characteristic curve of activated charcoal proceedings of the academy of sciences, Phys. Chem. Sect. USSR 55 (1947) 331–333.
[35] A. Drozdetskiy, C. Cole, J. Procter, G.J. Barton, JPred4: a protein secondary structure prediction server, Nucleic Acids Res. 43 (W1) (2015) W389–W394 (Web Server issue).
[36] J.C. Payne, M.A. ter Horst, H.A. Godwin, Lead fingers: Pb^{2+} binding to structural zinc-binding domains determined directly by monitoring lead-thiolate charge-transfer bands, J. Am. Chem. Soc. 121 (1999) 6850–6855.
[37] C.M. Santiveri, J. Santoro, M. Rico, M.A. Jiménez, Factors involved in the stability of isolated β-sheets: turn sequence, β-sheet twisting, and hydrophobic surface burial, Protein Sci. 13 (2004) 1134–1147.
[38] A.B.T. Ghisaidoobe, S.J. Chung, Intrinsic tryptophan fluorescence in the detection and analysis of proteins: a focus on förster resonance energy transfer techniques, Int. J. Mol. Sci. 15 (2014) 22518–22538.

[39] L.N. Neupane, J. Park, J.H. Park, K. Lee, Turn-on fluorescent chemosensor based on an amino acid for Pb(II) and Hg(II) ions in aqueous solutions and role of tryptophan for sensing, Org. Lett. 15 (2013) 254–257.
[40] O.A. Plotnikova, A.G. Mel'nikov, G.V. Mel'nikov, T.I. Gubina, Quenching of tryptophan fluorescence of bovine serum albumin under the effect of ions of heavy metals, Optic Spectrosc. 120 (2016) 65–69.
[41] A. Jarosławiecka, Z. Piotrowska-Seget, Pb resistance in micro-organisms, J. Microbiol. 160 (2014) 12–25.
[42] K.P. Neupane, V.L. Pecoraro, Pb-207 NMR spectroscopy reveals that Pb(II) coordinates with glutathione (GSH) and tris cysteine zinc finger proteins in a PbS3 coordination environment, J. Inorg. Biochem. 105 (2011) 1030–1034.
[43] M.R. Jensen, G. Petersen, C. Lauritzen, J. Pedersen, J.J. Led, Metal binding sites in proteins: identification and characterization by paramagnetic NMR relaxation, Biochemistry 44 (2005) 11014–11023.
[44] F. Rollin-Genetet, C. Berthomieu, A.H. Davin, E. Quéméneur, *Escherichia coli* thioredoxin inhibition by cadmium: two mutually exclusive binding sites involving Cys32 and Asp26, Eur. J. Biochem. 271 (2004) 1299–1309.
[45] H.W. Hellinga, J.P. Caradonna, F.M. Richards, Construction of new ligand binding sites in proteins of known structure: II. Grafting of a buried transition metal binding site into *Escherichia coli* thioredoxin, J. Mol. Biol. 222 (1991) 787–803.
[46] S.V. Mohan, J. Karthikeyan, Removal of lignin and tannin colour from aqueous solution by adsorption onto activated charcoal, Environ. Pollut. 97 (1997) 183–187.
[47] J. Liu, X. Wang, Novel silica-based hybrid adsorbents: lead(II) adsorption isotherms, Sci. World J. (2013) 1–6 2013.
[48] M.A. Shaker, A.A. Yakout, Optimization, isotherm, kinetic and thermodynamic studies of Pb(II) ions adsorption onto N-maleated chitosan-immobilized TiO_2 nanoparticles from aqueous media, Mol. Biomol. Spectrosc. 154 (2016) 145–156.

Supplementary Information

Recombinant expression and purification of a functional bacterial metallo-chaperone PbrD-fusion construct as a potential biosorbent for Pb(II)

Keshav V, Achilonu I, Dirr HW, and Kondiah K

1. Gene amplification of *pbrD* from pGEX vector supplied by Genscript (USA).

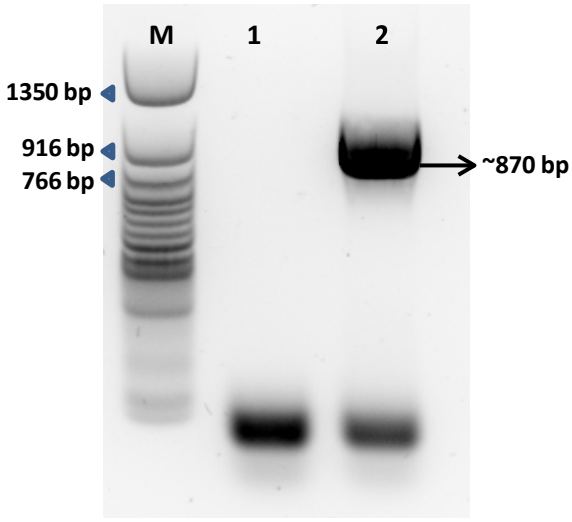

Figure S1 PCR amplification of *pbrD* gene. A 1.5% (w/v) agarose gel showing: lane M, Quick-Load® Purple 50 bp DNA Ladder (New England BioLabs® Inc,); lane 1, no template control and lane 2, amplified *pbrD* gene approximately 870 bp in size.

1. Expression and purification of fusion tag protein (pET32a) in *E. coli* BL21 (DE3) cells and its corresponding Western blot confirming the presence of the fusion tag protein.

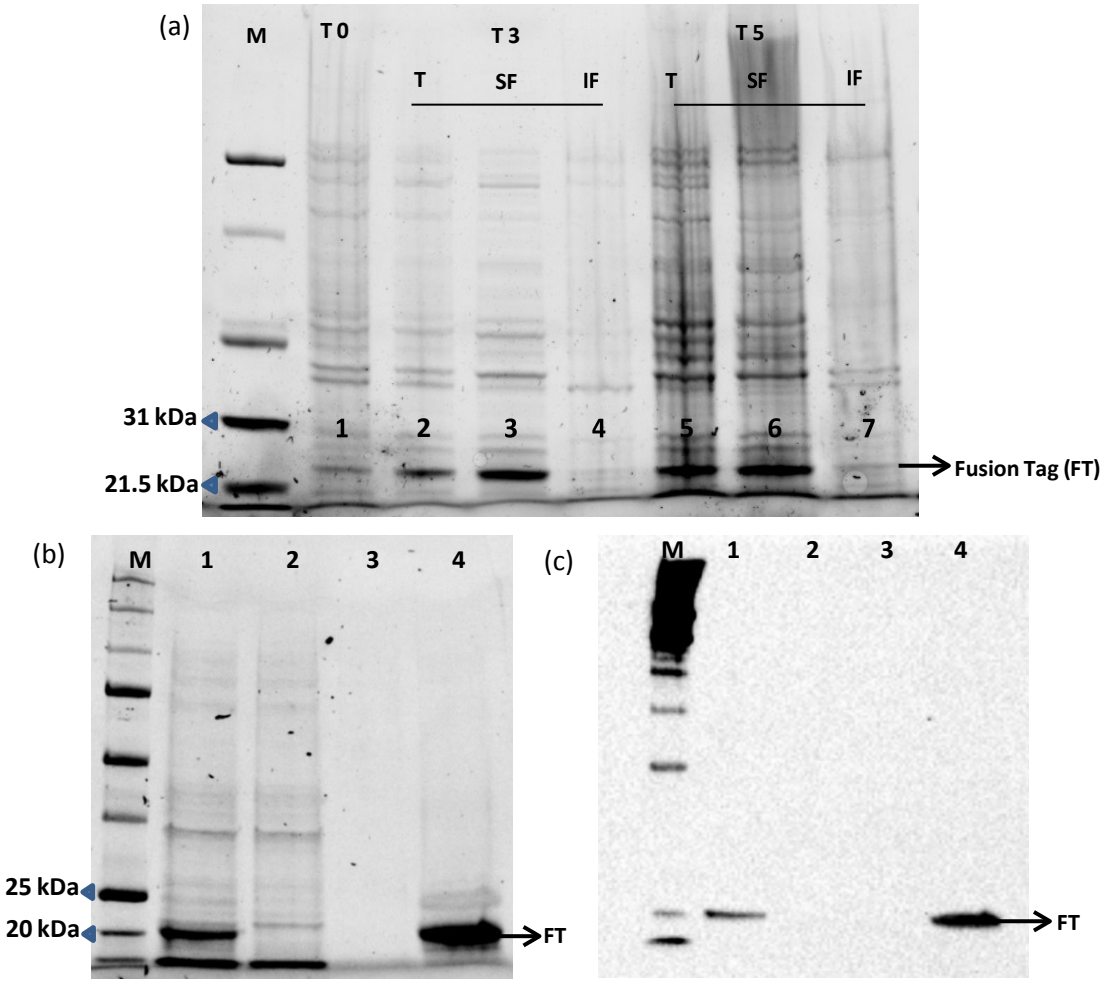

Figure S2 10 % normalized SDS-PAGE gel showing expression of soluble fusion tag protein (N-terminal Trx•Tag™, His•Tag® and S®Tag™) (a) purification of fusion tag through protein Ni-NTA IMAC chromatography (b) and corresponding Western blot analysis (c) conforming expression of fusion tag protein. In Figure (a): Lane M, SDS-PAGE Standards Low Range marker (Bio-Rad). Lanes 1, 2 and 5, total cell fraction (T) of *E. coli* BL21 (DE3) cell lysate at time 0, 3 and 5 hours, respectively post-induction; lanes 3 and 6, soluble fractions (SF) showing overexpression of

fusion tag protein, and lanes 4 and 7, insoluble fractions (IF) showing low expression of fusion tag. In Figure (b) and (c): Lane M, Precision Plus Protein™ Unstained Standards (Bio-Rad). Lane 1 represents the soluble protein fraction; Lanes 2, 3 and 4 represents the flow through, wash and elution fractions respectively. (c) Western blot showing bands correlating to the ~20 kDa protein band on the SDS-PAGE gel in the soluble (lane 1) and eluted fraction (lane 4) respectively.

2. Absorbance spectra of refolded rPbrD obtained from JASCO V-630 spectrophotometer with scan range from 240 to 340 nm.

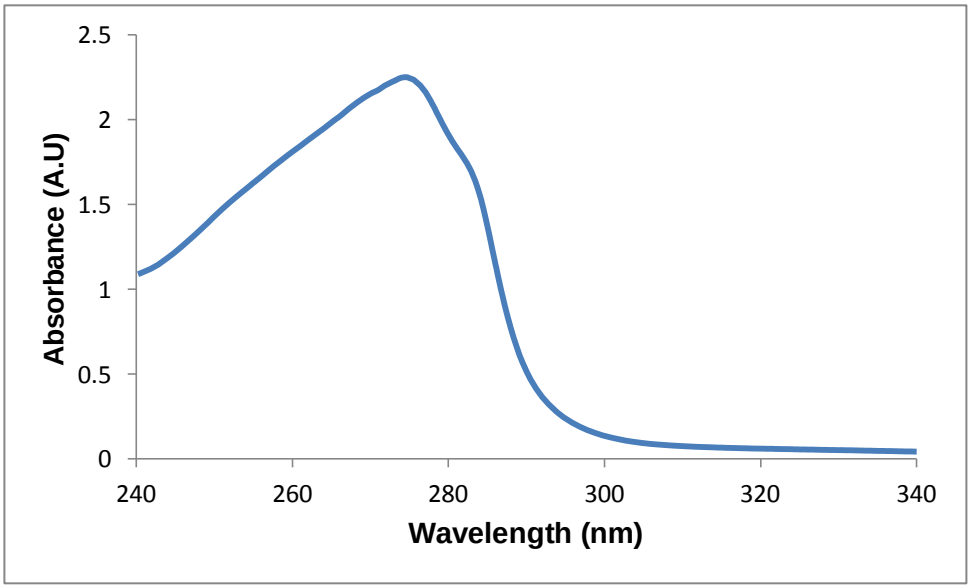

Figure S3 Absorbance spectra of refolded rPbrD. The spectra peak at 280 nm is indicative of a soluble protein sample. A peak between 300-340 nm was not visible indicating the absence of aggregation.

3. Refolded rPbrD analyzed with size exclusion - high performance liquid chromatography (SE – HPLC).

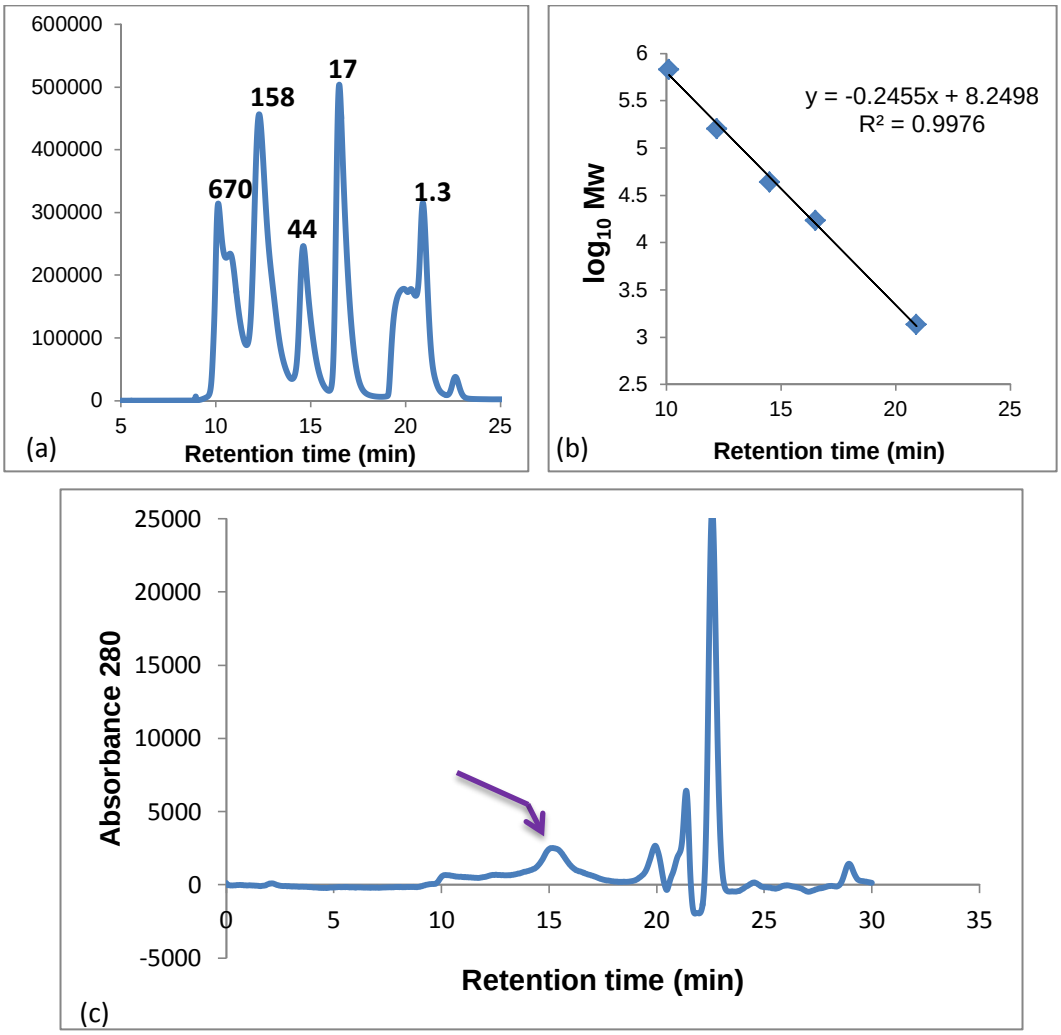

Figure S4 SE-HPLC elution profiles were prepared to assess the presence of protein aggregates in refolded rPbrD. (a) Elution profile of gel filtration standards (GE healthcare) consisting of conalbumin (75 kDa), ovalbumin (44 kDa), carbonic anhydrase (29 kDa), ribonuclease A (13.7 kDa) and aprotinin (6.5 kDa). (b) Standard curve showing the retention time of the gel filtration standards and (c) the elution profile of refolded rPbrD showing peaks at ~10 min (negligible aggregates due to the high content of cysteine residues) and ~14.75 min (rPbrD). Several peaks observed after 20 mins may represent possible contamination from the gel standards.

4. Predictive secondary structure of the fusion tag comprising of N-terminal Trx•Tag™, His•Tag® and S®Tag™.

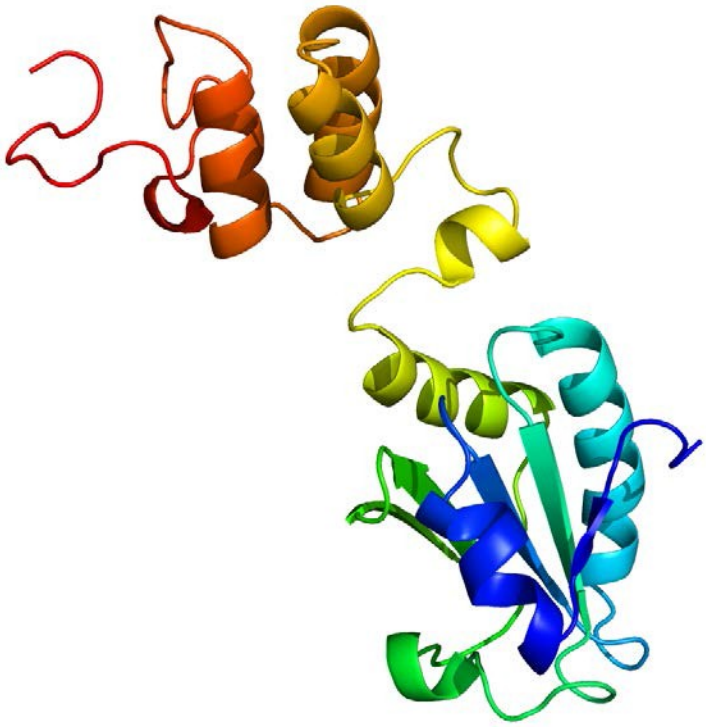

Figure S5 The hypothetical ribbon structure of fusion tag protein (N-terminal Trx•Tag™, His•Tag® and S®Tag™) constructed using Phyre2 (Kelley and Sternberg, 2009) and PyMol [version 1.7.4, Schrodinger] (DeLano, 2002). The model was built with 94 % confidence covering 177 residues and modeled at >90 % accuracy.

Chapter 4

Recombinant fusion protein PbrD cross-linked to calcium alginate nanoparticles for Pb remediation

Keshav, V., Franklyn, P and Kondiah, K.

American Chemical Society Omega, 2019 DOI: 10.1021/acsomega.9b01624

This paper reports the synthesis of rPbrD surface-cross-linked onto calcium alginate nanoparticles (CANPs) for the biosorption of Pb(II) from aqueous solution. Thus far, there are no homologs of PbrD and no other bacterial Pb binding metallo- chaperone has been reported for the remediation of Pb ions from wastewaters. Due to its specificity for Pb and the ability to bind the metal ions, rPbrD cross-linked onto CANPs could be used as an innovative biosorbent for Pb bioremediation.

Author contributions: Vidya Keshav contributed towards all the experimental work, data analysis, data curation, writing of initial drafts and revisions of manuscript. Dr Paul Franklyn contributed towards co-supervision and guidance on the formulation of nanoparticles. Dr Kulsum Kondiah contributed towards student supervision, data interpretation, data editing and proof reading of the manuscript.

ACS OMEGA

Article

http://pubs.acs.org/journal/acsodf

Recombinant Fusion Protein PbrD Cross-Linked to Calcium Alginate Nanoparticles for Pb Remediation

Vidya Keshav,[†] Paul Franklyn,[‡] and Kulsum Kondiah*[,†,§]

[†]School of Molecular and Cell Biology and [‡]School of Chemistry, University of Witwatersrand, Private Bag 3, Wits, 2050 Johannesburg, South Africa

[§]Department of Biotechnology and Food Technology, University of Johannesburg, P.O. Box 17011, Doornfontein, 2028 Johannesburg, South Africa

ABSTRACT: Lead (Pb) pollution arising from industrial and mining activities has led to widespread environmental toxicity, particularly in South Africa. Humans exposed to Pb are reported to suffer from detrimental health impacts that can lead to fatalities. As such, there is an urgent need to remediate Pb from the environment. In this study, we propose the use of a Pb-specific recombinant fusion metalloprotein, rPbrD surface-cross-linked onto calcium alginate nanoparticles (CANPs) for the biosorption of Pb(II) from aqueous solution. The prepared biosorbents were characterized using scanning electron microscopy, transmission electron microscopy, and dynamic light scattering. Their ability to biosorb soluble Pb(II) was determined by inductively coupled plasma mass spectroscopy and their adsorption mechanism was described according to the Langmuir, Freundlich, Temkin, and Dubinin−Radushkevich adsorption isotherms. The rate of Pb uptake for bare CANPs and rPbrD-CANPs at a concentration of 100 mg/L metal was 3.34 and 8.82 mg/g, respectively, within 30 min. The adsorption data for the bare CANPs best fit the Langmuir isotherm, whereas the adsorption data for rPbrD-CANPs best fitted the Freundlich isotherm. Based on the sorption intensity (n) and the separation factor (R_L), both biosorbents represent a favorable adsorption system. These findings suggest that the proposed nanobiosorbent is a promising candidate for the recovery of Pb ions present in high concentrations such as acid mine drainage or industrial effluent.

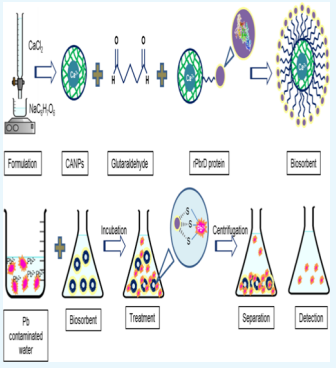

INTRODUCTION

Lead (Pb) toxicity is an environmental concern with a global impact on public health. Lead poisoning refers to the accumulation of the metal in the body, over time resulting in organ dysfunction, especially within the nervous system. It has caused permanent neurological damage in over 15 million children from developing countries.[1] An increase in industrialization and urbanization has contributed to copious amounts of metals like Pb being discharged into natural water resources; rendering it unfit for human consumption. In South Africa, 40% of the population lives in rural settlements that depend entirely upon ground and surface water for domestic use.[2] However, metal exposure is not only limited to communities in informal settlements but also the urban population when they consume the home-grown fruits and vegetables, which are sold as a source of income.[3] Several reports highlight the presence of Pb(II) in South African river systems exceeding the acceptable limit of 10 μg/L.[4] Fatoki and co-workers[5] detected 240−1110 μg/L of Pb(II) in the Umtata River, Eastern Cape, while in the Western Cape, 30−40 μg/L of Pb(II) was recorded in Eerste River.[6] Olujimi and co-workers[7] reported an annual average of between 17.6 and 52.9 μg/L Pb(II) in the river systems of the Western Cape. Although new policies, regulations, and legislations have been made to control the decanting of industrial waste, ambiguities in the system still remain.[8] Humphries and co-workers[9] suggested that although a natural wetland in the Klip River, Gauteng acts as a sink for metals like Pb (source of contamination—Central Witwatersrand Basin), increase in contaminated discharge could compromise the wetland, itself becoming a source of metal contamination that would lead to devastating effects on the region's water supply. Consequently, there is a focus on the development of effective strategies to remove or reduce the elevated concentrations of Pb(II) from wastewaters.

Remediation of Pb(II) from wastewaters using bacterial cells has been reviewed extensively[10,11] as it offers a cheap alternative to chemical treatments. Although biosorption may offer high adsorption capacity and short reaction times, the system is inefficient in targeting specific metal ions when present in a complex medium. Peptides targeting specific metal ions (biopanning) have been attached to bacterial cells for Pb(II) remediation.[12,13] However, introducing modified bacterial cells into water bodies is not yet feasible due to the uncertainty around their behavior in the environment.

In this study, we report the development of a novel nanobiosorbent that exploits the Pb(II) binding properties of the bacterial protein PbrD. PbrD is a metallochaperone found exclusively in *Cupriavidus metallidurans* CH_{34}[14] that binds

Received: June 3, 2019
Accepted: August 20, 2019

DOI: 10.1021/acsomega.9b01624
ACS Omega XXXX, XXX, XXX−XXX

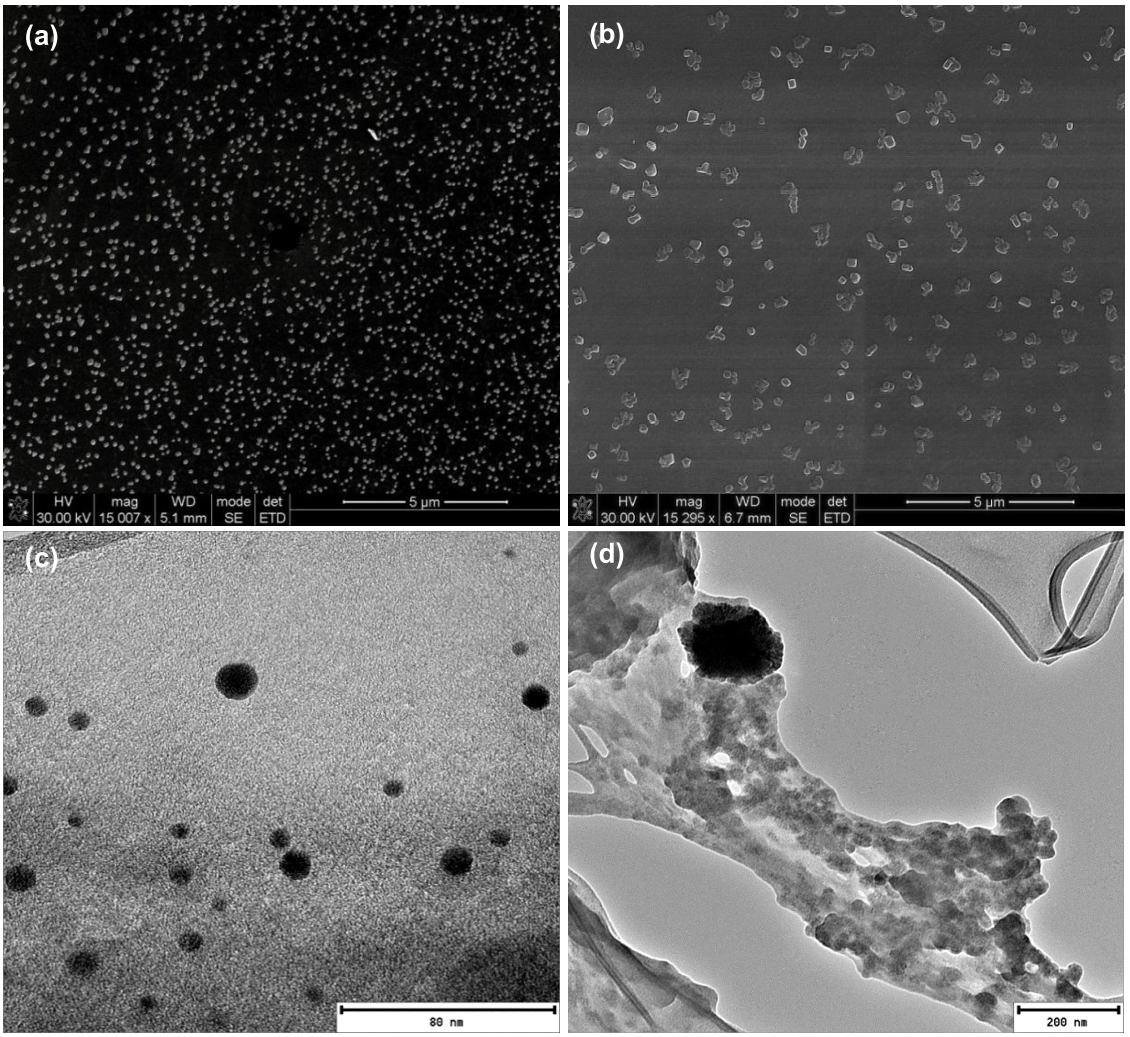

Figure 1. SEM and corresponding TEM images showing uniformly synthesized, monodispersed spherical CANPs ranging from 5 to 30 nm (a, c) and rPbrD-CANPs between 60 and 85 nm (b, d).

Pb(II) intracellularly, thereby reducing the cellular toxic effect of the metal at elevated concentrations.[10] A recombinant form of PbrD (rPbrD) was immobilized onto calcium alginate (CA) nanoparticles (CANPs) and assessed for its ability to biosorb Pb(II) in vitro. Calcium alginate nanoparticles afford stability to the biomolecule in terms of temperature and pH,[15−17] enhance Pb(II) remediation,[18−22] and are biodegradable.[19,23] Herein, we report the use of a synthetic protein-based nanobiosorbent to adsorb Pb(II) at 25 °C. Furthermore, we assess the theoretical adsorption properties of the newly developed nanobiosorbent by the Langmuir, Freundlich, Temkin, and Dubinin−Radushkevich (D−R) isotherms owing to its application to remediate Pb(II) from wastewater.

RESULTS AND DISCUSSION

Characterization of rPbrD-CANPs. *Electron Microscopy.*

Figure 1 shows the morphology and structure of bare CANPs and rPbrD-CANPs. Scanning electron microscopy (SEM) images for CANPs (Figure 1a) and rPbrD-CANPs (Figure 1b) reveal uniformly synthesized, monodispersed particles. Morphology of CANPs was of spherical nature, whereas rPbrD-CANPs were amorphous NPs. Transmission electron microscopy (TEM) micrographs further confirmed the formation of NPs with clear geometric boundaries. Bare CANPs with the size ranging from 5 to 30 nm were observed (Figure 1c) while rPbrD-CANPs appeared larger, between 60 and 85 nm in diameter (Figure 1d). The larger diameter of the rPbrD-CANPs was expected owing to the extended arm of glutaraldehyde and surface-cross-linked protein. When compared to the bare CANPs, rPbrD-CANPs remained in close proximity to each other. This can be attributed to the overall surface charge as well as low particle dispersion from reduced sonication that would otherwise lead to protein degradation.

Protein Loading. For the synthesis of the nanobiosorbent, two strategies used in the immobilization of rPbrD to the as-prepared CANPs were evaluated to determine which resulted in more efficient protein loading. When encapsulated within the CANPs, 66% of 5 μM rPbrD protein was loaded. However, when rPbrD was surface-cross-linked to the CANPs, 72% protein loading efficiency was achieved. The lower loading efficiency could be as a result of smaller pore size within the CANPs, which prevented the entry of rPbrD for binding.[24,25] When compared to encapsulation, chemical cross-linking has been noted to not only improve thermal stability but also protein loading.[25] All further characterization of the nanobiosorbent was performed with surface-cross-linked rPbrD-CANPs.

DOI: 10.1021/acsomega.9b01624
ACS Omega XXXX, XXX, XXX−XXX

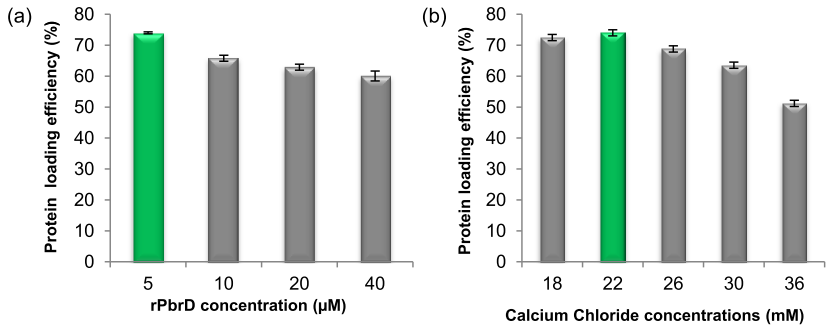

Figure 2. Protein loading efficiency (%). Graphs showing protein loading efficiency when different concentrations of rPbrD protein are cross-linked to CANPs (a), and different concentrations of $CaCl_2$ are used to vary the size of CANPs cross-linked to 5 μM rPbrD (b).

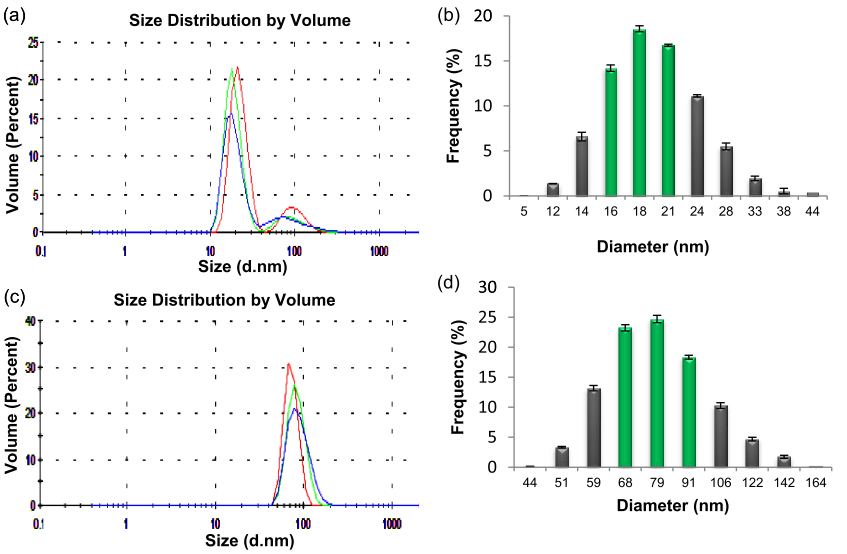

Figure 3. Size distributions of bare CANPs (a, b) and rPbrD-CANPs (c, d) showing the formulation of monodispersed particles with a mean diameter of approximately 12−40 and 50−140 nm, respectively. Error bars represent the standard deviation (SD) from triplicate treatments.

To improve the protein loading efficiency on surface-cross-linked CANPs, two additional parameters were assessed: the concentration of rPbrD and size of CANPs. Figure 2a shows that increasing the concentration of rPbrD from 5 to 40 μM did not increase loading efficiency. Similar trends were observed when the cellulase enzyme was immobilized onto calcium alginate beads,[17] and bovine serum albumin (BSA) was encapsulated in chitosan nanoparticles.[15] Both studies reported that an increase in protein concentration decreased the immobilization efficiency. The decrease in loading efficiency may occur due to the exclusion of binding to inner aldehydic groups by proteins diffusing from bulk solutions to the outer aldehydic chains, which are usually the first to be encountered.[26] A high protein concentration leads to rapid immobilization resulting in partial or total blockage of the pore. Another contributing factor could be that at higher concentrations, recombinant proteins may precipitate out of solution becoming unavailable for immobilization.

In addition, changing the particle size (diameter) may affect the protein loading efficiency. Therefore, 5 μM rPbrD was loaded onto CANPs formed with different concentrations of $CaCl_2$. An increase in $CaCl_2$ concentration resulted in a corresponding increase in particle size. However, as the size of CANPs increased, a decrease in the protein loading efficiency was noted (Figure 2b). These findings suggested a reduction in the surface area of NPs and therefore reduced the number of protein binding sites. Similarly, a decrease in the CANP size (18 mM $CaCl_2$) slightly reduced the protein loading efficiency. In this study, CANPs synthesized with 22 mM $CaCl_2$ showed the highest loading efficiency of 74% and hence was characterized further and used for downstream applications. The stability of rPbrD cross-linked onto CANPs was monitored by measuring the protein concentration in the supernatant of the stored samples over a period of 7 days. There was no appearance of degeneration or leakage of the rPbrD protein in the supernatant, indicating the stability of the system.

Particle Size Distribution and ζ Potential. Particle size and surface charge of NPs are two important factors in their application due to their effect on dissolution. Dynamic light scattering (DLS) data indicated the particle size distribution of bare CANPs to be between 12 nm (±1.29) and 44 nm (±0.46) with an average polydispersity index (PDI) of 0.288 and rPbrD-CANPs to be between 50 nm (±2.57) and 140 nm (±1.95) with an average PDI of 0.326 (Figure 3a,c, n = 3). The peak of high intensity shows a relatively narrow size distribution typical of monodispersed NPs. The DLS data correlates with the data obtained from SEM images.

The surface charge of NPs determines its ability to interact with other molecules. In this study, an average ζ potential of −26 mV (±0.85) and −31.1 (±0.3) were recorded for bare CANPs and rPbrD-CANPs, respectively (Figure 4a,b, n = 3).

DOI: 10.1021/acsomega.9b01624
ACS Omega XXXX, XXX, XXX−XXX

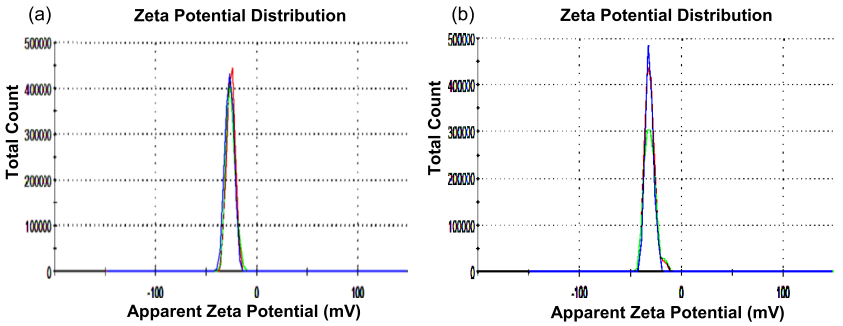

Figure 4. ζ potentials of bare CANPs (a) and rPbrD-CANPs (b) indicating the formation of stable NPs.

The overall negative surface charge is due to the high content of carboxyl and hydroxyl groups of alginate.[27] Immobilization of rPbrD to the surface of the CANPs results in increased particle stability. In addition, an increase in the ζ potential for rPbrD-CANPs was indicative of the success of protein immobilization by surface-cross-linking. These results suggest a stable colloidal system that would allow interaction with Pb(II) cations.

Biosorption Efficiency of rPbrD-CANPs. To determine the biosorption efficiency of the nanobiosorbent, both bare CANPs and rPbrD-CANPs were incubated separately in the presence of increasing concentrations of Pb(II) from 0.001 to 100 mg/L. The supernatant was analyzed using inductively coupled plasma mass spectroscopy (ICP-MS) to indirectly detect the amount of bound Pb(II). Additionally, control samples containing the same concentration range of Pb(II) were prepared without the biosorbent and analyzed with ICP-MS. The control showed no change in the concentration of Pb(II). Figure 5 shows that the biosorption efficiency of

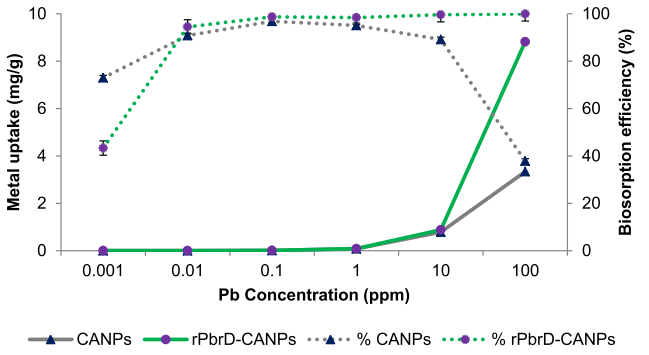

Figure 5. Rate of metal uptake (mg/g) and corresponding biosorption efficiency (%) of bare CANPs and rPbrD-CANPs in the presence of increasing concentrations of Pb(II). An increase in the rate of uptake for both CANPs and rPbrD-CANPs was observed with an increase in the Pb concentration. The biosorption efficiency for bare CANPs gradually decreased after 1 mg/L, whereas rPbrD-CANPs maintained its Pb(II) binding efficiency up to 100 mg/L Pb. Error bars represent the standard deviation from triplicate treatments.

rPbrD-CANPs increased (44−99%) with an increase in Pb(II) concentration (0.001−100 mg/L). At low concentrations of Pb(II), there is a surplus of active binding sites as the ratio of binding sites to metal concentration is high. These binding sites may include the carboxylate (−COO) and hydroxyl (OH) groups characteristic of CA particles[20] as well as the cysteine residues of the protein rPbrD.[10] A similar trend, where biosorption efficiency increased with an increase in the initial Pb concentration, was noted in other biosorption studies.[28,29] This pattern may be attributed to an increased driving force for mass transfer, causing higher collisions between the sorbate and biosorbent,[30,31] thereby leading to an enhanced uptake of Pb(II).

In addition to the apparent increase in the biosorption efficiency, the rate of Pb uptake for rPbrD-CANPs also significantly increased from 3.82×10^{-5} to 8.82 mg/g with an increase in the Pb concentration (0.001−100 mg/L). This trend is attributed to the increased electrostatic attractions and mass transfer resistances between the Pb ions and the metal-binding sites.[32] However, since this is the first study to report on a nanobiosorbent constructed from a recombinant protein, a true comparison with other reported nanobiosorbents is not possible.

Bare CANPs also showed an increase in Pb(II) uptake from 0.001 mg/L (74%) to 0.1 mg/L (97%) until saturation was obtained. Thereafter, the biosorption efficiency began to gradually decrease dropping to 37.85% at 100 mg/L Pb(II). The decrease in metal sorption at higher concentrations of Pb is attributed to the fully occupied metal-binding sites, where the biosorbent has reached a state of equilibrium. At this stage, there is constant sorption−desorption of metals ions, and therefore no further decrease in the residual metal concentration is observed unless the bound metals are desorbed by a change in solution parameters. This trend is typical of the adsorption Langmuir isotherm where the metals occupy the finite number of vacant adsorption sites in a monolayer formation, i.e., one metal ion per metal-binding site.[27] These results are further confirmed with the adsorption isotherm data obtained for CANPs in this study. Similar results were obtained by Khezri and co-workers,[19] who showed a 99% adsorption of bare CANPs in the presence of 25 mg/L $Pb(NO_3)_2$ and also discovered that as the initial metal ion concentration increased, the biosorption of Pb(II) decreased owing to the limited number of binding sites on CANPs.

As expected, these results showed that both CANPs and rPbrD-CANPs are capable of binding Pb. However, when comparing the rate of uptake between the biosorbents, rPbrD-CANPs significantly biosorbed [Table 1, $p < 0.05$ analysis of variance (ANOVA)] more metal per gram of biomass compared to CANPs for all concentrations tested except at 0.001 mg/L. The increase in the rate of metal uptake in rPbrD-CANPs is due to the additional metal-binding sites available on rPbrD (cysteine residues) and its hypothesized specificity for binding Pb(II). At the highest concentration of Pb tested (100 mg/L), rPbrD-CANPs biosorbed almost all of the metals (99%) at a rate of 8.82 mg/g of nanobiosorbent, whereas CANPs biosorbed only 38% at a rate of 3.34 mg/g

DOI: 10.1021/acsomega.9b01624
ACS Omega XXXX, XXX, XXX−XXX

Table 1. Rate of Pb Uptake between CANPs and rPbrD-CANPs at Different Concentrations of Pb(II) (Single-Factor ANOVA)

Pb conc (mg/L)	CANPs (Q_{max})	rPbrD-CANPs (Q_{max})	sum of squared differences (SS)	degrees of freedom (df)	F	P-value	F crit
0.001	0.00006	0.00004	0.0010	1	76.90	0.0009*	7.71
0.01	0.00080	0.00083	0.0016	1	1.12	0.35	7.71
0.1	0.0085	0.0087	0.04	1	15.96	0.02*	7.71
1	0.08	0.09	12.90	1	17.58	0.014*	7.71
10	0.79	0.88	8772.53	1	898.37	0.0011*	18.51
100	3.34	8.82	29 915 269.38	1	2692.68	0.0004*	18.51

*Significant difference $p \leq 0.05$.

nanobiosorbent. A significant difference in the rate of Pb uptake between CANPs and rPbrD-CANPs was observed for all concentrations tested, except at a concentration of 0.01 mg/L, where the rate of Pb uptake did not differ significantly (Table 1, $p < 0.05$ single-factor ANOVA). These findings suggest that while CANPs are able to remove Pb from aqueous solutions when present in low concentrations, adding rPbrD to the CANPs significantly enhances the biosorption efficiency even under high concentrations of the metal. This is ideal not only for South African natural water systems currently contaminated with Pb concentrations ranging from 17 to >1000 μg/L as mentioned earlier but also globally in countries like India, China, Mexico, and Brazil amongst others.[33]

The findings from the present study show that surface-cross-linked rPbrD-CANPs are good nanobiosorbents for Pb(II) that maintain high biosorption efficiency even in the presence of elevated concentrations of the metal. Consequently, the nanobiosorbent would be suitable to recover Pb ions from wastewater.

The binding of Pb(II) to rPbrD-CANPs was further confirmed by performing SEM with energy-dispersive X-ray spectroscopy (EDS) analysis on the washed nanobiosorbent pellet before (Figure 6a) and after incubation (Figure 6b) with the metal. The EDS spectra of rPbrD-CANPs post-biosorption showed a strong signal for Pb and weak signals for carbon (C), chloride (Cl), and oxygen (O) elements (Figure 6b). The peaks of Pb originated from the successful binding of Pb(II) onto rPbrD-CANPs while those of C, Cl, and O were attributed to the formulation of the CANPs itself.

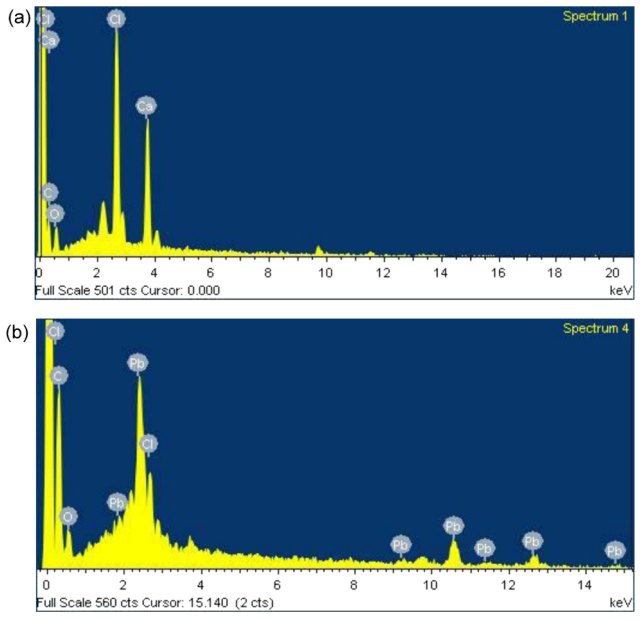

Figure 6. EDS analysis of rPbrD-CANPs before (a) and after (b) Pb biosorption.

Adsorption Isotherms. Adsorption isotherms were applied to understand the adsorption mechanism and compare the Pb(II) binding properties of rPbrD-CANPs to that of bare CANPs. For each isotherm, the values of the adsorption parameters and their respective linear regression line (R^2) were calculated from the linear plots (Figure 7) prepared using the adsorption equilibrium data. The results of the adsorption isotherm values are presented in Table 2.

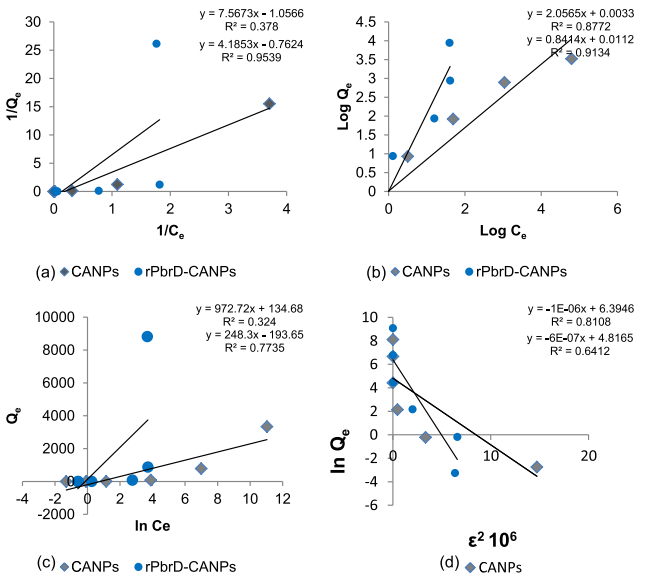

Figure 7. Adsorption isotherm plots of Langmuir (a), Freundlich (b), Temkin, (c) and Dubinin−Radushkevich (d) for Pb(II) adsorption onto bare CANPs and rPbrD-CANPs.

Based on linear regression, bare CANPs best fit the Langmuir isotherm suggesting a monolayer formation of Pb(II). This indicates that the surface of CANPs contains a finite number of binding sites.[19] The theoretical assumption correlates to the experimental data, where bare CANPs eventually reached saturation (at 0.1 mg/L Pb) and no further adsorption could occur. The linear regression data obtained for rPbrD-CANPs best fit the Freundlich isotherm, suggesting that Pb(II) binds in a multilayer formation, which is indicative of a nonrestrictive and exponential form of binding. In multilayer adsorption, the number of Pb(II) molecules is not necessarily identical to the exact number of active sites on the adsorbent surface due to the exponential adsorption of Pb ions, which occur due to interaction with other Pb molecules.[34] As a result, the experimental data showed the complete removal of Pb(II) (100 mg/L) within 30 min when using a concentration of 11 g/L of nanobiosorbent (rPbrD-CANPs). Furthermore, adding

DOI: 10.1021/acsomega.9b01624
ACS Omega XXXX, XXX, XXX−XXX

Table 2. Adsorption Parameters of the Langmuir, Freundlich, Temkin, and Dubinin−Radushkevich Isotherms for the Adsorption of Pb(II) onto Bare CANPs and rPbrD-CANPs

adsorption parameters	CANPs	rPbrD-CANPs
Experimental Adsorption Capacity		
Q_{max} (mg/g)	3.34	8.82
Langmuir Isotherm		
Q_{max} (mg/g)	0.24	0.13
K_L (L/mg)	5.49	7.16
R^2	0.9539	0.378
Freundlich Isotherm		
$1/n$	0.84	2.06
n	1.19	0.49
K_f (mg/g)	1.03	1.01
R^2	0.9134	0.8772
Temkin Isotherm		
A_t (L/mg)	2.18	1.15
B_t	9.98	2.55
B (J/mol)	248.3	972.7
R^2	0.7735	0.324
Dubinin−Radushkevich Model		
Q_s (mg/g)	123.53	598.60
K_{ad} (mol^2/kJ^2)	6×10^{-7}	1×10^{-6}
E (J/mol)	912.87	707.106
R^2	0.6412	0.8108

rPbrD to the CANPs enhanced the maximum rate of adsorption of bare CANPs experimentally from 3.34 to 8.82 mg/g (rPbrD-CANPs). These findings are also supported by the maximum adsorption data (Q_s) obtained from the Dubinin−Radushkevich model with values for bare CANPs of 123.53 mg/g and rPbrD-CANPs of 598.60 mg/g of Pb(II)/g biosorbent, respectively. The differences between the adsorption capacity of bare CANPs and rPbrD-CANPs may be attributed to the different surface adsorption properties and particle size.[20,27,28] The surface properties of rPbrD-CANPs differ from that of the CANPs due to the addition of rPbrD, which provides additional functional groups (amino acids) to the biosorbent. This changes the overall ionic strength and the surface charge of the biosorbent. Additionally, an increase in the surface area (size) of a particle consequently increases the number of binding sites on the biosorbent, thereby increasing its ability to interact/bind to Pb ions. On the other hand, the hypothesized maximum adsorption capacity values obtained from Langmuir and Freundlich isotherms (q_{max} and K_f) were relatively low (<1 mg/g). Due to the immense differences between the adsorption capacity values for all isotherms, no approximate value can be stated. Based on the Langmuir isotherm, the separation factor (R_L) for each Pb(II) concentration used in this study was calculated and shown in Table 3. The R_L values for both bare CANP and rPbrD-CANPs fell in the range $0 > R_L > 1$, indicating a favorable adsorption. Based on the Freundlich isotherm, the adsorption intensity ($1/n$) indicates the binding strength between the biosorbent and Pb(II). The exponent values showed $1/n < 1$ (0.84) for bare CANPs indicating a normal adsorption, whereas $1/n > 1$ (2.06) for rPbrD-CANPs indicating a cooperative adsorption. Normal adsorption is usually favored by monolayer coverage, whereas cooperative adsorption is favored by a multilayer coverage. Furthermore, the n value should lie between 1 and 10, as obtained from the Freundlich

Table 3. Separation Factor of the Biosorbents Obtained from the Langmuir Isotherm

initial [Pb(II)]	R_L (CANPs)	R_L (rPbrD-CANPs)
0.001	0.99	0.99
0.01	0.95	0.93
0.1	0.65	0.58
1	0.15	0.12
10	0.02	0.01
100	1.80×10^{-3}	1.4×10^{-3}

data for both sorbents, then the adsorption process is favorable.[35] The Temkin isotherm constant B explicitly indicates the maximum binding energy or the heat of adsorption that occurs with the coverage of the nanobiosorbent.[36] Based on this data, the values obtained for bare CANPs (248.3 J/mol) and rPbrD-CANPs (972.7 J/mol) showed that the adsorption process is exothermic, representing a physical adsorption system. Additionally, the calculated value of E (kJ/mol) obtained from the D−R isotherm was approximately 1 kJ/mol for bare CANPs and rPbrD-CANPs also, indicating a physisorption process.[37] However, based on the low linear regression line for rPbrD-CANPs ($R^2 = 0.3$) obtained from the Langmuir and Temkin isotherm, no conclusive outcome can be made. Nevertheless, since rPbrD-CANPs indicated a multilayer coverage, and based on the E value from the D−R isotherm, the interaction between Pb(II) and the proposed sorbent is most likely through a physisorption process.

CONCLUSIONS

In this paper, we report the synthesis and characterization of a novel recombinant protein-based lead (Pb) biosorbent for potential application in wastewater treatment. The metallochaperone PbrD was overexpressed and surface-cross-linked to CANPs to form spherical, monodispersed particles with an average diameter of 80 nm. The negative surface charge of the nanobiosorbent indicated a stable colloidal system with the ability to bind positively charged Pb(II). Although bare CANPs were able to bind Pb(II), the rPbrD-CANP nanobiosorbent showed enhanced uptake of the metal (99.9%) at a rate of 8.82 mg/g biosorbent even in the presence of elevated concentrations. The adsorption by rPbrD-CANPs best fitted the Freundlich and Dubinin−Radushkevich isotherms indicating that Pb(II) binding occurred by physical sorption in a multilayer formation. Further development of the nanobiosorbent will include optimizing its performance for real water samples where rPbrD protein is likely to preferentially remediate Pb ions. The nanobiosorbent offers several advantages over traditional biosorbents. It does not produce secondary waste, is biodegradable, and offers increased stability, specificity, sensitivity, and miniaturization of the process. Its incorporation into a small volume portable membrane filter or alternative incorporation into existing wastewater treatment systems could provide a suitable treatment strategy for the recovery of Pb(II) present from 1 μg/L to 100 mg/L, which covers the variability of metal concentration in wastewater effluent.

MATERIALS AND METHODS

Materials. Sodium alginate (SA, low viscosity grade; 15−25 cP, 1% H_2O), calcium chloride ($CaCl_2$), glutaraldehyde (70%), and lead nitrate ($Pb(NO_3)_2$) were purchased from Sigma-

DOI: 10.1021/acsomega.9b01624
ACS Omega XXXX, XXX, XXX−XXX

Aldrich (Missouri) and used without further purification. The experimental procedures were performed at ambient temperature (~25 °C) unless otherwise stated. All solutions were prepared with distilled water obtained from the Elix Essential Water Purification System (Merck, Germany).

Preparation of Recombinant PbrD Protein (rPbrD). The PbrD protein was expressed in *Escherichia coli* BL21 (DE3) cells carrying the constructed vector pPET32Xa/LIC-*pbrD*. This vector was constructed to carry the full-length *pbrD* gene fused to an N-terminal Trx·Tag, His·Tag, and STag; the resulting fusion protein is hereafter referred to as rPbrD. Optimal expression of rPbrD (~50 kDa) was achieved at 37 °C, 5 h post-induction with 1 mM isopropyl *β*-D-1-thiogalactopyranoside. Overexpressed rPbrD was purified by Ni-NTA affinity chromatography under denaturing conditions using 8 M urea. Purified protein (>85%) was eluted in elution buffer (50 mM NaH_2PO_4, 300 mM NaCl, 8 M urea, 400 mM imidazole, pH 8) and refolded by dialysis into buffer containing reduced concentrations of urea and dithiothreitol (DTT) (50 mM Tris, 0.5 M L-arginine, 1 M urea, 10% (v/v) glycerol, 1 mM DTT, pH 8). The refolded protein was further dialyzed into phosphate-buffered saline buffer [containing 0.5 M L-arginine, 1 mM DTT, 10% glycerol (v/v), pH 8] and used for immobilization onto CANPs.

Preparation of CANPs. Calcium alginate nanoparticles were synthesized according to the method described by Daemi and Barikani[23] with slight modification. A solution of 0.06% (w/v) SA was prepared in distilled water under constant agitation and heated to 60 °C until the polymer was completely dissolved. Simultaneously, 22 mM $CaCl_2$ solution was prepared by dissolving in distilled water and titrated into the SA solution at a flow rate of 0.05 mL/min using a peristaltic pump (EP-1 Econo Pump, Bio-Rad) under continuous homogenization. The solution was further agitated for 1 h to achieve the complete formation of the NPs. The homogenized solution was centrifuged at 15 000*g* for 10 min (Heraeus Multifuge X1R Centrifuge, Thermo-Fisher Scientific) to remove impurities. The pellet was reconstituted in 10 mL distilled water and pulse-sonicated with three cycles of 15 s each at 50% amplitude (Q125 sonicator, Qsonica) for even dispersion of prepared NPs.

Preparation of rPbrD-CANPs. Purified rPbrD was either encapsulated within or surface-cross-linked to the CANPs using glutaraldehyde as a cross-linker.

Preparation of Encapsulated rPbrD-CANPs. Separate solutions of 0.06% (w/v) SA and 22 mM $CaCl_2$ were prepared as described earlier. Glutaraldehyde solution (0.5%) was added to the dissolved SA solution and agitated for 30 min at room temperature. Thereafter, 5 *μ*M rPbrD protein was added to the solution and further agitated for 30 min to allow maximum binding of the protein. To form nanoparticles, prepared $CaCl_2$ solution was titrated into the polymer solution containing rPbrD as described earlier and was further agitated for 1 h. The homogenized solution was centrifuged at 15 000*g* for 10 min to remove impurities, and the supernatant containing unbound protein was quantified to determine protein loading efficiency using the Qubit protein assay kit together with the Qubit quantification platform fluorometer (Thermo Scientific). Pre-diluted bovine serum albumin (BSA) standards were used to calibrate the Qubit fluorometer prior to protein quantification.

Preparation of Surface-Cross-Linked rPbrD-CANPs. Calcium alginate nanoparticles were prepared as described earlier. Glutaraldehyde solution (0.5%) was added to the prepared CANPs and agitated for 30 min. A final concentration of 5 *μ*M rPbrD protein was added to the solution and further agitated for 30 min. The surface-cross-linked CANPs were purified by centrifugation at 15 000*g* for 10 min, and the protein loading efficiency was determined using the Qubit protein assay kit together with the Qubit Quantification Platform fluorometer (Thermo Scientific) as previously described. The amount of protein loaded on surface-cross-linked CANPs was found to be consistently higher in replicate preparations than for encapsulated CANPs. Subsequently, further development of the nanobiosorbent was based on the surface-cross-linked method to prepare rPbrD-CANPs.

Protein Loading Efficiency of rPbrD-CANPs. To obtain maximal protein loading efficiency of rPbrD onto the CANPs, protein concentration and nanoparticle size were varied. Several concentrations of the protein (5, 10, 20, and 40 *μ*M) were surface-cross-linked to the as-prepared CANPs and incubated for 30 min. The solution was centrifuged at 15 000*g* for 10 min, and the concentration of the unbound protein in the supernatant was quantified using the Qubit Quantification Platform fluorometer (Thermo Scientific) as previously described. Alternatively, CANPs of variable sizes were prepared using different concentrations of $CaCl_2$ (18, 26, 30, and 36 mM) with a standard concentration of 5 *μ*M rPbrD and evaluated for protein loading. All samples were prepared in a minimum of triplicates, and the results reported are representative of the mean ± SD.

Characterization of CANPs and rPbrD-CANPs. *Scanning Electron Microscopy (SEM) and Energy-Dispersive X-ray Spectroscopy (EDS).* Bare and rPbrD-CANP samples (10 *μ*L) were mounted onto a carbon-coated aluminum stub and placed in a desiccator to dry for 24 h. The prepared stubs were then sputter-coated twice with carbon and once with gold palladium and analyzed using the FEI Nova NanoLab 600 FEG-SEM/FIB (FEI) operated at 30 kV coupled to the EDS. Samples were prepared in triplicates, and images were recorded in a minimum of triplicates.

Transmission Electron Microscopy (TEM). Twenty microliters of bare CANPs or rPbrD-CANPs were placed onto a copper mesh grid and dried at room temperature for 24 h. TEM measurements were performed on an FEI Tecnai T12 instrument (FEI) operating at 120 kV.

Particle Size Distribution and ζ Potential. Dynamic light scattering (DLS) for particle size distribution and ζ potential measurements was carried out on a Zen 3600 Laser Particle Size Analyzer (Malvern Instruments). Samples were pulse-sonicated at a low amplitude of 15%, and 1 mL sample was transferred into a sterile cuvette for analysis at a wavelength of 532 nm. All measurements were performed at 25 °C. For each preparation, an average of three separate measurements was reported, and the results are representative of the mean ± SD.

Pb Binding Assay with CANPs and rPbrD-CANPs. Biosorption studies were conducted using 11 g/L of CANPs and rPbrD-CANPs, respectively. The biosorbents were incubated separately with increasing concentrations of Pb-$(NO_3)_2$ solution (pH 8) ranging from 0.001 to 100 mg/L for 30 min under constant agitation (150 rpm) to facilitate Pb(II) binding. The samples were then centrifuged at 24 000*g* for 20 min. The supernatant containing unbound Pb(II) was collected, adjusted with 1% nitric acid, and analyzed using an Agilent 7900 induction coupled plasma mass spectrometer (ICP-MS, ^{208}Isotope) (Agilent Technologies, Inc.) at the Council for Scientific and Industrial Research (South Africa)

DOI: 10.1021/acsomega.9b01624
ACS Omega XXXX, XXX, XXX−XXX

to indirectly detect the concentration of bound Pb(II). Appropriate controls using $Pb(NO_3)_2$ solutions of similar concentrations (0.001−100 mg/L) without the addition of nanoparticles were included. The adsorption experiments were performed in triplicate, and an average of three measurements are reported. The percentage of Pb removal (biosorption efficiency) and the adsorption capacity (Q_e) (mg/g) were determined using eqs 1 and 2,[38] respectively

$$\text{biosorption efficiency } (\%) = \left(\frac{C_i - C_e}{C_i}\right) \times 100 \quad (1)$$

$$\text{adsorption capacity } (\text{mg/g}) = \frac{(C_i - C_e)V}{w} \quad (2)$$

where C_i is the initial metal concentration (mg/L), C_e is the residual metal concentration (mg/L), V is the solution volume (L), and w is the amount of adsorbent in solution (g).

Statistical Analysis. Statistical hypothesis testing was performed on the biosorption data (rate of metal uptake) using the statistical program R, version 3.4.3. The single-factor ANOVA analysis was used to compare the rate of Pb uptake between CANPs and rPbrD-CANPs for each concentration evaluated in this study. All experiments were performed in triplicate to ensure statistical accuracy. A statistical difference was considered significant when the p-value (α-level) is ≤ 0.05 (95% confidence).

Adsorption Isotherm. Modeling experimental adsorption data of new biosorbents is essential to provide a proper understanding and interpretation of the adsorption mechanisms they follow. Consequently, their commercial potential and application feasibility[39] can be evaluated. Therefore, the four frequently reported adsorption isotherms (Langmuir, Freundlich, Temkin, and Dubinin−Radushkevich) were used to model the adsorption mechanism of both bare and rPbrD-CANPs in the presence of Pb(II) for the purpose of this study. However, it is crucial to apprise that the data obtained from these isotherms are only theoretical and not experimental and therefore are purely descriptive and used as a guide for downstream application.[40] The following summarizes the different adsorption isotherms, linear equations, and adsorption properties, which were applied using the adsorption equilibrium data from the biosorption study.

Langmuir Isotherm. The Langmuir adsorption isotherm was initially developed to study the gas−solid-phase adsorption onto activated carbon.[41] This isotherm depicts a homogenous sorbent surface containing a limited number of metal-binding sites that are similar in size and shape. If the experimental data best fit the Langmuir isotherm, then the following is predicted: Pb(II) forms a monolayer coverage on the surface of CANPs or rPbrD-CANPs and no further adsorption occurs. The isotherm further predicts the separation factor based on the following: if $R_L > 1$ indicates unfavorable adsorption, if $R_L = 1$ indicates linear adsorption, and if R_L $0 < R_L < 1$ then it is favorable and if $R_L = 0$ then it is an irreversible sorption.

The adsorption parameters (Q_{max} and K_L) and the separation factor (R_L) were determined from the slope and intercept of the $1/C_e$ versus $1/Q_e$ plot based on the linearized eqs 3 and 4[36]

$$\frac{1}{Q_e} = \frac{1}{Q_m} + \frac{1}{Q_m K_L C_e} \quad (3)$$

$$R_L = \frac{1}{1 + (1 + k_L C_0)} \quad (4)$$

where Q_e is the amount of Pb adsorbed per gram of the sorbent at equilibrium, Q_m is the maximum adsorption capacity (mg/g), C_0 is the initial metal concentration, K_L is the Langmuir equilibrium constant (mg/L), and R_L is the equilibrium/separation factor.

Freundlich Isotherm. The Freundlich adsorption isotherm determines the empirical relationship between the amount of gas adsorbed per gram of biosorbent at a specific pressure and temperature.[42] This isotherm depicts a heterogeneous sorbent surface that binds metal ions in a nonrestrictive manner until saturation pressure is reached. If the experimental data best fit the Freundlich isotherm, then the following is predicted: Pb(II) forms a multilayer coverage on the surface of CANPs or rPbrD-CANPs indicative of the exponential distribution of Pb(II). The isotherm further predicts the adsorption intensity based on the following: $n = 1$ indicates a more heterogeneous surface, $1/n < 1$ indicates normal adsorption, and $1/n > 1$ indicates cooperative adsorption. The adsorption parameters (K_f and n) were determined from the slope and intercept of the $\log Q_e$ versus $\log C_e$ plot based on the linearized equation presented as eq 5[37]

$$\log Q_e = \log K_f + \frac{1}{n} \log C_e \quad (5)$$

where K_f is the Freundlich adsorption constant (mg/g) relating to the bonding energy and n is the adsorption intensity between Pb and sorbent.

Temkin Isotherm. The Temkin adsorption model considers the effects of indirect adsorbate−adsorbate interactions during the adsorption process and best fits with a monolayer coverage. Considering only the intermediate ion concentrations, the model assumes that as metal ions bind and cover the surface of the biosorbent, the heat of adsorption would decline linearly rather than logarithmically.[43] If the experimental data best fit the Temkin isotherm, then the following is predicted: a positive B (heat) value would indicate that Pb(II) binds to CANPs or rPbrD-CANPs in an exothermic process, whereas a negative value would indicate an endothermic process. The adsorption parameters (A_t and B_t) were determined from the slope and intercept of the Q_e versus $\ln C_e$ plot based on the linearized equation as presented in eq 6 and the heat of the adsorption (B) was determined from eq 7[35]

$$Q_e = \frac{RT}{B_t} \ln(A_t) + \frac{RT}{B_t} \ln(C_e) \quad (6)$$

$$B = \frac{RT}{B_t} \quad (7)$$

where R is the Universal gas constant [8.314 J/(mol k)], T is the absolute temperature in kelvin (298 K), A_t is the equilibrium binding constant, B_t is the Temkin isotherm constant related to the heat of sorption, and B is the constant related to heat of sorption (J/mol).

Dubinin−Radushkevich isotherm. The Dubinin−Radushkevich (D−R) adsorption isotherm is an empirical isotherm which indicates the sorption energy (B_{DR}) distribution between metal ions and the biosorbent.[44] The physisorption prediction best fits a multilayer coverage displaying van der Waals forces of interactions, whereas the chemisorption process best fits monolayer coverage displaying covalent

DOI: 10.1021/acsomega.9b01624
ACS Omega XXXX, XXX, XXX−XXX

bond formation.[45] If the experimental data best fit the D−R isotherm, then the following is predicted: If a low enthalpy (<20 kJ) is measured, then the nature of bonding between Pb(II) and CANPs or rPbrD-CANPs is a physisorption process. Similarly, a high enthalpy (>200 kJ) would depict a chemisorption process. The adsorption parameters (Q_s and K_{ad}) were determined from the slope and intercept of the ln Q_e versus ε^2 plot based on the linearized equation as presented in eqs 8−10[46]

$$\ln Q_e = \ln Q_s - K_{ad}\varepsilon 2 \quad (8)$$

$$\varepsilon = RT \ln\left(1 + \frac{1}{C_e}\right) \quad (9)$$

$$E = \frac{1}{\sqrt{2B_{DR}}} \quad (10)$$

where ε is the Polanyi potential, Q_s is the theoretical saturation capacity (mg/g), K_{ad} is the D−R adsorption energy constant (mol^2/kJ^2), and B_{DR} is the isotherm constant related to the mean free sorption energy.

AUTHOR INFORMATION

Corresponding Author

*E-mail: kuslumk@uj.ac.za. Tel: +27 011 559 6102.

ORCID

Vidya Keshav: 0000-0002-7785-5280

Kulsum Kondiah: 0000-0003-4174-7496

Notes

The authors declare no competing financial interest.

ACKNOWLEDGMENTS

This project was financially supported by the National Research Foundation of South Africa for the Thuthuka grant (Grant No. TTK13062820091). The funders had no role in the design of the study, collection, analyses, interpretation of data, writing of the manuscript, or in the decision to publish the results.

REFERENCES

(1) Sirangala, T. G. Lead Bioremediation with Respect to Mining and Industrial Effluents. *Int. Res. J. Environ. Sci.* **2014**, *3*, 58−61.

(2) *Water for Growth and Development in South Africa*; Department of Water Affairs and Forestry (DWAF): South Africa, 2008.

(3) Bvenura, C.; Afolayan, A. J. Heavy Metal Contamination of Vegetables Cultivated in Home Gardens in the Eastern Cape. *S. Afr. J. Sci.* **2012**, *108*, No. 696.

(4) World Health Organization. *Childhood Lead Poisoning* [Online]; WHO Press: Geneva, Switzerland, 2010; p 37. https://www.who (accessed June 03, 2018).

(5) Fatoki, O. S.; Lujiza, N.; Ogunfowokan, A. O. Trace Metal Pollution in Umtata River. *Water SA* **2002**, *28*, No. 5160.

(6) Reinecke, A. J.; Snyman, R. G.; Nel, J. A. J. Uptake and Distribution of Lead (Pb) and Cadmium (Cd) in the Freshwater Crab, *Potamonautes perlatus* (Crustacea) in the Eerste River, South Africa. *Water, Air, Soil Pollut.* **2003**, *145*, 395−408.

(7) Olujimi, O. O.; Fatoki, O. S.; Odendaal, J. P.; Oputu, O. U. Variability in Heavy Metal Levels in River Water Receiving Effluents in Cape Town, South Africa. In *Research and Practices in Water Quality* [Online]; Lee, T. S., Ed.; Intech Open, 2019; pp 193−211 (accessed March 03, 2019).

(8) Oelofse, S. H. Mine Water Pollution—Acid Mine Decant, Effluent and Treatment: A Consideration of Key Emerging Issues That May Impact the State of the Environment. In *Mining: Environment and Health Concerns* [Online]; Krishna, C. S., Ed.; Icfai University Press, 2009; pp 84−91. http://researchspace.csir.co.za/dspace/handle/10204/5025 (accessed July 14, 2016).

(9) Humphries, M. S.; McCarthy, T. S.; Pillay, L. Attenuation of Pollution Arising from Acid Mine Drainage by a Natural Wetland on the Witwatersrand. *S. Afr. J. Sci.* **2017**, *113*, No. 2016-0237.

(10) Jarosławiecka, A.; Piotrowska-Seget, Z. Lead Resistance in Micro-organisms. *Microbiology* **2014**, *160*, 12−25.

(11) Naik, M. M.; Dubey, S. K. Lead Resistant Bacteria: Lead Resistance Mechanisms, their Applications in Lead Bioremediation and Biomonitoring. *Ecotoxicol. Environ. Saf.* **2013**, *98*, 1−7.

(12) Maruthamuthu, M. K.; Ganesh, I.; Ravikumar, S.; Hong, S. H. Evaluation of zraP Gene Expression Characteristics and Construction of a Lead (Pb) Sensing and Removal System in a Recombinant *Escherichia coli*. *Biotechnol. Lett.* **2015**, *37*, 659−664.

(13) Nguyen, T. T.; Lee, H. R.; Hong, S. H.; Jang, J. R.; Choe, W. S.; Yoo, I. K. Selective Lead Adsorption by Recombinant *Escherichia coli* Displaying a Lead-binding Peptide. *Appl. Biochem. Biotechnol.* **2013**, *169*, 1188−1196.

(14) Taghavi, S.; Lesaulnier, C.; Monchy, S.; Wattiez, R.; Mergeay, M.; van der Lelie, D. Lead (II) Resistance in *Cupriavidus metallidurans* CH_{34}: Interplay between Plasmid and Chromosomally-located Functions. *Antonie van Leeuwenhoek* **2009**, *96*, 171−182.

(15) Masalova, O.; Kulikouskaya, V.; Shutava, T.; Agabekov, V. Alginate and Chitosan Gel Nanoparticles for Efficient Protein Entrapment. *Phys. Procedia* **2013**, *40*, 69−75.

(16) Shilpa, A.; Agrawal, S. S.; Ray, A. R. Controlled Delivery of Drugs from Alginate Matrix. *J. Macromol. Sci., Polym. Rev.* **2003**, *43*, 187−221.

(17) Viet, T. Q.; Minh, N. P.; Dao, D. T. A. Immobilization of Cellulase Enzyme in Calcium Alginate Gel and its Immobilized Stability. *Am. J. Res. Commun.* **2013**, *1*, 254−267.

(18) Huang, Y.; Wang, Z. Preparation of Composite Aerogels based on Sodium Alginate, and its Application in Removal of Pb^{2+} and Cu^{2+} from Water. *Int. J. Biol. Macromol.* **2018**, *107*, 741−747.

(19) Khezri, M.; Jalilpour, Y.; Abedi, S.; Ashjari, H. R. Synthesis of Calcium Alginate Nanoparticles for Removal of Lead Ions from Aqueous Solutions. *Russ. J. Appl. Chem.* **2016**, *89*, 1177−1182.

(20) Mousa, N. E.; Simonescu, C. M.; Pătescu, R. E.; Onose, C.; Tardei, C.; Culiţă, D. C.; Oprea, O.; Patroi, D.; Lavric, V. Pb^{2+} Removal from Aqueous Synthetic Solutions by Calcium Alginate and Chitosan Coated Calcium Alginate. *React. Funct. Polym.* **2016**, *109*, 137−150.

(21) Nesamony, J.; Singh, P. R.; Nada, S. E.; Shah, Z. A.; Kolling, W. M. Calcium Alginate Nanoparticles Synthesized through a Novel Interfacial Cross-linking Method as a Potential Protein Drug Delivery System. *J. Pharm. Sci.* **2012**, *101*, 2177−2184.

(22) Ren, H.; Gao, Z.; Wu, D.; Jiang, J.; Sun, Y.; Luo, C. Efficient Pb (II) Removal Using Sodium Alginate−carboxymethyl Cellulose Gel Beads: Preparation, Characterization, and Adsorption Mechanism. *Carbohydr. Polym.* **2016**, *137*, 402−409.

(23) Daemi, H.; Barikani, M. Synthesis and Characterization of Calcium Alginate Nanoparticles, Sodium Homopolymannuronate salt and Its Calcium Nanoparticles. *Sci. Iran.* **2012**, *19*, 2023−2028.

(24) Misson, M.; Zhang, H.; Jin, B. Nanobiocatalyst Advancements and Bioprocessing Applications. *J. R. Soc., Interface* **2015**, *12*, No. 20140891.

(25) Mohamad, N. R.; Marzuki, N. H. C.; Buang, N. A.; Huyop, F.; Wahab, R. A. An Overview of Technologies for Immobilization of Enzymes and Surface Analysis Techniques for Immobilized Enzymes. *Biotechnol. Biotechnol. Equip.* **2015**, *29*, 205−220.

(26) Adriano, W. S.; Filho, E. H. C.; Silva, J. A.; Giordano, R. L. C.; Gonçalves, L. R. B. Stabilization of Penicillin G Acylase by Immobilization on Glutaraldehyde-activated Chitosan. *Braz. J. Chem. Eng.* **2005**, *22*, 529−538.

(27) Dubey, R.; Bajpai, J.; Bajpai, A. K. Chitosan-alginate Nanoparticles (CANPs) as Potential Nanosorbent for Removal of Hg (II) Ions. *Environ. Nanotechnol. Monit. Manage.* **2016**, *6*, 32−44.

DOI: 10.1021/acsomega.9b01624
ACS Omega XXXX, XXX, XXX−XXX

(28) Bée, A.; Talbot, D.; Abramson, S.; Dupuis, V. Magnetic Alginate Beads for Pb (II) Ions Removal from Wastewater. *J. Colloid Interface Sci.* **2011**, *362*, 486−492.
(29) Kumari, S.; Mahapatra, S.; Das, S. Ca-alginate as a Support Matrix for Pb (II) Biosorption with Immobilized Biofilm Associated Extracellular Polymeric Substances of *Pseudomonas aeruginosa* N6P6. *Chem. Eng. J.* **2017**, *328*, 556−566.
(30) Pathania, D.; Sharma, S.; Singh, P. Removal of Methylene Blue by Adsorption onto Activated Carbon Developed from *Ficus carica* bast. *Arabian J. Chem.* **2017**, *10*, S1445−S1451.
(31) Tewari, N.; Vasudevan, P.; Guha, B. K. Study on Biosorption of Cr (VI) by *Mucor hiemalis*. *Biochem. Eng. J.* **2005**, *23*, 185−192.
(32) Gonte, R.; Balasubramanian, K. Heavy and Toxic Metal Uptake by Mesoporous Hypercrosslinked SMA Beads: Isotherms and Kinetics. *J. Saudi Chem. Soc.* **2016**, *20*, S579−S590.
(33) Clune, A. L.; Falk, H.; Riederer, A. M. Mapping Global Environmental Lead Poisoning in Children. *J. Health Pollut.* **2011**, *1*, 14−23.
(34) Liu, S. Cooperative Adsorption on Solid Surfaces. *J. Colloid Interface Sci.* **2015**, *450*, 224−238.
(35) Dada, A. O.; Olalekan, A. P.; Olatunya, A. M.; Dada, O. Langmuir, Freundlich, Temkin and Dubinin−Radushkevich Isotherms Studies of Equilibrium Sorption of Zn^{2+} Unto Phosphoric Acid Modified Rice Husk. *IOSR J. Appl. Chem.* **2012**, *3*, 38−45.
(36) Foo, K. Y.; Hameed, B. H. Insights into the Modeling of Adsorption Isotherm Systems. *Chem. Eng. J.* **2010**, *156*, 2−10.
(37) Shaker, M. A.; Yakout, A. A. Optimization, Isotherm, Kinetic and Thermodynamic Studies of Pb (II) Ions Adsorption Onto N-maleated Chitosan-immobilized TiO_2 Nanoparticles from Aqueous Media. *Spectrochim. Acta, Part A* **2016**, *154*, 145−156.
(38) Taşar, Ş.; Kaya, F.; Özer, A. Biosorption of Lead (II) Ions from Aqueous Solution by Peanut Shells: Equilibrium, Thermodynamic and Kinetic Studies. *J. Environ. Chem. Eng.* **2014**, *2*, 1018−1026.
(39) Volesky, B. Biosorption and Me. *Water Res.* **2007**, *41*, 4017−4029.
(40) Ayoob, S.; Gupta, A. K. Insights into Isotherm Making in the Sorptive Removal of Fluoride from Drinking Water. *J. Hazard. Mater.* **2008**, *152*, 976−985.
(41) Langmuir, I. The Constitution and Fundamental Properties of Solids and Liquids. Part I. Solids. *J. Am. Chem. Soc.* **1916**, *38*, 2221−2295.
(42) Freundlich, H. M. F. Over the Adsorption in Solution. *J. Phys. Chem. A* **1906**, *57*, 1100−1107.
(43) Temkin, M. I.; Pyzhev, V. Kinetics of Ammonia Synthesis on Promoted Iron Catalysts. *Acta Physicochim. URSS* **1940**, *12*, 327−356.
(44) Dubinin, M. M. The Equation of the Characteristic Curve of Activated Charcoal. *Dokl. Akad. Nauk SSSR* **1947**, *55*, 327−329.
(45) Itodo, A. U.; Itodo, H. U. Sorption Energies Estimation using Dubinin-Radushkevich and Temkin Adsorption Isotherms. *Life Sci. J.* **2010**, *7*, 31−39.
(46) Hemalatha, R.; Chitra, R.; Rathinam, X. R.; Sudha, P. N. Synthesizing and Characterization of Chitosan Graft Co Polymer: Adsorption Studies for Cu (II) and Cr (VI). *Int. J. Environ. Sci.* **2011**, *2*, 805−828.

DOI: 10.1021/acsomega.9b01624
ACS Omega XXXX, XXX, XXX−XXX

Chapter 5

Conclusions and Direction for Future Research

This chapter presents a general discussion on the findings from chapters 3 and 4 and how they collectively address the aim of the study. Concluding remarks on the expression and purification of rPbrD and its Pb binding efficiency, along with the synthesis and cross-linking of rPbrD to CANPs and its Pb binding efficiency are stated. A basic summary on the cost of production and the advantages and disadvantages of the developed biosorbent are outlined with recommendations for future work in method validation and environmental application.

5.1 Discussion and Conclusions

This research demonstrated the *in vitro* synthesis of a Pb specific metallo-chaperone protein PbrD and further investigated its Pb binding function for future application as a biosorbent for Pb-contaminated wastewater. This is the first published report (Chapter 3) on the expression and purification of a functional PbrD fusion protein using an *E. coli* expression system.

For this study pET32 Xa/Lic vector was chosen to facilitate the expression of PbrD, as the vector system is designed for ligation independent cloning which would ensure the insertion of *pbrD* gene in the correct orientation. Additionally the vector contains a thioredoxin tag (109 aa) which is reported to increase the solubility of recombinant proteins expressed in *E. coli* and the histidine tag further assists with protein purification and identification by Western blot using easily available resources. Results from Chapter 3 showed that *pbrD* gene was transformed into *E. coli* BL21 (DE3) cells with high transformation efficiency. Overexpression of rPbrD in *E. coli* BL21 (DE3) was successful however, majority of the protein was found in the insoluble fraction. This is likely to occur under conditions of high level protein expression where the recombinant protein is rapidly expressed higher than the cellular protein which then aggregates into inclusion bodies (Singh *et al.,* 2015).

Generally, two strategies are available to recover the recombinant protein from inclusion bodies; (a) reducing the rate of protein synthesis by changing the expression parameters to promote solubility or alternatively (b) *in vitro* denaturing and refolding of the recombinant protein from inclusion bodies using denaturing reagents (Yamaguchi and Miyazaki, 2014). Despite several attempts to improve protein solubility (by supplementing the growth media

(chemical agents), utilizing a commercial kit (EnPresso® B growth system, Sigma), tuning IPTG concentrations and lowering growth temperatures), majority of the protein was still expressed in inclusion bodies. Consequently, the recombinant PbrD was recovered from the inclusion bodies under denaturing conditions as described in Chapter 3. IMAC purification of denatured PbrD was successfully performed and the purified PbrD protein containing the N-terminal Trx•Tag™, His•Tag® and S®Tag™ (rPbrD) was refolded *in vitro* by dialysis following several optimization procedures in the presence of protein stabilizers to increase the final concentration of soluble protein. The identity of the recombinant rPbrD (~50 kDa) that was subsequently used to prepare the nanobiosorbent was confirmed by Western blot and peptide sequencing. One of the downfalls of recombinant proteins is that they are often unstable when separated from the fusion tag. In order to maintain its stability and to minimize purification and enrichment costs, the decision was made to retain the fusion tag on PbrD protein for its intended use as a commercially available biosorbent.

Characterization of a protein is important to understand its physical, chemical and biological properties. To date, the only literature available on PbrD refers to a probable mechanism of Pb binding within its host strain *C. metallidurans* CH34. There is no homolog of PbrD and thus far no 3D structure of a bacterial Pb metallo- chaperone has been deposited in the protein data bank (PDB) as it has never been crystallized. Therefore, in this study bioinformatics was applied to predict the secondary structure of PbrD and rPbrD. Results obtained from JPred 4 server (Drozdetskiy *et al.,* 2015) and Phyre2 and PyMoL software [version 1.7.4, Schrodinger] (DeLano, 2002) displayed a partially structured protein with some contribution from β-sheet and helical structure, part of which originated from the fusion tag on rPbrD. This structure further correlated to CD data analyzed with BeStSel software (Micsonai *et al.,* 2018). Interestingly, it was observed that in the presence of its ligand Pb(II), rPbrD assumes a more ordered structure composed primarily of antiparallel β-sheets. This is in line with the mechanism of PbrD within *C. metallidurans* CH34 where Pb(II) that accumulates intracellularly is bound by PbrD which acts as a molecular chaperone (Taghavi *et al.,* 2009). The coupled folding and binding of disordered regions in proteins is characteristic of molecular switches that adopt an ordered conformation (Sandhu and Dash, 2007) when molecular recognition, in this case Pb(II), occurs. The ordered protein then serves as a regulator of biological function.

To assess whether the recombinant protein had refolded into the appropriate conformation for

Pb binding to occur, intrinsic fluorescence was applied. It is reported that proteins that contain aromatic amino acids (cysteine, phenylalanine, tryptophan and tyrosine) act as fluorophores which facilitate the study of structural changes in the protein conformation and intermolecular interactions based on the highly sensitive indole chromophore (Chen and Barkley, 1998). Since, binding of Pb(II) is known to occur through interactions with three Cys molecules (Cangelosi *et al.,* 2017) Cys fluorescence of rPbrD in the presence of Pb(II) would be an ideal technique to verify its functionality. However, Cys molecules exhibits weak signals and may produce inaccurate measurements therefore Trp which produces a strong signal when excited at 295 nm was used to assess the functionality of denatured and refolded rPbrD. Based on the bioinformatics analysis, rPbrD contains twelve Trp residues of which five are exposed in its native fold while theoretically all Trp residues should be exposed in the denatured form. In the presence of Pb(II), rPbrD quenched the intrinsic fluorescence more than the denatured sample indicating intermolecular interactions between Pb(II) and refolded rPbrD. These results further infer that the refolded rPbrD protein had presumably formed a “correct structural conformation” (native fold) during the refolding process thus maintaining its functionality to bind Pb(II) *in vitro*.

To further assess the functionality of rPbrD, Pb binding analysis was performed using a ten-fold increment in the concentration of Pb(II). As the thioredoxin protein present on the fusion tag may contribute to Pb binding by means of its metal binding motif (CxxC) (Su *et al.,* 2007) known to bind Ni(II), Cd(II), Cu(II) and Hg(II), the fusion tag Trx•Tag™, His•Tag® and S®Tag™ was itself expressed and purified as a soluble protein (~20 kDa) and analyzed as a control in the Pb binding assay. The findings from the assay revealed that the fusion tag contributed between 10-30 % of Pb(II) binding in the absence of other divalent metals whereas rPbrD was able to bind 78– 99% of Pb(II). Generally, an increase in metal concentration past the saturation concentration is known to result in a decrease in the biosorption efficiency as metal binding sites on the biosorbent are fully occupied. However, rPbrD exhibited a reverse effect i.e. the biosorption efficiency increased with an increase in metal concentration as indicated by the adsorption isotherm data. Within the native organism low concentrations of Pb(II) are removed via the initial efflux mechanisms (PbrA and PbrT) however, at elevated concentrations, Pb(II) enters into the cytoplasm and is stored by PbrD which protects the organism from cellular malfunctioning. In this regard, it is postulated that the initial concentrations of Pb(II) used in this study were too low to induce a change in the structural conformation of the rPbrD and therefore perhaps weakly bound and disassociated from rPbrD in solution causing the reverse effect. While the fusion tag also contributes to

the binding of Pb(II) and could be argued as a suitable biosorbent, the small protein size (unstable) and its non-specificity to Pb(II) encumbers its application as a Pb targeted biosorbent. Although PbrD is reported to preferentially bind Pb(II) within its native organism, its specificity and preferential order of binding metal ions in natural water systems still needs to be elucidated. Nonetheless, these results suggest that the GE protein indeed maintained its function *in vitro* and could be used as a Pb-specific biosorbent.

Owing to the delicate nature of proteins the use of a recombinant protein by itself is not feasible as a biosorbent especially in harsh conditions characteristic of wastewater. Furthermore recovery of protein-metal complex from treatment sites is unattainable. For these reasons, CANPs were formulated as a support matrix for rPbrD. The inherent physicochemical characteristics of several nanomaterial's like CANPs make them suitable for the support and preservation of the structure and function of biomolecules. Subsequently, there is a combined sorption effect from PbrD and CANPs for the enhanced uptake of Pb ions from solution.

Although synthesis of CANPs has been documented, several reaction parameters were optimized in order to attain suitable particles in terms of size, morphology and distribution for the immobilization of rPbrD as discussed in the paper presented as Chapter 4. Data obtained from the comparison of two immobilization strategies (cross-linking and entrapment) showed a higher protein loading efficiency when rPbrD was surface-cross-linked to the CANPs. A loss in protein loading efficiency during the entrapment method was perhaps due to the pore diffusion limitations of rPbrD into the alginate matrix as compared to rPbrD immobilized externally on the support matrix via the cross-linking method. Characterization of both bare CANPs and CANPs surface cross linked to rPbrD (CANP-rPbrD) showed the formation of uniformly synthesized, monodispersed particles with an average diameter of 18 and 80 nm respectively. However, images obtained from SEM and TEM revealed that bare CANPs were of spherical nature whereas rPbrD-CANPs were more amorphous NPs perhaps owing to the structure and direction in which the protein was attached during cross-linking.

It is well reported that the particle size and surface area of the constructed NPs majorly affects their interaction with the target molecules (Wang *et al.,* 2018). Therefore, to further assess the relationship between the size of rPbrD-CANPs and maximum protein loading efficiency different formulations of various particle size and protein concentrations were evaluated. These results showed that decreasing the size of CANPs increased the surface

area for higher protein loading efficiency which was achieved using the lowest concentration of rPbrD. One of the drawbacks post immobilization of proteins is that the particles may become unstable and aggregate. Therefore, DLS and zeta potential were applied to verify the particle distribution and stability of the formulations. A narrow size distribution typical of monodispersed NPs with a low PDI were observed implying no aggregation in both CANP and rPbrD-CANP formulations. Additionally, the negative surface charge of the CANP and rPbrD-CANPs indicated a stable colloidal system with the ability to bind positively charged Pb(II). These parameters indicate how the rPbrD-CANP biosorbent would distribute in aqueous solution, how they would respond and bind to Pb(II) and further indicate how the metal ions could be separated from the matrix for further desorption studies.

Another problem often encountered with protein immobilization is that the activity of protein is reduced or completely lost after their immobilization. To verify whether the activity of rPbrD was maintained post immobilization, Pb(II) binding analysis was performed. The binding of Pb(II) by bare CANPs was also analyzed since CANPs are known to interact with the metal. Data from the Pb(II) binding assay for rPbrD- CANPs showed a similar biosorption trend as free rPbrD, where the biosorption efficiency increased with an increase in Pb(II) concentration until it reached a state of equilibrium (Chapter 4). Similar biosorption trends were observed in other biosorbent studies where the authors attributed this pattern to an increased driving force for mass transfer due to the increased sorbate concentration; thereby leading to more uptake of Pb(II) at higher concentrations in this study. However as discussed in Chapter 4, this is the first study to report on a biosorbent constructed from a recombinant protein and therefore a true comparison with other reported biosorbents was not possible. Bare CANPs also showed an increase in Pb(II) uptake with increasing metal concentration though the particles reached saturation at a much lower Pb(II) concentration when compared to rPbrD-CANPs. Additionally, rPbrD- CANPs significantly biosorbed more Pb per g biomass (rate of uptake) compared to CANPs (statistical data shown in Chapter 4). These findings suggest that although CANPs adsorb Pb(II), adding rPbrD to the CANPs significantly enhanced the biosorption efficiency even at elevated metal concentrations as high as 100 mg/L Pb(II).

When designing a new biosorption system, adsorption isotherms are useful in providing information on the theoretical sorption mechanism, surface properties and affinity assumptions that play a key role in its application at industrial or environmental level. Based on the biosorption data obtained in this study, the Langmuir, Freundlich, Temkin and Dubinin-Radushkevich adsorption isotherms were employed to describe the relationship between Pb(II)

and rPbrD and rPbrD-CANPs (Chapter 4). Modeling of the binding data to these isotherms, suggest that binding of Pb(II) to both rPbrD and rPbrD-CANPs occurred as a favourable physisorption process although binding to rPbrD correlated more to the Temkin model (r^2=0.9783) while binding to rPbrD-CANPs correlated to the Langmuir model (r^2=0.9539) followed closely by the Freundlich model (r^2=0.9134).

Stability of biomolecules is a key factor in the production and commercialization of biosorbents, especially for a protein-based biosorbent. Leakage or degradation of the protein during storage and application would result in obvious reduced binding rendering the system substandard. One of the advantages of the immobilization process is that this technique offers stability of the captured protein (Masalova *et al.,* 2013). When rPbrD-CANPs were stored at 4^{o} C and monitored for protein loss by measuring the protein concentration in the supernatant of the stored samples over seven days, no protein leakage was observed. These results showed that rPbrD was stably cross-linked to CANPs. Additionally, EDS spectra of the rPbrD-CANPs before and after incubation further displayed the successful binding of Pb(II).

To conclude, this is the first report on the expression, purification and immobilization of a functional recombinant PbrD protein. Both rPbrD and rPbrD-CANPs showed the ability to bind Pb(II) at concentrations higher than the reported levels in ground/surface water in South Africa implying its use in the treatment of Pb-rich industrial waste water both locally and globally.

The successful immobilization of rPbrD to CANPs resulted in a novel eco-friendly protein-based nanosorbent that binds Pb(II) in an exponential multilayer manner with adsorption intensity indicative of a cooperative physisorption process. The simplicity of the biosorbent system would enable easy integration into portable membrane filters for use in domestic households that rely on naturally sourced water or scale-up for water treatment plants.

5.2 Advantages and Disadvantages of the Protein-based Biosorbent

The following is a summary of the benefits and drawbacks that a protein-based biosorbent could present in the bioremediation of industrial wastewater.

Advantages:

1) Eco-friendly biosorbent

2) Specificity for Pb(II) remediation
3) Sensitivity in recovering low concentrations of Pb(II)
4) Increased stability achieved from cross-linking method
5) NPs offer miniaturization of process
6) Inexpensive (after recommended modifications suggested hereafter)
7) Does not produce secondary waste post treatment
8) The overall concept can be applied for targeting other toxic metals

Disadvantages:

1) Based on the sensitive nature of protein, pre-treatment of wastewater such as addition of lime or limestone may be added to increase the pH of acid mine water prior to treatment.
2) Environmental factors such as pH, salts, temperature, non-polar solvents etc. may affect the activity of rPbrD protein. Subsequently, microbial degradation may affect the stability of the protein. Therefore, the optimum parameters for rPbrD-CANPs to maintain its Pb(II) binding activity in real wastewater samples still need to be elucidated.

5.3 Cost of the Protein-based Biosorbent

One of the major reasons for diversions into bioremediation is the high cost of existing chemical treatment systems such as ion-exchange resin and activated carbon. In this regard, several excellent biosorbents have been reported thus far. However, immobilization can drastically increase the biosorbent cost impeding its commercialization. Fosso-Kankeu and Mulaba-Bafubiandi (2014) reported that the existing market for new biosorbents materials in America cost an estimate of 30 million US dollars due to its increasing demand in water treatment.

Development of a novel biosorbent often requires a high capital cost due to various uncertainties encountered during the development process. However, once the biosorbent is developed and demonstrates great biosorption efficiencies, the biosorbent cost may be re-evaluated for large scale application. The cost involved in developing rPbrD-CANPs biosorbent for the purpose of the present study is detailed in Table 5.1. The table only provides an estimate cost for material required to synthesize 1 g/L of rPbrD-CANPs at laboratory scale. For commercialization, factors such as equipment cost, water and electricity usage etc. would be incorporated. The recommendations for cost reduction are discussed in section 5.4.

Table 5.1 Cost estimation for the formulation of 1 g/L rPbrD-CANPs

Preparation of biosorbent	Materials	Cost in ZAR*
Expression culture (1 L)	LB Amp broth	55.56
	IPTG	200.64
Solubilization of IB	Bugbuster	369.24
	Buffer A without urea	1.50
	Buffer B with urea (~2 mg/mL denatured protein)	3.34
Purification	HisTrap HP column	2502.42
Purification buffers	Binding buffer	33.50
	Wash buffer	33.50
	Elution buffer	121.00
Dialysis	Cassette/tube	309.00
Refolding buffers	Buffer A	932.33
	Buffer B	758.80
	Buffer C	550.01
	Buffer D	517.01
Total protein cost	~0.650 mg/mL refolded protein	6387.85
Nanoparticles (200 mL)	Sodium alginate	0.20
	Calcium chloride	38.00
	Glutaraldehyde	188.00
Total NP cost	200 mL CANPs	226.20
Protein	0.235 mg/mL	2309.45
CANPs	5 mL (~1.7 g)	5.66
Consumables	Tips, tubes, filters, gloves, ethanol etc.	1723.00
Biosorbent cost at 11 g/L	rPbrD-CANPs	4038.11
Biosorbent cost at 1 g/L	rPbrD-CANPs	367.10

**The above cost estimation was calculated based on 2018 pricelist*

In summary, to treat 1 L of effluent containing a maximum of 100 mg/L Pb one would require 11 g/L of rPbrD-CANPs to effectively reduce the concentration of Pb which would cost ~R4000.00. Understandably, this cost appears high compared to other biosorbents however, it should be taken into account that the cost was calculated for consumables/reagents at lab scale. It can be assumed that large-scale production of the biosorbent would significantly reduce the cost of the biosorbent.

5.4 Recommendations for Future Work

Further development of the biosorbent for industrial applications should take into consideration the following points.

5.4.1 Improved production

As indicated in Table 5.1, majority of the cost of production was incurred due to the affinity purification and refolding of rPbrD protein since it was expressed in insoluble form. Large scale production of rPbrD in soluble form would alleviate these costs making the system more attractive for commercialization. There are several strategies of improving solubility of recombinant proteins in *E. coli* (Gopal and Kumar, 2013; Rosano and Ceccarelli, 2014); some of which were analyzed to obtain soluble PbrD with little success as described in section 5.1. Fusion tags are known to increase the solubility of proteins (Terpe, 2003). However, different fusion tags rescue different proteins and should therefore be tested empirically for each protein which can take some time. The Expresso® solubility and expression screening system offered by Lucigen, USA contains seven different cleavable solubility tags. The solubility of the expressed protein can be rapidly tested with a single PCR amplicon transformed into a suite of cloning-ready pSol vectors each carrying one of seven fusion tags. Such a system could prove useful in the rapid evaluation of fusion tags that facilitates solubility of PbrD protein in *E. coli*.

5.4.2 Optimization and specificity

Efficient biosorption is dependent on factors such as pH, temperature, contact time, concentration of biosorbent and the presence of competing cations. A change in pH and temperature may lead to the alteration of functional groups thereby affecting the surface charges of the biosorbent, or the alteration of the oxidation state of metals in aqueous solution (Taşar *et al.,* 2014). For the purpose of this study rPbrD-CANPs were stored at 4 ^{o}C. However, the immobilization strategy was applied to increase the stability of rPbrD-CANPs complex. A change in temperature may affect the stability of the complex and therefore it will be necessary to monitor the biosorbent at various temperatures to determine their maximum thermal stability. A balance between the number of available binding sites and contact time is important to ensure maximum uptake of metal per g of biosorbent. Therefore it will be necessary to investigate the effect of each of these parameters on the stability of the proposed biosorbent and its ability to biosorb Pb. Polluted freshwater generally contains a consortium of metals and other inorganic material. Since metal binding functional groups are non-specific, other metal ions could behave in a synergistic or antagonistic manner in the uptake of Pb by rPbrD-CANPs

and would need to be evaluated. Post-optimization, the activity of the biosorbent in real life water samples from different locations and during seasonal variations should be assessed. Additionally, a method validation will be performed to test the sensitivity and efficiency of rPbrD-CANPs when used in synergy with existing treatment systems.

5.4.3 Regeneration and recycling

For environmental significance it is important that once removed from the water, the metal bound to the biosorbent is desorbed and recycled back to industry. Additionally, in the interest of commercialization the biosorbent should be regenerated for several cycles of application to reduce the process cost (Shaker and Yakout, 2016). The choice of metal desorbent (acids, complexing agents) should preferably remove all of the bound metals without compromising the original state or function of the biosorbent (Alluri, *et al.,* 2007). As previously described protein is sensitive in nature which limits the range of desorbents that can be used with rPbrD- CANPs. Therefore, a chelating agent like Ethylenediaminetetraacetic acid (EDTA) which is commonly used with protein can be evaluated for its desorption efficiency of Pb(II) from rPbrD-CANPs. Any structural changes of the nanobiosorbent post desorption is monitored by SEM and CD while the maximum number of cycles for reuse of the biosorbent will be determined through the Pb binding assay.

5.4.4 Commercialization

A number of factors (from lab to application) are evaluated when considering a technology for commercialization. Volesky (2007) describes preliminary assessments (competing technologies, market size, cost evaluation, potential partners) required for evaluating the economic feasibility of a biosorbent for commercialization. Successful expression of soluble PbrD and validation of the nanobiosorbent performance with real wastewater samples will be the first stage towards commercialization. The long term goal of this research is to incorporate rPbrD-CANPs into a membrane filter for treatment of small water volumes that address the needs of local communities in South Africa who source their water for domestic use from natural rivers prone to contamination with industrial effluent.

The present study focused on finding a solution to manage Pb pollution in the South African context. However, Pb pollution is a global threat; indeed, there has been a recent outcry on the state of Pb poisoning in America. The application of the protein- based biosorbent described here is not limited to South Africa but could present as a bioremediation solution globally. For these reasons a nation phase patent application was filed in South Africa, United States of

America, Canada and Australia (WO 2017/051370 A1).

5.5 References

1. Alluri, H.K., Ronda, S.R., Settalluri, V.S., Bondili, J.S., Suryanarayana, V. and Venkateshwar, P., 2007. Biosorption: An eco-friendly alternative for heavy metal removal. *African Journal of Biotechnology*, *6*(25).
2. Cangelosi, V., Ruckthong, L. and Pecoraro, V.L., 2017. Lead (II) binding in natural and artificial proteins*. Metal ions in Life Sciences,* 17. https://doi.org/10.1515/9783110434330-010
3. Chen, Y. and Barkley, M.D., 1998. Toward understanding tryptophan fluorescence in proteins. *Biochemistry*, *37*(28), pp.9976-9982. https://doi.org/10.1021/bi980274n
4. DeLano, W.L. (2002) The PyMOL Molecular Graphics System. Delano Scientific, San Carlos.
5. Drozdetskiy, A., Cole, C., Procter, J., Barton, G.J. (2015) JPred4: a protein secondary structure prediction server, *Nucleic Acids Res.* Web Server issue.
6. Fosso-Kankeu, E. and Mulaba-Bafubiandi, A.F., 2014. Review of challenges in the escalation of metal-biosorbing processes for wastewater treatment: Applied and commercialized technologies. *African Journal of Biotechnology*, *13*(17).
7. Gopal, G.J. and Kumar, A., 2013. Strategies for the production of recombinant protein in *Escherichia coli*. *The Protein Journal*, *32*(6), pp.419- 425. https://doi.org/10.1007/s10930-013-9502-5
8. Masalova, O., Kulikouskaya, V., Shutava, T. and Agabekov, V., 2013. Alginate and chitosan gel nanoparticles for efficient protein entrapment*. Physics Procedia*, *40*, pp.69-75. https://doi.org/10.1016/j.phpro.2012.12.010
9. Micsonai, A., Wien, F., Bulyáki, É., Kun, J., Moussong, E., Lee, Y.H., Goto, Y., Réfrégiers, M. and Kardos, J., 2018. BeStSel: A web server for accurate protein secondary structure prediction and fold recognition from the circular dichroism spectra. *Nucleic Acids Research*, *46*(W1), pp.W315-W322. https://doi.org/10.1093/nar/gky497
10. Rosano, G.L. and Ceccarelli, E.A., 2014. Recombinant protein expression in *Escherichia coli*: Advances and challenges. *Frontiers in Microbiology*, *5*, p.172. https://doi.org/10.3389/fmicb.2014.00172
11. Sandhu, K.S. and Dash, D., 2007. Dynamic α-helices: Conformations that do not

conform. *Proteins: Structure, Function, and Bioinformatics*, 68(1), pp.109- 122. https://doi.org/10.1002/prot.21328

12. Shaker, M.A. and Yakout, A.A., 2016. Optimization, isotherm, kinetic and thermodynamic studies of Pb (II) ions adsorption onto N-maleated chitosan-immobilized TiO_2 nanoparticles from aqueous media. *Spectrochimica Acta Part A: Molecular and Biomolecular Spectroscopy*, *154*, pp.145-156. https://doi.org/10.1016/j.saa.2015.10.027
13. Singh, A., Upadhyay, V., Upadhyay, A.K., Singh, S.M. and Panda, A.K., 2015. Protein recovery from inclusion bodies of *Escherichia coli* using mild solubilization process. *Microbial Cell Factories*, *14*(1), p.41. https://doi.org/10.1186/s12934-015-0222-8
14. Su, D., Berndt, C., Fomenko, D.E., Holmgren, A. and Gladyshev, V.N., 2007. A conserved cis-proline precludes metal binding by the active site thiolates in members of the thioredoxin family of proteins. *Biochemistry*, *46*(23), pp.6903- 6910. https://doi.org/10.1021/bi700152b
15. Taghavi, S., Lesaulnier, C., Monchy, S., Wattiez, R., Mergeay, M. and van der Lelie, D., 2009. Lead (II) resistance in *Cupriavidus metallidurans* CH34: interplay between plasmid and chromosomally-located functions. *Antonie Van Leeuwenhoek*, 96(2), p.171. https://doi.org/10.1007/s10482-008-9289-0
16. Taşar, Ş., Kaya, F. and Özer, A., 2014. Biosorption of lead (II) ions from aqueous solution by peanut shells: equilibrium, thermodynamic and kinetic studies. *Journal of Environmental Chemical Engineering*, *2*(2), pp.1018-1026. https://doi.org/10.1016/j.jece.2014.03.015
17. Terpe, K., 2003. Overview of tag protein fusions: from molecular and biochemical fundamentals to commercial systems. *Applied Microbiology and Biotechnology*, *60*(5), pp.523-533. https://doi.org/10.1007/s00253-002-1158-6
18. Volesky, B., 2007. Biosorption and me. *Water Research*, *41*(18), pp.4017- 4029. https://doi.org/10.1016/j.watres.2007.05.062
19. Wang, Y., Cui, Y., Zhao, Y., Zhao, Q., He, B., Zhang, Q. and Wang, S., 2018. Effects of surface modification and size on oral drug delivery of mesoporous silica formulation. *Journal of Colloid and Interface Science*, *513*, pp.736-747. https://doi.org/10.1016/j.jcis.2017.11.065
20. Yamaguchi, H. and Miyazaki, M., 2014. Refolding techniques for recovering biologically active recombinant proteins from inclusion bodies. *Biomolecules*, *4*(1), pp.235-251.